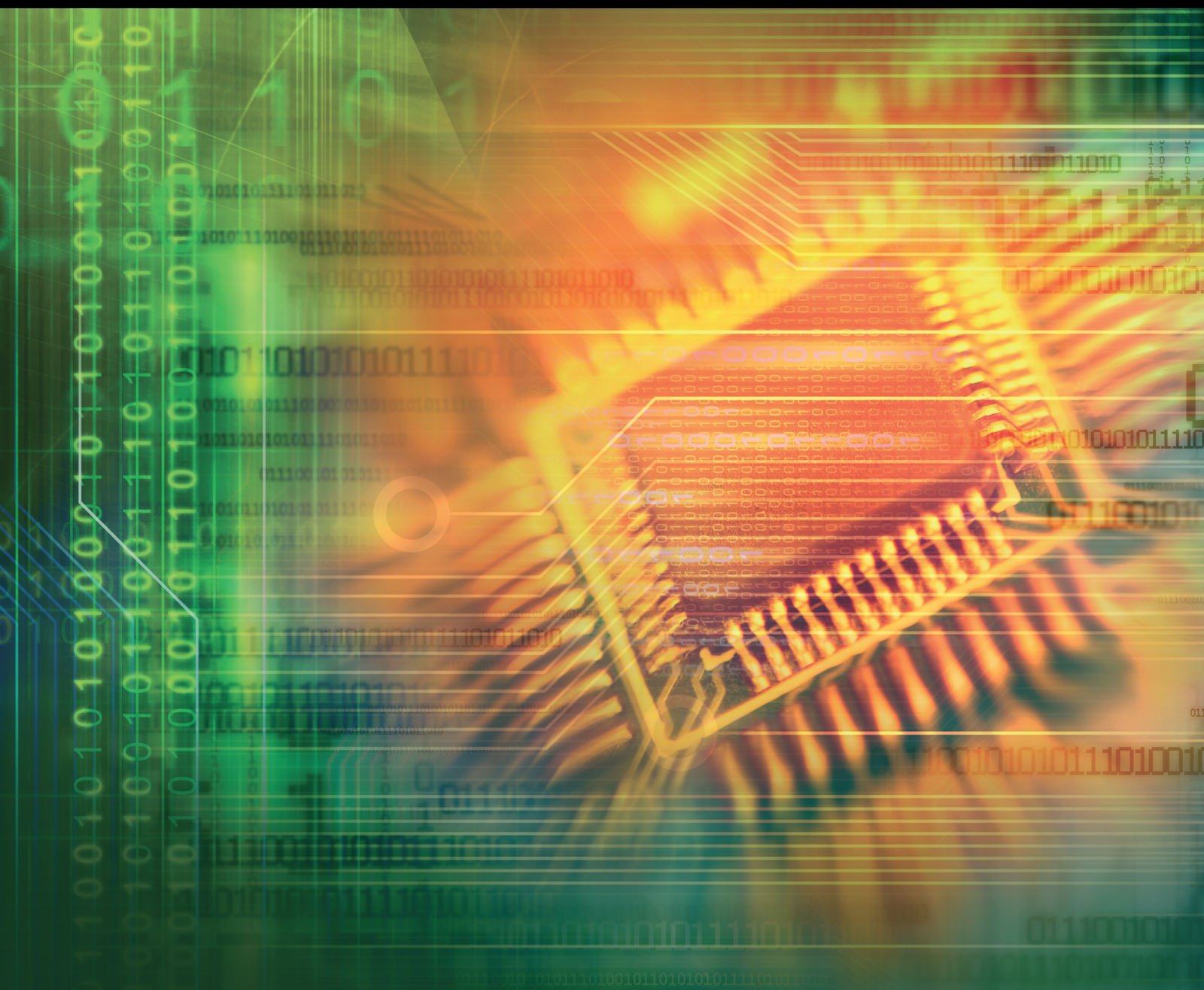


# Computational Intelligence Applied to Smart Grids

Lead Guest Editor: Carlos R. Minussi

Guest Editors: Anna Diva Plasencia Lotufo, Fernanda Caseño Trindade Arioli, Mauro de Souza Tonelli-Neto, and Om P. Malik





---

# **Computational Intelligence Applied to Smart Grids**



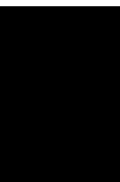
Journal of Electrical and Computer Engineering

---

## **Computational Intelligence Applied to Smart Grids**

Lead Guest Editor: Carlos R. Minussi

Guest Editors: Anna Diva Plasencia Lotufo,  
Fernanda Caseño Trindade Arioli, Mauro de Souza  
Tonelli-Neto, and Om P. Malik



---

Copyright © 2021 Hindawi Limited. All rights reserved.

This is a special issue published in "Journal of Electrical and Computer Engineering." All articles are open access articles distributed under the Creative Commons Attribution License, which permits unrestricted use, distribution, and reproduction in any medium, provided the original work is properly cited.

## Circuits and Systems

Muhammad Taher Abuelma'atti , Saudi Arabia  
Domenico Bianchi, Italy  
Luca Cassano, Italy  
Henry Chen , USA  
M. Jamal Deen, Canada  
Prince Jain, India  
Jayshri Kulkarni, USA  
Arjuna Madanayake , USA  
Shibendu Mahata, India  
Shun Ohmi , Japan  
Susana Ortega-Cisneros , Mexico  
Ping-Feng Pai , Taiwan  
R. Palanisamy , India  
Jose R. C. Piqueira , Brazil  
Egidio Ragonese , Italy  
Gabriel Robins, USA  
Raj Senani , India  
Vincenzo Stornelli , Italy  
Ephraim Suhir, USA  
Hannu A. Tenhunen, Finland  
George S. Tombras , Greece  
Suman Lata Tripathi , India  
Gurvinder S. Virk , United Kingdom

## Communications

Islam Abdellah , USA  
Mominul Ahsan , United Kingdom  
Bhargav Appasani , India  
Nihal Areed , Egypt  
Shonak Bansal, India  
Francesco Benedetto , Italy  
Giulio Maria Bianco , Italy  
Yogesh Kumar Choukiker , India  
René Cumplido, Mexico  
Luca De Nardis , Italy  
Rajesh Khanna , India  
Kiseon Kim , Republic of Korea  
Tho Le-Ngoc , Canada  
Jit S. Mandeep , Malaysia  
Montse Najar , Spain

John N. Sahalos , Greece  
Vinod Sharma, India  
Kuei-Ping Shih , Taiwan  
Iickho Song , Republic of Korea  
Sangeetha Subbaraj , India  
Andrea Tani , Italy  
George Tsoulos , Greece  
Neng Ye , China

## Power Systems

Hadi Nabipour Afrouzi , Malaysia  
Ayman Al-Quraan , Jordan  
Mahendra Bhadu , India  
Antonio Bracale , Italy  
Vito Calderaro, Italy  
Vincenzo Di Dio , Italy  
Salvatore Favuzza , Italy  
Rajendra Kumar Khadanga , India  
Alessandro Lidozzi , Italy  
Giovanni Lutzemberger , Italy  
Sheila Mahapatra , India  
Luca Maresca , Italy  
Antonio J. Marques Cardoso , Portugal  
Fabio Massaro , Italy  
Daniele Menniti , Italy  
Manuela Minetti, Italy  
Dillip Mishra , USA  
Vitor Monteiro, Portugal  
Nicola Pasquino , Italy  
Luigi Piegari , Italy  
Renato Procopio , Italy  
Daniela Proto , Italy  
Michele Riccio , Italy  
Renato Rizzo , Italy  
Gulshan Sharma , South Africa  
Iouliia Skliarova , Portugal  
Jayesh Soni, USA  
Nicola Sorrentino , Italy  
Kusum Verma , India  
Chao Zhai , China

## Signal Processing







---

Raid Al-Nima , Iraq  
Aleksandar Dogandzic , USA  
Martin Haardt , Germany  
Jiri Jan, Czech Republic  
Ramash Kumar K , India  
Chi Chung Ko, Singapore  
James Lam , Hong Kong  
William Sandham, United Kingdom  
Ravi Sankar, USA  
Ari J. Visa, Finland  
Gongping Yang , China

## Contents

---

### **Energy Management Strategies for Smart Green MicroGrid Systems: A Systematic Literature Review**

Chaimaa Essayeh , Mohammed Raiss El-Fenni , Hamza Dahmouni , and Mohamed Aymane Ahajjam 

Review Article (21 pages), Article ID 6675975, Volume 2021 (2021)

### **Solar Photovoltaic Power Forecasting**

Abdelhakim El hendouzi  and Abdennaser Bourouhou

Review Article (21 pages), Article ID 8819925, Volume 2020 (2020)

### **Bus Voltage Stabilization Control of Photovoltaic DC Microgrid Based on Fuzzy-PI Dual-Mode Controller**

Yu Zhang , Shuhao Wei, Jin Wang, and Lieping Zhang 

Research Article (10 pages), Article ID 2683052, Volume 2020 (2020)

## Review Article

# Energy Management Strategies for Smart Green MicroGrid Systems: A Systematic Literature Review

Chaimaa Essayeh <sup>1</sup>, Mohammed Raiss El-Fenni <sup>1</sup>, Hamza Dahmouni <sup>1</sup>,  
and Mohamed Aymane Ahajjam <sup>2</sup>

<sup>1</sup>Department of Communication Systems, INPT, Madinat Al Irfane, Rabat, Morocco

<sup>2</sup>TICLab, International University of Rabat, Rabat, Morocco

Correspondence should be addressed to Chaimaa Essayeh; [chaimaa.essayeh@gmail.com](mailto:chaimaa.essayeh@gmail.com)

Received 2 November 2020; Revised 16 January 2021; Accepted 31 January 2021; Published 25 February 2021

Academic Editor: Anna Diva Plasencia Lotufo

Copyright © 2021 Chaimaa Essayeh et al. This is an open access article distributed under the Creative Commons Attribution License, which permits unrestricted use, distribution, and reproduction in any medium, provided the original work is properly cited.

Having neither precise definition nor a commonly accepted scope, the term “MicroGrid” tends to be used differently across researchers and practitioners alike. The management of energy usage within a microgrid is one of the topics that was handled from numerous perspectives. This study presents systematic literature review (SLR) of research on architectures and energy management techniques for microgrids, providing an aggregated up-to-date catalogue of solutions suggested by the scientific community. The SLR incorporated 45 papers selected according to inclusion/exclusion criteria and defined a priori. The selection process was based on an automated search and covered three known digital libraries. The extraction process covers three main questions. (i) The architectures of microgrids including their components, their bus configuration, and the adopted utility grid policy. (ii) The employed methods to ensure an optimal usage of energy under uncertainty. (iii) The confronted challenges and constraints of the suggested strategies. The findings of this SLR indicate a great diversity of methods and a rich background. Finally, the SLR suggests that future research should take into account the uncertainty aspect relating to energy management rather than the direct use of historical data as it is commonly done in most research papers. A sensitivity analysis should be provided in the latter case.

## 1. Introduction

The ever-increasing demand for electrical energy is a worldwide phenomenon which is the product of different changes happening across the nations. Coupled with a poor consumer awareness with regards to energy efficiency, the explosion in population growth and the wide spread and adoption of electronic devices in daily life are driving this trend to continue well beyond a couple of decades. This surge of demand imposes critical challenges facing grid utilities. Currently, the majority of electrical networks are relying on ageing infrastructures that restrict the performance of power delivery. As a result, the expansion of the grid proves to be complicated necessitating a radical transformation of the grid architecture and components. The installation of distributed generation units comes as an

alternative solution to fill the continually expanding gap between demand and supply.

The use of distributed supply points presents many benefits especially in term of energy loss. In fact, the closer the generation to the consumer is, the less energy loss it undergoes. However, at the same time, this alternative solution faces some challenges. A distributed energy network will require its monitoring unit to migrate from the old-fashion centralized strategy presented by a unique monitoring unit to a new decentralized strategy. This implies more implication of computer technology and infrastructure. On the contrary, fossil fuels remain the dominant sources for both centralized and distributed power generation. Such sources of energy are exhaustible and are going to disappear in the short future. With the rise of new green technologies such as



PV panels, wind turbines, and electrochemical batteries, new ways of generating and consuming energy emerge. It is considered that the integration of such clean distribution units can have many advantages to the electrical network. It can help mitigate climate change, alleviate load from the main utility grids, and avoid the blackout/brownout.

“MicroGrid” ( $\mu$  grid) is flowering in the scientific community as the future of the electrical grid. Although it has neither well standardized definition nor defined scope, there is a common agreement that the  $\mu$  grid is a small-scale energy network composed of loads and distributed energy resources. The integration of renewable energy resources (RER) puts more pressure on the monitoring units. In fact, the natural phenomena on which the RER rely are intermittent and the result is an unpredictable power supply. The fluctuations in the RER power output may cause network instability and yield to a demand-supply imbalance. Researchers suggested different methodologies to overcome these problems as well as to further advance green technologies incorporation. Particularly, managing energy within a  $\mu$  grid has been studied widely using a variety of techniques in various contexts.

This paper provides a current state of the art regarding the application of energy management strategies in  $\mu$  grids. The overview was performed following a defined methodology that is presented in Section 2. The results of the overview are divided into four parts and are presented in the remaining sections. The emphasize is first directed to the adopted architectures. We focus in this part on the common components that compose a  $\mu$  grid, the different modes of its operation, the policy of connecting a  $\mu$  grid to the main grid and the specifications associated with it, and finally the bus configurations that structure the connection of heterogeneous electric devices. In Section 3, we shed the light on the proposed methods presented in the research field to manage the energy usage in  $\mu$  grids. Attention is then paid to various algorithms and simulation tools that are utilized to put into practice the suggested methods. As aforementioned, an efficient energy usage in  $\mu$  grids faces many challenges and constraints. Those latter will be discussed in Section 5. The section that follows explains the limitation of our study and the difficulties that we encountered. Section 7 concludes the paper and opens on further suggestions.

## 2. The Review Process

The review process has been carried out, and the following steps are structured into three phases: planning, conducting, and documenting the review. Each phase involves several activities. In this section, we present how the review was planned and conducted. The planning phase includes the identification of the research questions and the development of the search process. Then, we proceed to the review conducting phase by selecting relevant studies and performing data extraction process.

TABLE 1: Search terms.

Facet	Search term
Microgrid	Microgrid
	Micro-grid
	Smart grid
	Smart building
Energy management	Energy balance
	Energy management
	Load balance
Optimization	Optimization
	Optimal

*2.1. The Research Questions.* The main objective of this study was to answer the following research question:

RQ: how do researchers and modellers tackle the problem of uncertainties of the RERs to ease their penetration in the future electrical grids?

The question was broken down into several “sub-questions” that will help us focus on many facets of the implementation of  $\mu$  grids.

RQ1: what are the suggested architectures of a  $\mu$  grid?

RQ2: what are the proposed methods for an efficient energy usage?

RQ3: what are the challenges faced and what constraints are commonly taken into consideration?

*2.2. The Search Process.* We searched the following three electronic databases:

(i) Elsevier Science Direct (<http://www.sciencedirect.com/>)

(ii) IEEEExplore (<http://www.ieeexplore.ieee.org/Xplore/>)

(iii) SpringerLink (<http://www.springerlink.com/>)

The search process was not evident to apply. The energy management in the  $\mu$  grid could take many forms. For instance, the term “energy management” could not figure in the elements searched (title, abstract, . . .) even if the paper tackles the subject. This could be load shifting, energy balance, state of charge management, energy scheduling, etc. Besides, for many studies, there is a mingling of the terms  $\mu$  grid, smart grid, and smart building. We were obliged to enlarge our research target in order to include any relevant study. Table 1 lists the different synonyms, abbreviations, and alternative spellings of each of the individual facets of the study. The search terms of each facet were gathered using a Boolean “OR” operator, while the different facet items were combined using the Boolean “AND” operator.

A first selection based on the search strategy cited above turned out to be nonrelevant since a huge number of papers were returned. Thus, the search process was done in an iterative way, following the best practices of the agile methods. In fact, the search process has been updated throughout the review conducting phase as to ensure the selection of the most relevant papers. The aforementioned lack of standards and specifications regarding the management of  $\mu$  grids has been very apparent during this study

selection. For Science Direct library only, we found 604 papers based on our first search. We were obliged to narrow the scope of our search by applying a supplementary filter on papers. The filter selects only the papers in which one of these terms: PV, wind, solar, or “renewable energy” figures, since our interest is more oriented on how researchers tackle the problem of the intermittent aspect of RERs. Table 2 gives the final command that was used for the study selection in every database.

Table 3 reflects the number of papers found in each library after applying the search command, but before proceeding to the selection, thus providing a general idea about the papers published in the field of energy usage management for  $\mu$  grids. With a growing yearly number of published papers in this topic, the research community’s interest is apparent.

**2.3. The Study Selection.** We restrict our study to the first 15 relevant papers of each database. The papers selected for the study were subject to the following inclusion/exclusion criteria.

Inclusion:

- (i) Only papers written in English were selected
- (ii) The paper, be it a primary or secondary study, must propose an energy management strategy for green  $\mu$  grids

Exclusion:

- (i) Papers considering the whole smart grid network since our study is more lenient towards a user-driven low voltage networks.
- (ii) Papers conducting research on the wireless micronetworks and communication.
- (iii) Papers that focus on the communication facet of  $\mu$  grids and optimize the communication energy among the network nodes.
- (iv) Papers proposing energy forecasting techniques relating to RERs such as wind turbine and PV panels without proposing an energy management for  $\mu$  grids.
- (v) Papers not including a type of a RER since the focus of the study is on *green*  $\mu$  grids.
- (vi) Papers not including a type of energy storage. The models we are interested in include a type of energy storage that will increase the autonomy of the system be it working under an on-grid mode, off-grid mode, or hybrid mode.
- (vii) Papers focusing on the charging/discharging scheduling of electric vehicles (EV) since their inclusion in  $\mu$  grids is beyond the scope of our SLR.

**2.4. The Data Extraction Process.** After the selection was made, we proceed to processing the selected papers and extracting specific pieces of information that will help us answer the defined research questions:

- (i) The components of the  $\mu$  grid, namely, the exploited RER, the storage, and the bus configuration
- (ii) The operational mode of the  $\mu$  grid, namely, on, off, and on/off modes
- (iii) The adopted pricing model of the utility for the grid-connected and the switched mode  $\mu$  grids
- (iv) The adopted policy of energy flow with the main grid when dealing with grid-connected and switched modes
- (v) The developed methods to overcome the problem of uncertainty and make an optimal usage of energy
- (vi) The challenges and the constraints of the suggested strategies

In the remaining sections, we cover the last phase of the SLR and answer the defined research questions.

### 3. RQ1: Architectures

In this section, we will focus on the electrical architectures proposed in the selected papers for  $\mu$  grid systems. Table 4 summarizes the first part of the findings of the review. We will focus as a first step on the different components that make up a  $\mu$  grid. Next, we will discuss the management of power flow between these components. Finally, we will differentiate between the various bus system configurations for green  $\mu$  grids.

We note that an efficient operation of a  $\mu$  grid depends not only on its electrical configuration but also on its communication architecture. In fact, the projection of a monitoring infrastructure onto the already existing power system is what made a  $\mu$  grid an actuality.

**3.1. Integration of RERs in  $\mu$  Grids.** RERs, also known as Renewable Energy Sources (RES) or nondispatchable sources, are the type of technologies that provide energy from renewable natural phenomena such as solar intensity, wind speed, waves, tides, and geothermal heat. They usually have low greenhouse gas emissions compared to their fossil fuels counter parts and thus are considered a prominent player in climate change mitigation. While some RERs are implemented in large-scale projects, others were found to be suitable for small-scale implementations such as  $\mu$  grids. The most implemented RERs in  $\mu$  grids are PV panels and wind turbines.

**3.1.1. PV-Based Systems.** Recently, there has been a dramatic fall of PV panels’ prices in the market. Coupled with other advantageous aspects (e.g., high conversion efficiency, light weight, and possibility of installation in the most unconventional conditions), PV panels became the most popular type of renewable energy to be implemented in a  $\mu$  grid scale.

Generally, PV panels installed on rooftops convert solar irradiance into electric energy. The paper [14] introduces a new idea of hybrid PV thermal systems (PVT) producing either thermal or electrical energy. The thermal energy production can be used for heating water or air and

TABLE 2: Search commands.

Database	Search command
Science Direct	Title, abstract, and keywords: (microgrid OR micro-grid OR “smart building” OR “smart grid”) AND (“energy management” OR “energy balance” OR “load balance”) AND (optimal OR optimization) Find articles with these terms: (PV OR wind OR solar OR “renewable energy”) AND storage Years: 2015–2018
IEEEExplore and SpringerLink	(“Smart grid” OR microgrid OR micro-grid OR “smart building”) AND (“energy management” OR “energy scheduling” OR “load balance” OR “energy balance”) AND (optimal OR optimization) AND (PV OR wind OR solar OR “renewable energy”) AND storage Years: 2015–2018

TABLE 3: Number of papers’ result of the search command.

	2015	2016	2017	2018	Total
ScienceDirect	50	64	89	114	317
IEEEExpore	865	1104	1336	1858	5163
SpringerLink	159	170	271	423	1023
Total	1074	1338	1696	2395	6503

supplying thermal energy for domestic use. This implementation increases the efficiency of the system since the process of providing thermal energy passes through one step conversion (i.e., conversion to thermal energy) instead of passing through a two-step conversion (i.e., conversion to electric energy and then to thermal energy), saving losses related to the conversion process. Authors in [4] exploited a new potential of PV systems and studied the PV installation on facades.

Different equations were used to calculate the PV power output. The equation below is given in [1, 9], incorporating all important parameters that impact the PV output such as the temperature and the solar radiation:

$$P_{PV} = P_{PV}^{nom} \times \frac{G}{G_{ref}} \times \left[ 1 + K \times \left( T_{amb} + \left( \frac{NOCT - 20}{800} G \right) - T_{ref} \right) \right], \quad (1)$$

where (i)  $P_{PV}^{nom}$ : nominal power of PV at standard test conditions, (ii)  $G$ : solar radiation ( $W/m^2$ ), (iii)  $G_{ref} = 1 kW/m^2$ : reference solar radiation, (iii)  $K$ :

temperature coefficient of power, (iv)  $T_{amb}$ : ambient temperature, (v)  $T_{ref} = 25^\circ C$ : reference temperature at standard conditions, and (vi) NOCT: nominal operation temperature.

Some papers (e.g., [6, 22]) neglect the term  $((NOCT - 20)/800)G$  to give a simpler equation. Other simplified expressions for the output can be found in [6, 7, 32]. A detailed expression is presented in [14]. These equations showcase the relationship between the output with manufacturing parameters (e.g., short-circuit current  $I_{sc}$ , open-circuit voltage  $V_{oc}$ , the maximum points of voltage  $V_{mpp}$ , and current  $I_{mpp}$ ) as well with weather parameters (i.e., temperature and irradiance).

**3.1.2. WT-Based Systems.** For relatively large  $\mu$  grids, PV panels can be combined with wind sourced energy. This technology is very suitable for rural areas and isolated regions since it allows to compensate the lack of PV output in cloudy periods. The WT power output depends on the wind speed as

$$P_{WT} = \begin{cases} 0, & V_{WT} < V_{cut-in}, V_{WT} > V_{cut-out}, \\ P_{WT}^{nom} \times \left( \frac{V_{WT}^3}{V_{nom}^3 - V_{cut-in}^3} - \frac{V_{cut-in}^3}{V_{nom}^3 - V_{cut-in}^3} \right), & V_{cut-in} \leq V_{WT} < V_{nom}, \\ P_{WT}^{nom}, & V_{nom} \leq V_{WT} < V_{cut-out}, \end{cases} \quad (2)$$

where (i)  $V_{WT}$ : wind speed, (ii)  $V_{nom}$ : nominal wind speed, (iii)  $P_{WT}^{nom}$ : nominal power of the WT, (iv)  $V_{cut-in}$ : cut-in wind speed, and (v)  $V_{cut-out}$ : cut-out wind speed.

This equation is used in [1, 9, 22, 42]. Other expressions, namely, equation (3), integrate power coefficients and air

density and are given in [11, 32, 36, 43]. A more detailed expression is presented in [36, 43]:

$$P_{WT} = \frac{\rho}{2} \times A \times C_p(\lambda, \beta) \times V_{WT}^3, \quad (3)$$



TABLE 4: Suggested architectures.

Ref	ON/OFF	Utility pricing	RER	DER	Injection	ESS	Injection
[1]	OFF	—	PV WT	DG	—	BESS	—
[2]	ON	Dynamic pricing	PV	—	Y	BESS	Y
[3]	OFF	—	PV WT	—	—	BESS (lead-acid)	—
[4]	ON	Dynamic pricing	PV	—	Y	BESS (Li-ion)	Y
[5]	ON/OFF	—	PV	DG	Y	BESS (lead-acid)	—
[6]	OFF	—	PV	Fuel cell	—	BESS (Li-ion), hydrogen	—
[7]	ON	TOU	PV	—	Y	BESS	N
[8]	ON	Dynamic pricing	PV	—	Y	Ice storage	N
[9]	OFF	—	PV WT	—	—	Pump ESS	—
[10]	ON	—	PV	—	Y	BESS	Y
[11]	OFF	—	PV WT MHP	BMG	—	BESS	—
[12]	OFF	—	PV	DG	—	BESS	—
[13]	OFF	—	PV	GT	—	BESS (lead-acid)	—
[14]	ON	RTP	PV WT	MT FC	Y	BESS	Y
[15]	ON	Flat	PV	CHP	Y	BESS (Li-ion), thermal storage	N
[16]	ON	Dynamic pricing	PV WT	—	Y	BESS	Y
[17]	ON	—	PV WT	—	—	BESS	—
[18]	ON	Dynamic pricing	PV WT	—	N	BESS	N
[19]	ON	Quadratic	RER	—	N	ESS	N
[20]	ON	Time-varying linear function	RER	—	N	ESS	N
[21]	OFF	—	PV WT	DG MT	—	BESS (VRB), supercapacitor	—
[22]	OFF	—	PV WT	DG	—	BESS (Li-ion)	—
[23]	ON	TOU	PV	—	N	BESS (Li-ion)	N
[24]	OFF	—	PV	—	—	BESS	—
[25]	OFF	—	PV WT	DG	—	BESS, hydro-pumped storage	—
[26]	ON	Dynamic pricing	PV WT	—	N	ESS	N
[27]	ON	Dynamic pricing	PV	—	Y	BESS	Y
[28]	ON/OFF	Dynamic pricing	PV WT	DG	Y	BESS	Y
[29]	OFF	—	PV WT	MT	—	BESS	—
[30]	ON/OFF	TOU	PV	—	Y	BESS	—
[31]	ON/OFF	Dynamic pricing	PV WT	DG	Y	BESS (VRB, Li-ion), supercapacitor	—
[32]	ON	TOU	PV WT	DG, FC, MT	Y	BESS	N
[33]	ON	—	PV WT	—	N	BESS	N
[34]	ON	TOU	PV WT	—	Y	BESS (lead-acid)	N
[35]	ON	Dynamic pricing	PV WT	—	—	BESS	—
[36]	OFF	—	PV WT	FC	—	BESS	—
[37]	ON	Flat price	PV	—	Y	BESS	N
[38]	ON/OFF	Dynamic pricing	PV	DG	Y	BESS	N
[39]	OFF	—	PV WT	DG	—	BESS (Li-ion)	—
[40]	ON	TOU	PV	MT, BMG	Y	BESS, thermal storage	—
[41]	ON	RTP	PV WT	MT, FC	Y	BESS	—
[42]	ON	Auction price	PV WT	—	Y	Pumped storage	—
[43]	OFF	—	PV	DG	—	BESS	—
[44]	ON	TOU	RER	—	Y	ESS	Y
[45]	ON	TOU	PV	—	Y	BESS (Li-ion)	N

where  $\rho$  is the air density,  $A$  is the swept area of the blade, and  $C_p$  is the power coefficient that depends on the pitch angle  $\beta$  and the tip speed ratio  $\lambda$ .

**3.1.3. Micro-Hydropower System (MHP).** A MHP system transforms the energy of flowing water into electrical energy. A turbine, a pump, or a waterwheel is used to convert the flowing power into rotational energy. The latter is then converted into electrical energy using a generator. The authors in [11] compute the power output of the MHP system using

$$P_{\text{MHP}} = \frac{9.8 \times H_{\text{net}} \times \eta_{\text{MHP}} \times \rho_w \times Z}{1000}, \quad (4)$$

where  $H_{\text{net}}$ : net head,  $\eta_{\text{MHP}}$ : efficiency of the MHP system,  $\rho_w$ : water density, and  $Z$ : available discharge.

**3.2. Conventional Energy Resources.** The conventional energy resources or the dispatchable energy resources are small-scale energy generators relying on a specific type of fuel. Usually, they are used as a backup energy supply to overcome outage power events or as control sources to regulate frequency and voltage deviations. Common

examples of conventional energy resources include natural gas turbines [13], microturbines [14], combustion turbines, biomass generators, and distributed generators.

**3.2.1. Biomass Gasifier (BMG) System.** The BMG systems are energy systems that rely on biomass as a fuel source to generate power or heat. Several biomass materials can be used, such as wood chips, animal waste, farm waste, and paper waste. Equation (5) from [11] calculates the power output of a BMG system:

$$P_{\text{BMG}} = \frac{Av \times CV_{\text{BMG}} \times \eta_{\text{BMG}} \times 1000}{365 \times 860 \times \text{Op}} \quad (5)$$

where  $Av$  is the biomass availability (tons/year),  $CV_{\text{BMG}}$  is the system's calorific value,  $\eta_{\text{BMG}}$  is the overall conversion efficiency from biomass to electricity, and  $\text{Op}$  is the operating hours per day.

The burning of biomass generates a significant amount of carbon dioxide, but it has less environmental impact than fossil fuels which is already included in the natural cycle of the biomass. BMG systems are then considered to be "cleaner" than the fossil fuel systems, but less "cleaner" than the RERs.

**3.2.2. Distributed Generators (DGs).** DGs convert the mechanical power into electric power. They consist of an engine that drives motors operating with gasoline, diesel [1, 27], natural gas, propane [39], etc. The most known DGs are diesel generators.

$P_{\text{DG}}$ , the output power of DGs in [22], is assumed to be proportional to the fuel consumption  $\varrho_{\text{DG}}$  with a coefficient of proportionality  $a_{\text{DG}}$  (i.e., fuel consumption coefficients):

$$\varrho_{\text{DG}}(t) = a_{\text{DG}} P_{\text{DG}}(t) \quad (6)$$

**3.2.3. Fuel Cells.** Fuel cells are another type of energy converters. These electrochemical cells transform the chemical energy of the fuel into electricity. There are five major types of fuel cells generally available in the market: alkaline fuel cell (AFC), phosphoric acid fuel cell (PAFC), molten carbonate fuel cell (MCFC), solid oxide fuel cell (SOFC), and proton exchange membrane fuel cell (PEMFC) [43].

In [1], the relation between  $P_{\text{FC}}$ , the output power of FC, and  $\varrho_{\text{FC}}$ , the consumption of fuel, is given by

$$\varrho_{\text{FC}} = a_{\text{FC}} P_{\text{FC}} + b_{\text{FC}} P_{\text{FC}}^{\text{nom}} \quad (7)$$

where  $a_{\text{FC}}$  and  $b_{\text{FC}}$  are coefficients of fuel consumption. A similar equation is given in [40]. A detailed formula for calculating the output voltage of a fuel cell is given in [36]. The expression includes among other parameters: the universal gas constant (8.3145 J/(mol·K)), the Faraday constant (96485 A s/mol), the number of moving electrons, the charge transfer coefficient, the operating temperature (K), the partial pressure of hydrogen inside the stack (atm), and the partial pressure of oxygen inside the stack (atm).

**3.3. Energy Storage System (ESS) Integration.** Electrical energy cannot be stored in the way it is generated. The ESSs are technologies that allow us to store another type of energy such as chemical energy or mechanical energy and convert it into electrical energy when needed. There is a large variety of ESSs in the market. These include electrochemical battery, super-capacitor, compressed air energy storage, and flywheel energy storage. When the  $\mu$  grid is working as a standalone system, the main roles of an ESS are ensuring a continuous energy supply as well as stabilizing the DC bus voltage. When connected to the grid, the ESS (especially the battery) works in coordination with the other elements of the  $\mu$  grid to meet its objectives as well be defined in Section 5.1.

The authors in [46] give a comprehensive overview of different ESSs and their roles when integrated in  $\mu$  grids. Their technical roles and functions include the following: grid voltage and frequency support, grid angular (transient) stability, load levelling/peak shaving, spinning reserve, imbalanced load compensation, power quality, and reliability improvement.

There is a huge tendency in the  $\mu$  grid research field that considers the battery of electric vehicles (EV) as an ESS and integrates it in the energy management policy; such systems can be the sole subject of another review. In fact, when an EV is present, its stored energy can be consumed in the system. Although, this can introduce additional constraints in the system (i.e., EV battery should be fully charged at some predefined periods).

**3.3.1. Battery Energy Storage Systems (BESSs).** Batteries are the common solution for energy storage in a  $\mu$  grid scale. Their price is still not very affordable for household economy. Besides, the rigorous maintenance this type of ESS needs (e.g., requiring a dry and cool place and huge volume) does not encourage customers to adopt it as a solution. Still, it is the best choice compared with the aforementioned ESS solutions. When the type of battery is mentioned, it is either lead-acid or lithium-ion. The latter is getting more and more popular thanks to its high efficiency rate, its extended lifetime, and its deep depth of discharge (DoD).

The charging/discharging equation of a battery is as follows:

$$SE(t + \Delta t) = SE(t) \times (1 - \delta) + \left[ \eta_{\text{char}} \times \beta_{\text{char}} - \frac{\beta_{\text{dis}}}{\eta_{\text{dis}}} \right] \times \Delta t \quad (8)$$

With  $\delta$  is the self-discharging rate,  $\eta_{\text{char}}$  and  $\eta_{\text{dis}}$  are, respectively, the charging and discharging efficiencies,  $\beta_{\text{char}}$  and  $\beta_{\text{dis}}$  are, respectively, the charging and discharging rates, and  $\Delta t$  is the time step. Some assumptions could be made to simplify the equation:

- (i) Neglect the self discharging rate (0.002)
- (ii) Take  $\Delta t$  equal to one hour
- (iii) Take  $\eta_{\text{char}} = \eta_{\text{dis}}$
- (iv) Consider that the battery is either charging or discharging at a single time step

This will lead to

$$SE(t+1) = \begin{cases} SE(t) + \eta \times \beta_{\text{char}}, & \text{charging mode,} \\ SE(t) - \frac{\beta_{\text{dis}}}{\eta}, & \text{discharging mode.} \end{cases} \quad (9)$$

**3.3.2. Other ESSs.** In [15], a thermal storage is used as a buffer storage. The authors in [9] used a pumped-storage plant under two operation modes: a pump mode and a discharge mode. They developed the water to power conversion equation and set the constraints related to the operation of the pump storage. In [8], the authors integrate an ice storage model for which the mathematical modelling is described in [47].

**3.4. ON/OFF Modes of Operation.** There are three types of  $\mu$  grid operation: off-grid, on-grid, and on/off-grid. The off-grid mode, also known as stand-alone power system (SAPS), is an isolated mode or islanded mode. In this mode, the  $\mu$  grid works autonomously without being connected to the utility grid. This mode of operation is very common in rural areas or in regions with harsh geographical conditions. The use of an ESS is very crucial since they store the energy during the period of peak production (i.e., when the generation exceeds the load demand, use it when the local generation becomes insufficient). A backup supply is also a plus in off-grid implementations since it will support the load in the worst case scenarios. Consequently, a precise design should be done to define the capacity of the local resources as well as the capacity of the ESS to ensure a good functioning of such systems and to avoid power outage.

When a  $\mu$  grid is connected to the utility grid, we say that it is working under on-grid mode, connected mode, or grid-tied mode. This mode is widely used in homes and businesses or any building located in zones supported by a utility grid company. The first version of this mode describes only DER with no ESS. Thus, any generated energy excess was exported to the grid for which the customer gets paid with a feed-in-tariff; any deficiency is supported by the utility grid. The significant drop in the price of ESS, especially batteries, encouraged their integration in such  $\mu$  grids. This helps the  $\mu$  grid to get the best of both worlds. The ESS is charged from the excess and discharged when needed. The utility acts as a backup supply providing the  $\mu$  grid with energy when both generated and stored energy fail to fulfill the demand. With this type of operation, ESS is able to be charged from the utility during off-peak periods. The option of exporting the generated excess to the grid or charging the ESS from the grid will be further detailed in Section 3.5.

The last mode of operation is the on/off-grid mode. This mode is very similar to the on-grid mode with the only additional feature of being able to disconnect from the utility grid upon request. Generally, this type of  $\mu$  grids works under an on-grid mode. When a fault occurs in the utility grid, the system switches to the off-grid mode in which it has

to work autonomously and rely basically on the local resources. Similar to an off-grid  $\mu$  grid, this system needs a good sizing to calculate the capacity of its components in order to ensure their operation under the partial autonomous mode. A basic layout scheme of the different modes of operation is shown in Figure 1.

**3.5. Energy Exchange Policy with the Grid.** The bidirectional flow of energy is only available for the on-grid or on/off-grid modes. From the 30 papers that suggested the on-grid mode, 22 papers used the bidirectional flow of energy as a valid option for the operation of the  $\mu$  grid. Nevertheless, the possibility of exporting the local generated energy to the grid is not legally approved in many countries. In fact, the structure of the electrical grid that is currently implemented in almost all countries has a hierarchical aspect. At the highest level, we have the power plants where the energy is generated and transmitted to the high voltage (HV) stations, also called transmission networks; then, it passes through the medium voltage (MV) stations (or distribution networks) to the low voltage (LV) networks, from where it is delivered to consumers. As it is illustrated in Figure 2, the connection between different levels of power voltage is done via transformers. The traditional type of transformers has a limited performance preventing the bidirectional flow of energy, particularly from a lower to a higher level. Upgrading this equipment (and others) turns out to be very costly, and many utility companies around the world are not ready yet to take this step, as long as there is no incentive from the governmental institutions. Countries allowing the injection of energy into the public grid define a grid export limit. In Australia, for example, export is limited to 10 kW. This limit is imposed to avoid signal disturbances occurring in transmission lines. The  $\mu$  grid inverters must accurately respect the voltage and the frequency of the public grid, which are generally 240 V at 50 Hz or 120 V at 60 Hz. Yet, from all the papers that allow the bidirectional flow of energy, only a few touched on the bound on the energy to be exported to the grid [16, 21, 27, 31, 38]. On the contrary, the export limit puts more constraint on the size of the  $\mu$  grid system. Thus, the customer should make good decisions concerning the capacity of the implemented system in order to increase its return on investment and reduce the power waste.

The exchange of energy between the ESS and the utility grid is less common. Papers that allow the ESS to be charged from the utility grid are few; the ones that allow both charging and discharging from/to the grid are even fewer [2, 4, 10, 28]. As a general case, the ESS is implemented to improve the reliability of the system and increase its autonomy. As a matter of fact, it is more common to see ESSs only charging from the excess of the local generated energy and discharging when needed by the customer.

**3.5.1. Utility Pricing.** The utility companies can adopt a static pricing or a dynamic pricing. In the former, the price is flat and does not change with time or demand.



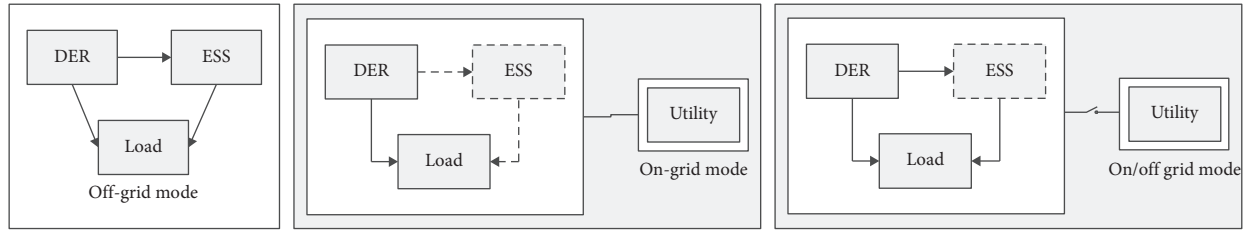


FIGURE 1: Modes of operation.

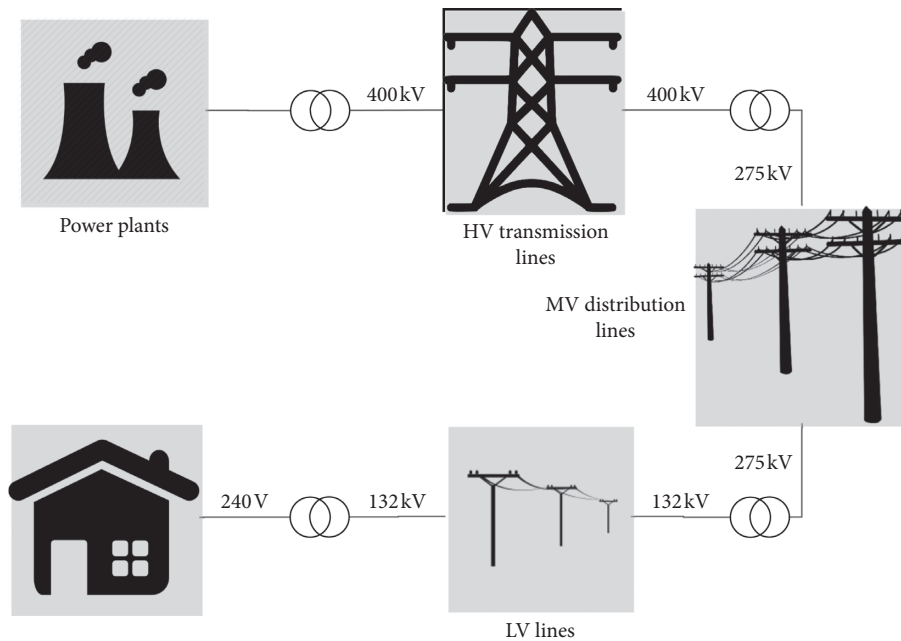


FIGURE 2: Example of a general structure of the public grid.

While in the latter, the price is not fixed and can change depending on several parameters such as the quantity of requested energy, the time of the day, and the period of the year. The static pricing is beneficial to neither the customer nor the supplier. In fact, during the peak periods (e.g., in early evening), the utilities are often obliged to activate “peak-plants” to catch up to the high demand of energy in this period. This type of plant is very costly and the solution proves to be inefficient. Therefore, to compensate the extra cost of activating the “peak plants,” the company splits the cost evenly on the whole period of the day. And, this means that a customer who is running the washing machine or the dryer at 10 am is then overpaying the cost of energy they consume. The idea of a dynamic pricing model to incentive customers is to shift/reduce their energy consumption from peak periods by rewarding them with lower prices for doing so.

Dynamic pricing models have been recently adopted by electricity companies not only for the benefits they provide but also because this was mandated by the governmental legislatures in some regions. Authors in [48] present an analysis of dynamic pricing in electricity grids and investigate the issues facing the integration of such pricing models in the energy market. They also listed the different existing

models of dynamic pricing. Almost all the selected papers for this study stated that they have adopted a dynamic pricing for the energy drawn from the utility, but they do not provide the model used. When mentioned, the model of dynamic pricing is TOUP (Time-Of-Use Price) or RTP (Real Time Pricing). TOUP determines two or three levels of energy prices; each level for a certain period of the day. The price levels are predetermined and can be changed only once or twice a year (i.e., summer period TOUP and winter period TOUP). In RTP, instead of predetermining the price levels, the exact price value for each period is calculated and announced to the user only at the beginning of the trading slot.

**3.5.2. Feed-in-Tariff (FiT).** The FiT is the pricing policy created to promote investments in RERs. It is adopted by countries that encouraged the penetration of RERs in their power systems. The first FiT was introduced in the US during the late 1970s, and by the end of 2010, it has been enacted in 50 countries from which we cite Algeria, Germany, Iran, and Australia. The FiT provides a long-term agreement between the RER users and electricity companies and defines the price that the customer gets paid for injecting energy into the grid and the limit of quantity to be injected.

**3.6. Bus Configuration.** RERs as well as batteries provide direct current (DC) energy. Most of the distributed generators supply alternating current (AC). The load is composed of both appliances that have to be fed by AC, such as washing machines and refrigerators, and others by DC, such as lighting and battery-powered devices. Therefore, many suggestions focusing on bus configuration for green  $\mu$  grids exist in the literature.

The traditional method is the centralized DC bus configuration. It is very common especially in the implementation of isolated (off-grid) architectures. Figure 3 gives a general scheme of such configurations. The system is connected by a central DC bus to which the AC components are connected via AC/DC inverters. Several papers in the selection adapted this type of configuration, e.g., [2, 6, 17, 22, 24, 27]. They justify their choice by stating that the DC configuration has more efficiency, less cost, less occupied space, lower lifetime cost, and high reliability [34]. Besides, implementing a DC configuration helps avoiding the frequency violation problem since only voltage stabilization is dealt with. However, this method presents several drawbacks. In fact, in a DC coupled system, the battery inverter is responsible for delivering the power. During the generated peak energy, the capacity of resources surpasses the capacity of the battery, resulting in a loss of the generated energy and limiting the performance of the system.

The centralized AC bus configuration shown in Figure 4 is a relatively more recent innovation. It provides an AC medium to govern the interactions between different components. The DC components are connected to the AC main bus through DC/AC converters or inverters. For example, in such configurations, the PV panels are connected to the AC bus through an AC inverter, and the batteries are either connected via a bidirectional converter or paralleled inverter and rectifier. The centralized AC configurations work under a higher operating voltage which results in fewer losses in wire cables. Moreover, unlike the DC configurations, the RERs can provide directly the power to home appliances. This enhances the expected lifetime of the battery by reducing its charge/discharge cycles and leads to a better exploitation of the RER. Nevertheless, this configuration requires additional safety measures (e.g., frequency stabilization) in addition to having a slightly higher installation cost than that of DC coupled systems. Compared to this latter, only fewer papers have adopted the AC configuration (i.e., [16, 21, 25, 43]).

The last and the newest configuration is a hybrid DC-AC coupling bus configuration (Cf. [1, 5, 10, 11, 23, 26]). This bus configuration contains two main buses: an AC bus connecting the AC components and a DC bus connecting the DC components, as shown in Figure 5. The two buses are connected to each other via a bidirectional inverter. This configuration has the advantage of benefiting from both previous configurations. It necessitates minimum conversion requirements and reduced power converters, since every component is connected to either the DC or the AC bus, depending on its technical functioning, leading to a reduced system cost. Yet, such

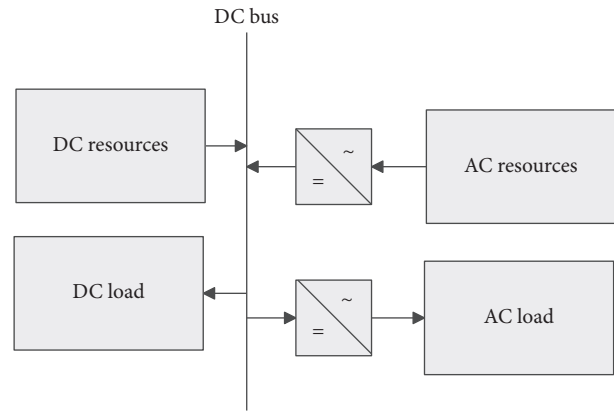


FIGURE 3: Centralized DC bus configuration.

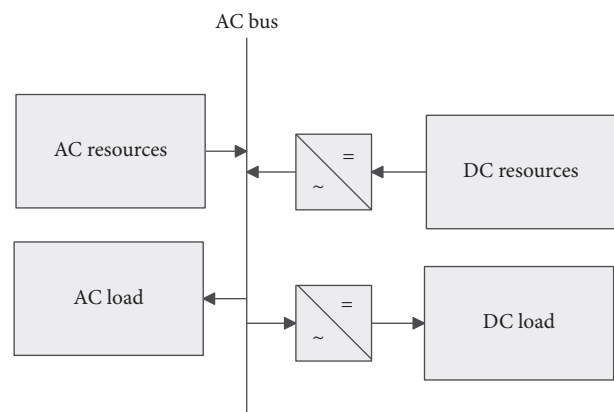


FIGURE 4: Centralized AC bus configuration.

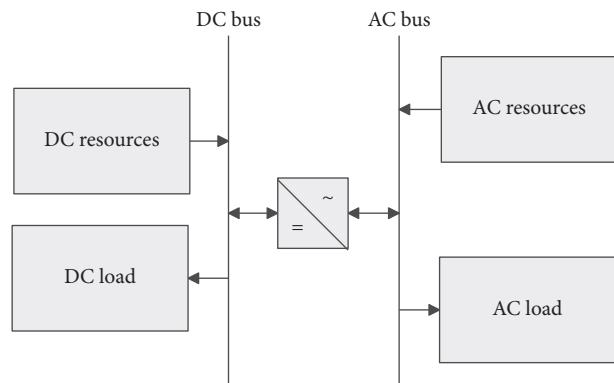


FIGURE 5: Hybrid AC/DC bus configuration.

configuration requires more coordination between DC and AC buses in terms of control strategy. In fact, coordinated bus voltage (and frequency) operations need to be considered.

In search of the most efficient configurations, many researchers conducted comparative studies of the different configurations. In [49], for instance, they deduced that hybrid AC/DC coupled systems offer some compelling advantages compared to other configurations. The system that underwent the study was composed of a genset, PV

array, and a battery. Another study [50] concluded that the hybrid coupled AC/DC is beneficial in all the investigated scenarios.

#### 4. RQ2: Methods

The major grid imbalances causing instability are frequency deviations, overloads, loss of synchronism, and voltage collapses [51]. As mentioned before, the system has to work with a 240 V at 50 Hz or with 120 V at 60 Hz. Any deviation from the specified range of voltage/frequency operation will lead to system instability. The synchronism is lost when there is a phase shift in the signal angles, while overloads occur when there is an imbalance between the supply and the demand. Energy management strategies address the problem of overloads by ensuring a continuous energy balance within the system, while control strategies address the rest of the imbalances and propose some adjustment mechanisms to frequency and voltage.

The second part of the findings are listed in Table 5, outlining the different strategies employed in prior studies.

*4.1. Control Strategies.* It is challenging for systems integrating RERs to provide reliable and stable power to load demand. On the one hand, the intermittent characteristic of RERs may cause some fluctuations in the power they generate. On the other hand, RERs generate low power compared to the conventional sources. Control strategies (CS) aim to address these types of problems; their main role is to ensure a coordinated control of multiple sources and avoid network violations through controlling variables such as voltage, current, and frequency. The architecture (i.e., bus configuration and mode of operation) determines the tasks that should be handled by a CS. In fact, under a DC-bus configuration [17], only one component needs to be stabilized which is the DC power. In this case, the source providing a stable voltage output operates in a voltage-controlled mode to regulate the DC bus voltage, while the other sources operate in the current-controlled mode. In the case of an AC-bus configuration, the adopted control scheme depends on whether the  $\mu$  grid is isolated or grid-connected. In fact, if it was isolated, four components should be taken into account, namely, voltage, frequency, and active and reactive powers. Indeed, voltage and frequency are controlled through the  $V/f$  control scheme that is implemented in the AC inverter to avoid related violations; while the other nodes operate under the PQ control scheme regulating the active and reactive powers. If the  $\mu$  grid was connected to the main grid, this latter takes charge of voltage and frequency regulation. Thus, only two components are left to the  $\mu$  grid to control which are active and reactive powers. They are implemented in nodes using either a PQ or a PV control scheme [52]. Flowchart in Figure 6 summarizes the different control schemes adopted by different  $\mu$  grid configurations. We note that the most employed schemes are the PQ control scheme to regulate the active/reactive powers and the  $V/f$  control scheme to stabilize the voltage and frequency violations.

*4.1.1. The  $V/f$  Control Scheme.* The  $V/f$  control ensures that the output voltage is proportional to the nominal frequency. The voltage control maintains the nominal voltage amplitude by adjusting the reactive output of the  $\mu$  grid. Similarly, the frequency control keeps the system working under the nominal frequency (e.g., 50 Hz) by adjusting the active output of the system. The two equations of a  $V/f$  control are shown below:

$$\begin{aligned} V_i &= V_i^* - m(Q_i - Q_i^*), \\ f_i &= f_i^* - n(P_i - P_i^*), \end{aligned} \quad (10)$$

where  $V_i$ ,  $f_i$ ,  $P_i$ , and  $Q_i$  are the voltage amplitude, frequency, and active and reactive powers relative to the input electrical signal, while  $V_i^*$ ,  $f_i^*$ ,  $P_i^*$  and  $Q_i^*$  are their references.  $m$  and  $n$  are the drop amplitude and frequency coefficients.

*4.1.2. PQ Control Scheme.* The PQ control ensures that the active power  $P$  and the reactive power  $Q$  are regulated to remain fairly constant. In fact, when connected to the grid, voltage and frequency stability of an AC  $\mu$  grid is handled by the main grid. While this keeps voltage amplitude and frequency varying within their allowable range, the PQ control scheme ensures that the active and reactive outputs remain unchanged. In addition of being implemented in connected  $\mu$  grids, the PQ control scheme is also applied by slave nodes in the isolated mode.

The control technique widely used in the literature to implement control schemes is Pulse Width Modulation (PWM) technique, which can be implemented via a PI controller [10, 19, 52]. Authors in [52] give a comprehensive review on the application of different control strategies in both on- and off-grid modes of operation. To ensure  $\mu$  grid stability, the control strategy is sometimes associated to a load management strategy, mainly a load shedding strategy. In [24, 43], for instance, the authors resorted to the latter strategy to keep voltage amplitude and frequency working under their predefined limits.

*4.2. Energy Management Strategies.* Energy strategy or energy management strategy is an umbrella term. It is widely known and used in utility companies and industrial settings. We can define the energy management strategy as the scheduling and the exploitation of different resources including RERs to handle the customer's demand load. Nevertheless, with the emergence of the  $\mu$  grid concept, energy management started gaining interest in residential setting as well, and it was coined *home energy management strategy* (HEMS). From hereafter, we refer to this as EM strategy.

$\mu$  grid systems incorporate one or more types of RERs, which raises several challenges due to their stochastic nature. Therefore, the task of energy balance between production and consumption becomes less evident to achieve. To tackle these problems, researchers focus their efforts to find opportunities that save energy and reduce routine energy waste while keeping track of the system's unpredictability.

TABLE 5: Energy management strategies.

Ref	Method	Objectives	Constraints	Algorithm	Simulation tool
[1]	Sizing	Min COE, max reliability	RF, BESS constraints	MOSaDE	—
[2]	EM	Min COE	Thermal limit violation, voltage stabilization, BESS constraints	GA + DSM	CEPLEX Matlab
[3]	Sizing	Min loss, max reliability	BESS constraints	Myopic	Matlab
[4]	Sizing	Ensure balance	—	Myopic	PVsys, Crmsolar
[5]	Sizing	Min NPC, min COE, min CO <sub>2</sub>	RF	(GAMS)	HOMER
[6]	EM	Max reliability, min loss, max lifetime	BESS, FC, hydrogen technical constraints	MPC + DSM	—
[7]	EM	Min COE	BESS, utility technical constraints	MPC	—
[8]	EM	Min peak demand	User comfort	Myopic + DSM	EnergyPlus
[9]	EM	Min operation cost	ESS, network and security constraints, user comfort	GAMS	SBB solver
[10]	CS + EM	—	BESS, utility technical constraints	Myopic	Matlab
[11]	EM	Min NPC	Reliability, BESS and generation constraints, excess of RER	Myopic + DSM	HOMER
[12]	EM	Min mismatch cost	BESS, generation and load constraints	Built algorithms	—
[13]	EM	Min operation cost, max reliability	BESS, generation and load constraints	MILP	SimplexLP
[14]	EM	Min operation cost	BESS and generation constraints	Backtracking search optimization algorithm (BSO)	—
[15]	EM	Min operation cost, max reliability	ESS constraints	MPC + rule-based control	Pyomo (CPLEX)
[16]	EM	Min cash flow, min CO <sub>2</sub> , max reliability	BESS and network constraints	Branch & bound	Matlab
[17]	CS	Network stabilization	Voltage stabilization	Time rate multiple pulse width modulation (TRM-PWM)	Matlab/ Simulink
[18]	EM	Min COE	Energy balance	PSO	Matlab
[19]	EM	Min COE	ESS constraints	Sliding-window-based sequential optimization	—
[20]	EM	Min COE	ESS and network constraints	Store-then-cooperate/cooperate-then-store	—
[21]	EM	Min COE, max reliability	BESS and generation constraints	MPSO	Matlab/ Simulink
[22]	EM	Min NPC, max reliability	BESS and generation constraints	Myopic	Matlab
[23]	EM	Min O&M cost, max reliability	BESS constraints	PSO	Matlab
[24]	CS	Voltage stabilization	BESS constraints	Myopic	PSCAD/ EMTDC
[25]	Sizing	Min annual cost, min CO <sub>2</sub>	BESS and generation constraints, reliability	Branch & cut	Matlab
[26]	Sizing	Min investment cost, min expected operation cost	Budget	—	—
[26]	EM	Min operation cost	BESS and load constraints, user comfort	Built algorithm	—
[27]	EM	Min cash flow, max reliability	BESS constraints	Belleman dynamic programming	—
[28]	EM	Min operation cost	BESS constraints, voltage stabilization, user comfort	Predictor corrector proximal multiplier (PCPM)	—
[29]	EM	—	—	Auction theory	—
[30]	EM	Min COE	BESS and generation constraints, islanding constraint, peak shaving constraint	Linear programming	MATlab CPLEX
[31]	EM	Min COE	BESS and generation constraints	regPSO	—
[32]	EM	Min operation cost, min PAR	BESS constraints	Ant colony	—
[33]	EM	Min operation cost	BESS constraints	Artificial neural network + linear programming	Matlab
[34]	EM	Min operation cost, min emissions (CO <sub>2</sub> , NO <sub>x</sub> , SO <sub>2</sub> )	BESS and generation constraints	Fuzzy-logic	Matlab/ Simulink

TABLE 5: Continued.

Ref	Method	Objectives	Constraints	Algorithm	Simulation tool
[35]	EM	Min cost, min emissions	BESS and generation constraints, user comfort	Myopic + shedding	Arduino/JADE
[36]	EM	Energy balance	BESS and generation constraints	Myopic + shedding	Matlab/Simulink
[37]	EM	Min COE, min mismatch cost	BESS, generation and load constraints, user comfort	Myopic + shedding	Matlab
[38]	EM	Min operation cost, min mismatch cost, max profit	BESS, generation, network constraints	Column-&- constraint generation algorithm (C& CG)	C++ (CPLEX)
[39]	Sizing EM	Min lifetime cost Min operation cost	BESS constraints BESS, generation and load constraints	Myopic shedding + shifting	Matlab —
[40]	EM	Min COE	Cooling/heating balances, electricity balances operational constraints	Piecewise linear robust MILP	—
[41]	EM	Min operation cost, min emissions	BESS and generation constraints	MOPSO	Matlab
[42]	EM	Max profit	ESS and generation constraints	MILP	GAMS (CPLEX)
[43]	CS	Min operation cost, min mismatch cost	BESS and generation constraints, voltage and frequency stabilization	—	Matlab
[44]	EM	Min energy bill	User comfort	Built algorithms	JADE
[45]	EM	Min operation cost, max reliability	BESS and generation constraints	—	GAMS (CPLEX)

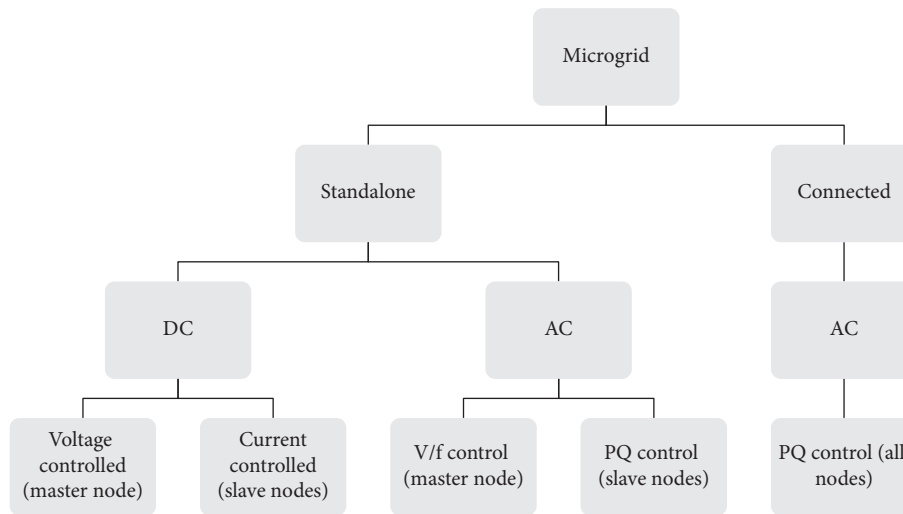


FIGURE 6: Summary of control schemes for microgrids.

The sizing (or design) of  $\mu$  grids is the long term EM strategy that aims to reduce the investment cost of the implementation for the whole duration of the project. A short term EM, commonly on a daily basis, can be done subsequently to increase the opportunities of saving money and energy. These techniques include resources scheduling, load scheduling, or a combination of both. In the following sections, we provide more details of the different EM strategies cited above.

It is noteworthy that the EM strategies developed below are presented from a technical aspect only. Although as important, other aspects (e.g., behavioural aspects) are out of the scope of this paper. These later require more attention from the organizational structures to raise energy awareness among customers by encouraging them to

replace inefficient equipments, install time switchers, and generally use less energy.

*4.2.1. Design and Sizing.* The optimal sizing is a techno-economic approach conducted with the goal of finding the best scenario that will return the highest Return On Investment (ROI). From a customer perspective, questions such as *what kind of DER technology best fulfil my needs? what should be the capacity of the implemented DER? what is the capacity of ESS that will increase the efficiency? and what if I increase the capacity of the DER, would it contribute to cost savings or would it be a waste of money because it would only generate unexploited energy excess?* will need convincing answers. By performing an optimal

sizing, we provide the customer with practical solutions for an optimal design of  $\mu$  grids suitable for their needs and capacities.

The sizing implicitly includes an EM strategy. It is usually intuitive and based on a simple process also known in prior works as the *myopic* strategy. This strategy consists of giving a priority to the different energy resources in the system. This strategy starts by fulfilling the demand from the first energy supply priority. When this energy supply is not enough to feed the load, the system then activates the next energy supply priority and so on. Figure 7 shows a general example of such strategies involving three energy supplies: RER as a primary supply, ESS as a second supply, and the utility grid as the backup supply. More complicated strategies can be integrated in the optimal sizing for performing EM. For instance, the authors in [13, 26, 34] performed a combined sizing and energy scheduling strategy. For a more detailed overview about the optimal sizing/design strategies for  $\mu$  grids, see [53].

The most common cost to minimize is the net present cost (NPC). There are two types of constraints to take into consideration: financial constraints defined by the budget and technical constraints that include capacity limits, generation limits, and load limits.

**4.2.2. Resource Scheduling.** The supply/resource scheduling, also known as optimal power flow (OPF), involves the scheduling of the controllable generators and ESS. It gives the optimal dispatch of resources over a time horizon during which the scheduling is performed, as showcased in [19, 33]. When the architecture contains only RER and ESS, the task is reduced to the optimal scheduling of charging/discharging of the ESS. The tools and algorithms the researchers used to perform the scheduling are detailed in Section 4.2.3. To tackle the problem of RER intermittency, the authors in [23, 34] combine a forecasting block with a scheduling strategy. The forecasting block predicts the weather data and the customer demand load.

**4.2.3. Load Scheduling.** Load scheduling is a part of the Demand Side Management (DSM)/Demand Response (DR) policies. It implicates load shifting, load shedding, and thermal load adjustment. Some papers consider the thermal load adjustment as a shifting technique. In fact, while the shifting impacts flexible (i.e., deferrable) loads for which the operation can be deferred over a specified period of time (i.e., washer-dryer and dishwasher), the thermal loads adjustment alters the power around the nominal power rating of power-level controlled appliances. Examples include heating, ventilation, and air conditioning systems (HVAC) and electric water heaters (EWH). For a short-term EM purpose, one or more of the aforementioned techniques can be combined.

(1) *Load Shifting.* Shifting appeared before the concept of smart grid. In fact, the industry has been the driving sector and the first one for which load shifting programs have been

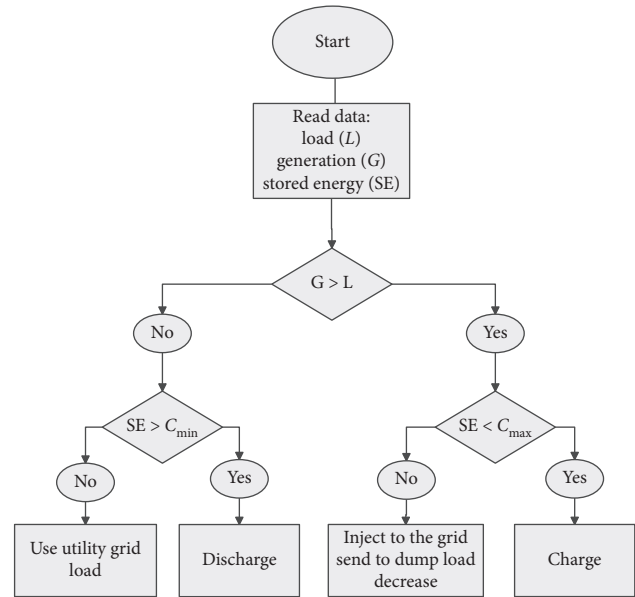


FIGURE 7: Example of myopic strategy.

deployed. Load shifting is a load rescheduling over time from on-peak hours to off-peak hours. The load rescheduling helps to reduce peak power to avoid overloads. The load shifting programs are always associated to an optimization of cost benefit, while respecting constraints such as customer preferences. The customer preferences are expressed via the classification of residential loads into different classes. The selected papers that used the shifting technique adopted various classifications, and we cite among others

- (i) Permanent loads, priority loads, and shiftable loads: permanent loads refer to those that run for long periods of time such as refrigerators. Priority loads are those that are used regularly and can create discomfort in users if shifted/shed (e.g., EWH). Shiftable loads include washers [11].
- (ii) Controllable (shiftable and elastic) and noncontrollable (nonshiftable and inelastic) loads: the latter refers to loads that cannot run on a scheduled date (e.g., electric cooker). Controllable loads on the other hand are divided into deferrable and power-level controlled loads. Deferrable loads have flexible starting-time operation (e.g., washing machine), while power-level controlled loads can vary their power around the nominal power of operation (e.g., water heater) [12, 27, 37].
- (iii) Low, medium, and high priority loads: priorities are set according to customer preferences defining the order of which loads are fed with energy. The highest priority demands are satisfied at the beginning, then the medium priority demands, and finally the lowest priority ones [44].

We can set priority for shiftable loads in order to plan the operation of a load over another governed by a set of parameters such as the starting and ending time limits.

(2) *Load Shedding*. Shedding is a traditional solution used to overcome the problem of overloads and network destabilization. The authors in [24] used it in their control strategy to keep the voltage network under a stable state. In [33, 35], loads were divided into critical and noncritical (i.e., ordinary) loads. In an event of overloads, the system starts dropping the noncritical loads starting with the least priority ones. In [36], loads were grouped into three categories based on their priority:  $L_1$ ,  $L_2$ , and  $L_3$ .  $L_1$  refers to loads that always have to be fed and  $L_3/L_2$  to loads that are shed if an energy deficit occurs.

Combining shedding and shifting is also a common EM strategy. The authors in [8] perform a power shifting of HVAC and lighting and shed less priority loads. A classification of loads into interruptible and deferrable loads was performed in [28], where an interruptible load can be shed and a deferrable load can be shifted.

### 4.3. Algorithms and Tools

**4.3.1. Algorithms.** The two main approaches that are commonly used for EM in  $\mu$  grids are rule-based approaches and optimization-based approaches. The former approaches follow a certain predefined criteria in order to make beneficial decisions for the system. They are mostly very simple with a low computational complexity but can provide efficient results. The myopic strategy, as it was demonstrated earlier in this paper, is an example strategy of this type of approaches. Papers using this method [8, 10, 11, 15, 21, 24, 35–37] proved the effectiveness of such strategies through simulations. More advanced techniques can be incorporated with rule-based approaches for higher efficiency. We cite as examples artificial neural networks (ANN) [33], fuzzy logic [34], and the adoption of multi-agent systems (MAS) [35–37, 44]. The use of the latter technique has garnered much interest lately. In fact, its incorporation helps to monitor the heterogeneous nodes (e.g., home devices, energy supplies, ESS, and communication nodes) composing a  $\mu$  grid system by representing each node as an autonomous and intelligent agent capable of taking decisions to better achieve the common goal.

The latter approach (i.e., optimization-based) is more sophisticated. It derives from mathematical models and aims to optimize an objective function while taking into consideration environmental constraints. When it comes to optimizing the energy in the  $\mu$  grid, it seems that heuristic algorithms and linear programming are the go-to tools.

Heuristic algorithms [54] are optimization algorithms that use the information currently gathered to help decide which candidate solution should be tested next or how the next individual can be produced. They are inspired from nature as they mimic the behaviour of living species. A variety of heuristics were used in the  $\mu$  grid field. We cite multiobjective self-adaptive differential evolution algorithm (MOSaDE) [1], genetic algorithms (GA) [2], ant colony optimization (ACO) [32], backtracking search optimization algorithm (BSOA) [14], and particle swarm optimization (PSO) [18, 24] and [21, 31, 41]. The authors

in the latter references used different versions of the same algorithm which are, respectively, modified PSO, regrouping PSO, and multiobjective PSO. In all of the referenced papers, results were compared with other heuristic algorithms and found that the PSO always gives better results.

Linear programming (LP), also called linear optimization, is the maximization/minimization of an objective linear function subject to linear constraints. The general form of a linear optimization is as follows:

$$\begin{aligned} \min_x \quad & f(x), \max_x f(x), \\ \text{s.t.} \quad & Ax \geq b, \quad Ax \leq b, \\ & Cx = d, \quad \text{s.t.} \quad Cx = d, \end{aligned} \quad (11)$$

where  $x$  is the variable,  $f$  is the linear objective function,  $A$  and  $B$  the parameters of the inequality constraint, and  $C$  and  $D$  are the parameters of the equality constraint. The resolution of a linear programming system returns the sets of vector  $x$  specifying the maximum/minimum value of the objective function. Many papers used linear programming to solve the energy usage optimization problem [13, 30, 40, 42].

**4.3.2. Tools.** Many tools are used for the simulation of an EMS. They can be grouped into three categories: tools for simulating the output of the different technologies, tools dedicated for sizing purposes, and solvers for rule-based or optimization approaches.

In the first category, we find WindSim. A tool based on computational fluid dynamics (CFD) for wind modelling. It returns several outputs, regarding the targeted terrain, the wind field, and the energy produced by the wind farms [3]. The authors in [4] simulated the PV system with the help of the software PVsyst for the annual yield and Crmsolar for the hourly simulations. To simulate the CS strategy suggested in [24], the authors used PSCAD/EMTDC which is a popular tool for this task (see [52]).

The second category covers numerous tools with HOMER (Hybrid Optimization Model for Electric Renewable) [5, 11] and MSDO (Matlab/Simulation Design Optimization) [3, 25, 39] being the most employed tool. A detailed list of the available tools can be found in the optimal sizing review in [53].

Matlab is also used for optimization purposes. It integrates a CPLEX solver for solving LP systems. Other software solutions providing CPLEX such as General Algebraic Modelling System (GAMS) [42, 45] and C++ are also used. In addition, Matlab can also be used to solving heuristic algorithms [2, 18, 21, 41] and to designing MAS systems [36, 37]. Other interesting tools for optimization are Pyomo that was used in [15]. Pyomo is a python-based optimization tool for LP, nonlinear programming, and mixed integer LP (MILP). JADE (java agent development environment) is also used for the modelling of MAS systems [35, 44].



## 5. RQ3: Challenges and Constraints

5.1. *Objectives.* Three main objectives are targeted when performing a microgrid optimization: Cost reduction, local resources use increase, and CO<sub>2</sub> emissions reduction.

5.1.1. *Cost Reduction.* Economic benefit is the major concern taken into account by modellers and researchers alike. Different sources of cost are considered: energy generation, energy consumption, in addition to NPC which includes Cost of Energy (COE), and others detailed below. The NPC is used for long-term optimization (i.e., sizing/design). It is usually mentioned in papers that use HOMER as a solver [5, 11]. The NPC represents the project's lifetime cost and includes the capital cost, replacement cost, operation and maintenance (O&M) costs, and fuel cost in case the architecture incorporates a conventional energy source:

$$\text{NPC} = \frac{C_{\text{ann,tot}}}{\text{CRF}}, \quad (12)$$

where  $C_{\text{ann,tot}}$  is the total annual cost and CRF is the capital recovery factor defined by

$$\text{CRF} = \frac{i(1+i)^n}{(1+i)^n - 1}, \quad (13)$$

where  $i$ : the annual real interest rate and  $n$ : the project lifetime. More detailed mathematical expressions describing how capital and replacement costs were distributed evenly on the project's lifetime can be found in [11].

The COE is the average cost of the electrical energy generated by the  $\mu$  grid in \$/kWh. It can be used for short- or long-term optimization. It is computed in [1] by

$$\text{COE} = \frac{\text{NPC}}{E_{\text{served}}} \times \text{CRF} = \frac{C_{\text{ann,tot}}}{E_{\text{served}}}. \quad (14)$$

Other costs were introduced in the papers such as the cost of generated energy [15, 23, 28, 38, 41], the cost of degradation of ESS [38], the cost of purchased energy from the grid [2, 14, 15, 19, 23, 28, 33, 37, 38, 41], the start-up/shut-down cost of DER [14, 38, 41], cost of fuel [13, 14, 43], and the comfort cost.

The comfort cost is the cost related to the nonsupplied energy [9] or to the action of shifting/shedding appliances [38, 43]. In [26], for instance, the authors introduce a discomfort cost that measures the user experience under a load scheduling  $x$  which deviates from their preferred power consumption  $y$ . It was called the mismatch cost in [12], and it penalized the change in the satisfaction of a user which was assumed to be proportional to the priority of the curtailed appliance. The same concept of cost was reproduced in [37] and was called the user drop. Lifetime was also included as a type of cost in [6], and it aims to increase the lifetime of devices by maximizing the state of health (SoH) of different components.

When a paper mentions an operation cost, it may refer to one or a combination of the costs listed above. In [40], for instance, the cost includes the cost of interacting with the grid, the ageing cost of the battery, the gas cost, and the O&M costs of RER. The losses are also expressed via a cost

function. In [6], the authors took into consideration the cost of power lost during the conversion process (e.g., electrical conversion losses and chemical conversion losses).

5.1.2. *Local Resources Use Increase/Reliability.* The autonomy of  $\mu$  grids is another concern for the scientific community. By increasing the use of local resources, we increase the autonomy of our system and implicitly attenuate the load from the main electric grid. In the studied papers, this metric has different mathematical expressions and is subject to minimization or maximization depending on the context.

- (i) In [1], the authors minimize the power supply probability (LPSP) which is the probability of power supply failure to meet load demand.
- (ii) In [3], the authors minimize the rate of nonsupplied demand load and the energy waste. The energy waste is the excess energy produced by RER which cannot be stored for ESS capacity limits.
- (iii) In [6], the authors penalize the unmet demand load.
- (iv) In [16], the authors maximize RER use as well as minimize utility grid use.
- (v) In [45], the authors aim to have a zero purchased energy from the grid (i.e., zero-net energy consumption).
- (vi) In [25], the authors take reliability as a constraint.

5.1.3. *CO<sub>2</sub> Emission Reduction.* RER are pollutant-free; this is the main incentive to their incorporation in the electric grid. Any hybrid system that includes a non-RER would generate an amount of greenhouse emissions. Two interesting expressions were used in the selected studies. Equation (15) was used in [5], where  $t_{\text{CO}_2}$  presents the total amount of CO emissions,  $m_f$  is the fuel quantity in litre,  $HV_f$  is the fuel heating value in (MJ/L),  $\text{CEF}_f$  is the carbon emission factor in (ton carbon/TJ), and  $X_c$  is the oxidized carbon fraction. We note that 3.667 g of CO<sub>2</sub> includes 1 g of carbon:

$$t_{\text{CO}_2} = 3.667 \times m_f \times HV_f \times \text{CEF}_f \times X_c. \quad (15)$$

In [25], the authors used another expression to penalize the CO<sub>2</sub> emissions:

$$C_{\text{CO}_2} = \omega_{\text{CO}_2} \times E = \omega_{\text{CO}_2} \times \sum_i T_{\text{DER}_i} [E_{\text{DER}_i}^{\text{op}} q_{\text{DER}_i}], \quad (16)$$

where  $\omega_{\text{CO}_2}$ : weight assigned based on the CO<sub>2</sub> cost European negotiation,  $E_{\text{DER}_i}^{\text{op}}$ : the CO<sub>2</sub> emissions generated by the operation of the unit  $\text{DER}_i$ ,  $q_{\text{DER}_i}$ : fuel consumption at one unit of time, and  $T_{\text{DER}_i}$ : the number of time units the unit  $\text{DER}_i$  was operating.

If the objective consists of increasing the use of RERs, it goes back to decreasing carbon emissions [13].

5.1.4. *Lifetime.* The authors in [6] introduced another metric, i.e., SoH.  $X_{\text{nom}}(t)$  and  $X_{\text{nom}}^0$  are, respectively, the actual nominal capacity (or power) and the initial nominal

capacity (or power). When the component is new, SoH = 1; when it reaches 0, the component is considered obsolete and must be replaced. This metric is governed by

$$\text{SoH}(t) = a \frac{X_{\text{nom}}(t)}{X_{\text{nom}}^0} - b, \quad (17)$$

where  $a > b$  and  $a$  and  $b$  are the coefficients that change depending on the component.  $X$  can be capacity or power.

Other metrics for calculating battery ageing are also introduced in the same reference such as the calendar ageing  $A_{\text{cal}}$  and the cycling ageing  $A_{\text{cyc}}$ .

An ESS's SoH is considered as an objective in some papers [6] and a constraint in others [16, 27], whereas, in [27], it was constrained by a minimum bound  $\text{SoH}_{\text{min}}$ .

**5.2. Challenges.** The intermittent aspect of RERs and the unpredictable behaviour of consumers are the main challenges faced with the implementation of RERs-based  $\mu$  grids. To tackle this problem, researchers mainly base their techniques on historical data. Nevertheless, other advanced solutions are employed in the literature including probabilistic models, forecasting models, and stochastic optimization.

**5.2.1. Historical Data.** This method is adopted mainly for sizing since, at this stage, EM can be performed from a macroscopic perspective (i.e., no need for real-time data). Yet, other papers rely on it to assess the performance of their suggested EM strategy. Many papers have adopted this method to simulate their systems (e.g., [1, 3, 17]). For instance, the authors in [2] used their own historical data (i.e., load profiles and PV output) for the proposed EM strategy. The authors in [5] performed sizing relying on NASA's historical data (i.e., weather data and load profile), while the authors in [14] developed an EM strategy using data originating from the technical report of NREL (National Renewable Energy Laboratory). Several websites provide free historical weather data of many regions of the world as well as load profiles of different energy scales (home, residential/commercial building, etc.).

**5.2.2. Probabilistic Models.** Probabilistic models assume that uncertain parameters such as demand load, wind speed, solar irradiation, and temperature follow a certain probability distribution function. From the selection, only one paper [43] used this type of models. The authors considered the speed of wind as a random variable following a Weibull distribution function with two parameters:

$$F(V_{\text{wind}}) = \frac{\eta}{c} \times \left(\frac{V_{\text{wind}}}{c}\right)^{\eta-1} \times \exp\left(-\left(\frac{V_{\text{wind}}}{c}\right)^{\eta}\right), \quad (18)$$

where  $V_{\text{wind}}$  is the wind speed (m/s),  $c$  is the scale factor of the Weibull distribution wind with unit of speed, and  $\eta$  is the shape factor of the Weibull distribution, which is dimensionless. Different methods exist for the computation of these parameters, and the authors in [43] used the following two expressions:

$$\eta = \frac{\sigma_w^{-1.086}}{V_{\text{mean}}}, \quad (19)$$

$$c = \frac{V_{\text{mean}}}{\gamma(1 + (1/\eta))},$$

where the  $\gamma$  is the gamma function,  $V_{\text{mean}}$  is the average value of the wind speed data, and  $\sigma_w$  is the standard deviation of the wind speed data. The accuracy of such models is verified through the comparison of their output with the existing actual data.

**5.2.3. Forecasting Models.** Forecasting is the process of estimating what will happen in the future based on the information possessed in the present and the past. It is a very useful method to handle the uncertainty issues within  $\mu$  grid systems. Table 6 gives an overview of the different forecasting models that were employed by the selection.

The most chosen candidates for forecasting are Model Predictive Controller (MPC), Two-Point Estimate Method (TPEM), and Artificial Neural Networks (ANN). The MPC was used in [6, 15] to determine the optimal output regarding the objective function in a time control horizon of 12 h in [6] and 6 h in [15]. Aside from the data forecasting stage used in [15], another stage was added to adjust the errors made by the predictive model.

Uncertainties with the market price changes, the load demand forecast error, and the RER output power changes were handled by TPEM in [14]. The authors in [9] used the same method to forecast the RER output and to estimate the load demand.

In [23, 42], the authors chose the MLPNN to model the system uncertainties and predict the day-ahead values. The predictions of PV power, wind speed, and load demand are modelled using neural networks in [33]. The authors in [34] applied a heterogeneous ANN composed from an aggregation of MLPNN, radial basis function neural network (RBFNN), and recurrent neural network (RNN) to make an hour-ahead forecasting of load demand and wind power generation and a 24 h ahead forecasting of solar power generation.

Other methods were used in the selection. We cite

- (i) General Collocated Velocity (GCV) solver [3] used to estimate the energy produced by wind farms
- (ii) Lagrange duality method used in [19, 20] as a stochastic off-line approach with a 6 h control horizon, and an online deterministic approach was juxtaposed to the first stage with a 10 min time slot interval
- (iii) Autoregressive Moving Average (ARMA) [36]
- (iv) Fast Fourier transformation (FFT) [45]

**5.2.4. Stochastic Optimization.** This method optimizes an objective function of a system under specific uncertainties. The application of stochastic optimization for smart grid applications was thoroughly reviewed in [55]. From the

TABLE 6: Algorithms for forecasting.

Ref.	Algorithm
[3]	GCV
[6, 15]	MPC
[9, 14]	TPEM
[19, 20]	Lagrange duality method
[23, 42]	MLPNN
[33, 34]	ANN
[36]	ARMA
[45]	FFT

selection, only the authors of two works [38, 40] employed this method, and they both adopted the robust optimization and a branch of the former, optimizing the output of a system under the worst case scenario.

### 5.3. Constraints

**5.3.1. Energy Balance.** The main constraint to consider is delivering noninterrupted energy to the consumer. This constraint is considered in all papers. It allows to keep customer comfort at a certain level and avoid the energy shortage and possible outage risks. The general expression of this constraint that has to be fulfilled at each time step of the control horizon is

$$\text{Load} - \text{Generation} = 0, \quad (20)$$

where the first term refers to the consumed energy by the customer's appliances and the second term refers to the energy produces locally by the DER and RER. During its charging phase, the ESS is considered a load and a generation when discharging. In [15], the energy balance constraint was split into two separate balances: electrical and thermal balance. The thermal balance constraint is further split in [40] into cooling balance and heating balance. The mathematical expression of this constraint gets complicated when dealing with shifting strategies. In fact, additional parameters are involved such as the schedule of each appliance  $i$  over the control horizon  $T$ :  $x_i = (x_i)_{0 < t \leq T}$ , and the binary variable  $u_i$  equal to 1 if the appliance is on, and 0 otherwise.

**5.3.2. Power and Capacity of Components.** The technical constraints of  $\mu$  grid components are expressed by the limitations on their nominal power or capacity.

**(1) Generation Units.** The power generation of the DER units  $P_{\text{DER}}$  is limited by an upper limit  $P_{\text{DER,max}}$  and a lower limit  $P_{\text{DER,min}}$  [6, 12, 21, 28, 31, 37].

In [38], the authors give a comprehensive set of constraints for DER concerning

- (i) The initial on-line/off-line requirements for the generation units.
- (ii) Minimum number of time periods the generator must remain on-line/off-line after the minimum off-line/on-line required time.

- (iii) Minimum number of time periods the generator must remain on-line/off-line at the end of the time horizon.
- (iv) A generator can change its power supply depending on its ramping rate  $r_{\text{DER}} \in ]0, 1]$ , which determines how fast the generation can be changed hourly, or when the generator is turned on or off a similar constraint figures in [28, 40], see equation (21).
- (v) Common constraints such as the lower and upper limits of each generator as well as start-up and shut-down costs' computation:

$$|P_{\text{DER}}(t) - P_{\text{DER}}(t-1)| < r_{\text{DER}} \cdot P_{\text{DER}}. \quad (21)$$

The capacity of the DER inverter  $s_{\text{DER}}$  was considered in [28], and the constraint related to it limits the active power  $P_{\text{DER}}$  and the reactive power  $q_{\text{DER}}$  of the DER:

$$P_{\text{DER}}^2(t) + q_{\text{DER}}^2(t) \leq s_{\text{DER}}^2. \quad (22)$$

In [25], the authors include an upper bound for the daily fuel consumption.

**(2) Utility Grid Unit (for the on-Grid Mode).** Some papers do not assign constraints on the utility grid, and this implies that the utility grid can provide the  $\mu$  grid with any amount of energy it needs, and in case of a bidirectional flow of energy, the  $\mu$  grid can inject all of its generation excess into the utility. Others, such as in [16, 21, 27, 31, 40], limit the power exchanged with the utility  $P_{\text{Grid}}$  by an upper limit  $P_{\text{Grid,max}}$  and a lower limit  $P_{\text{Grid,min}}$ . The upper limit is constrained by an upper bound  $P_{\text{peak}}$  in [16, 27, 30]. This last constraint is usually called the peak shaving constraint because it helps the network avoid overload events and reduces peak to average ratio (PAR). The term  $P_{\text{Grid,min}}$  limits the power to be injected into the grid:  $P_{\text{injected}} \leq |P_{\text{Grid,min}}|$ .

The authors in [38] have followed another policy: only the amount of energy exchanged under a firm contract is bounded, which means that the grid can exchange any amount with the  $\mu$  grid but with different price rates. If the exchanged amount is under a certain upper limit, the energy will be exchanged at a price  $F$  (Firm) and a price  $N$  (non-Firm) otherwise.

**(3) Load Unit.** For papers working with a load management strategy, constraints on the loads are considered. In [12, 13, 26, 37], a minimum and a maximum power consumption of each appliance is determined. This constraint is further split into two constraints in [28]: a constraint on the active power of the appliance, and another one on the reactive power.

**(4) Storage Units.** When considering the storage, many constraints should be taken into account: the capacity constraint, the charging/discharging rate constraint, and the charging/discharging limits. Since the majority of papers implement an electrical storage, we will focus first on the constraints on this type of storage. A deep discharging or an extra charging can damage the ESS. Batteries, for instance,

undergo a fast degradation if discharged under the optimal DoD. This constraint is expressed by the capacity of the ESS at a time  $t$   $C_{\min} \leq C(t) \leq C_{\max}$  or with the state of charge (SOC) of the ESS:  $\text{SOC}_{\min} \leq \text{SOC}(t) \leq \text{SOC}_{\max}$ . SOC defines the percentage of the stored amount compared to the total capacity of an ESS:  $\text{SOC}(t) = C(t)/C_{\max}$ . The charging (resp. discharging) rate is the rate at which a storage is charged (resp. discharged) relative to its capacity. The two parameters are bounded by an upper limit and a lower limit:

$$\begin{aligned} \beta_{\text{char},\min} &\leq \beta_{\text{char}} \leq \beta_{\text{char},\max}, \\ \beta_{\text{dis},\min} &\leq \beta_{\text{dis}} \leq \beta_{\text{dis},\max}. \end{aligned} \quad (23)$$

To simplify, the charging rate is taken equal to the discharging rate. Additional constraints on the electrical storage include the following. The SOC at the end must be equal to the SOC at the beginning of the time horizon as in [26]. Constraint on the storage inverter in [28] is

$$p_b^2(t) + q_b^2(t) \leq s_b^2, \quad (24)$$

where  $s_b^2$  is the inverter's capacity and  $p_b$  and  $q_b$  are, respectively, the battery's active and reactive powers.

Constraints on the thermal storage are identical to the electrical storage: bounds on capacity and charging/discharging rates (Cf. [40]). A detailed series of constraint equations for the pump-storage system can be found in [9, 42].

**5.3.3. Network Constraints.** The network constraints frequently considered are the bus voltage limit, the bus frequency limit (for the AC configurations), the active/reactive power limits, the feeder limit, and the physical capacity of the transmission lines.

**(1) Bus Voltage and Frequency Limits.** The bus voltage  $V$  should not exceed a voltage limit defined by the sum of the nominal voltage and a tolerance range (habitually  $V_{\text{nom}} \pm 5\%$  [9, 28]). In the expression below, the voltage is an absolute term and the two bounds are positives:

$$V_{\min} \leq |V| \leq V_{\max}. \quad (25)$$

The same rule applies on the frequency [43]. The bus operation frequency should be maintained within a 0.5 Hz around the nominal frequency:

$$f^{\min} \leq f \leq f^{\max}. \quad (26)$$

**(2) Active/Reactive Power.** In [9], the constraints on the active power  $P$  and reactive power  $Q$  are expressed by

$$\begin{aligned} P_{G,i} - P_{L,i} &= \sum_j |V_i| |V_j| Y_{ij} \cos(\theta_{ij} + \alpha_j - \alpha_i), \\ Q_{G,i} - Q_{L,i} &= \sum_j |V_i| |V_j| Y_{ij} \sin(\theta_{ij} + \alpha_j - \alpha_i), \end{aligned} \quad (27)$$

where  $V_i$  and  $V_j$  are the  $i/j$ -bus voltage,  $\alpha_j$  and  $\alpha_i$  are the voltage angle of bus  $i$  and  $j$  in rad, and  $\theta_{ij}$  angle of complex  $Y$ -bus element.

**(3) Feeder Flow Limit.** The apparent power flow  $S_{ij}$  from the bus  $i$  to the bus  $j$  in [9] was subject to a limit constraint:

$$S_{ij} \leq S_{ij}^{\max}. \quad (28)$$

**(4) Physical Capacity of the Transmission Lines.** These constraints were considered in [38]. In fact, each medium has a predefined capacity; transmitting a power flow higher than this capacity is called the thermal limit violation. Nevertheless, the voltage is the most important parameter of the transmission line since it gives an idea about the power that the line can hold. Therefore, if the voltage limit were respected, the capacity limitation is not considered.

**5.3.4. User Comfort.** For certain papers, the user comfort was included in the objective function as the cost of shifting appliances from the preferred period of operation. In other papers, the user comfort is expressed as a constraint.

In [8], three parameters were considered:

- (i) Thermal comfort was measured using the thermal comfort index: predicted mean vote (PMV)
- (ii) Visual comfort was measured by illuminance, which is an index for assessing the quantity of light
- (iii) The priority comfort was measured using the priority list of the customer

The user comfort constraint in [9] was expressed by the equation given below.  $D_f$  and  $D_{\text{init}}$  refer, respectively, to the demand load after DSM application and the initial demand load,  $e$  is the elasticity coefficient and it translates the willingness of the consumer to shift their loads, and  $\text{Pr}_0$  is the base utility price:

$$D_f = D_{\text{init}} \times \left[ 1 + e \left( \frac{\text{Penalty} - \text{Incentive}}{\text{Pr}_0} \right) \right]. \quad (29)$$

The load shifting was subject to the following constraint:  $|D_f - D_{\text{init}}| \leq x_{\%} D_{\text{init}}$ , where  $x_{\%}$  is the percentage of shifting that the DSM algorithm must not exceed.

**5.3.5. Budget Constraint.** The budget is an important parameter to consider when searching for an optimal sizing of the  $\mu$  grid. Unfortunately, only the authors in [26] have considered this condition and required that the sum of purchasing cost, installation cost, and O&M costs of equipment should not exceed an upper bound.

**5.3.6. Renewable Factor.** The authors in paper [1] consider the renewable factor as the quantity of power generated from the diesel generator compared to the amount generated from RERs:

$$\text{RF} = 100 \times \left( 1 - \frac{P_{\text{DG}}}{P_{\text{RER}}} \right). \quad (30)$$

The more RF approaches 100%, the more it is efficient because it means that the system covers its energy need

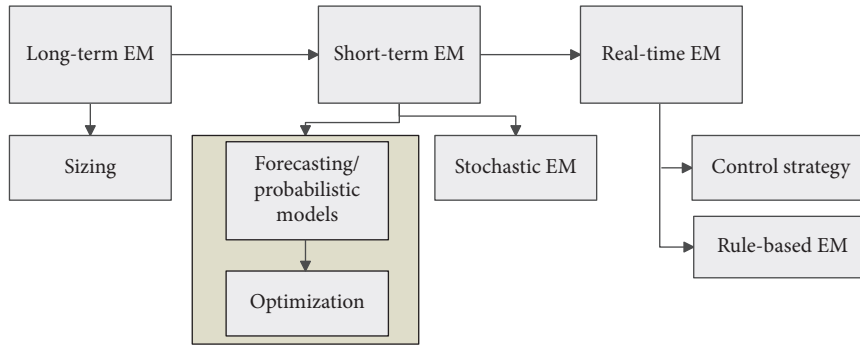


FIGURE 8: The proposed EM strategy.

mainly from RERs. While, in [5], the authors used a more generic expression. RF refers to the energy delivered to the load by RERs compared to non-RERs:

$$RF = 100 \times \left( 1 - \frac{P_{\text{non-RER}}}{P_{\text{Load}}} \right). \quad (31)$$

**5.3.7. Islanding Constraint.** In [30], the authors adapted the on/off  $\mu$  grid mode of operation. In case of a shortage event when the  $\mu$  grid has to switch between on-to off-mode, a minimum energy level for the total storage in the network is computed adaptively to ensure sufficient energy reserve.

## 6. Study Limitations

The first limitation that we had to face was the huge number of papers that cover the EM topic. The study would have been more interesting if we had covered all the papers from the selection process. Yet, due to their massive number, we were obliged to restrict our study to the 15 first relevant papers of each database. This restriction has the drawback of leaving behind papers that suggest worthwhile methods and strategies. After the selection was done and during the extraction process, we encountered a lack of information. In fact, important information was missing in some papers such as the adopted utility price policy or the type of batteries. A lot of papers did not mention the complexity of their suggested algorithms. Thus, we were not able to perform a quality assessment and apply a comparative study of the suggested algorithms.

## 7. Conclusion and Suggestions

Managing the energy usage in  $\mu$  grids has a vast impact in energy efficiency and sustainability research. This SLR proposes an overlook on different EM strategies suggested by researchers for green  $\mu$  grid systems. It starts by summarizing the different architectures proposed in the literature. This includes the components that compose a  $\mu$  grid, the different operation modes, and a brief discussion on the energy exchange policy with the main grid network. Then, the review proceeds to presenting the various methods,

algorithms, and tools that help perform EM and concludes with pointing out objectives and faced constraints.

As a result of this SLR, we propose a methodology for an efficient use of energy in a green  $\mu$  grid system. As shown in Figure 8, a good EM starts with a sizing study. The sizing will have the benefit of increasing the ROI in a long-term vision and help decrease the energy waste due to the frequent overgeneration. To perform the sizing, rule-based strategies and linear programming are the most appropriate for the task. The short term EM is a critical block since it is where the unpredictable behaviour of RERs is handled. It is usually performed in a daily basis and can be done in two different ways: utilize the stochastic optimization or combine a two-block strategy that includes a forecasting block and deterministic optimization block. The last part of the methodology is processed real time. It is generally a rule-based strategy. This part has the task of compensating the differences between the scheduled values and the actual values. The correction and the regulation of the system's electric signals are performed at this level as well.

A significant part that starts to emerge and that was not detailed in this paper regards the cooperative energy management strategies. In fact, by allowing  $\mu$  grids to collaborate, the costs resulting from losses can be significantly reduced, especially with the integration of an efficient distributed EM strategy. The peer-to-peer interconnection of numerous  $\mu$  grids in a distribution network will take us one step towards the future smart grid network. Therefore, it is essential to take into account the cooperative aspect in each step of the suggested methodology.

We have to bear in mind that EM strategies reviewed here are highly related to the communication infrastructure. In fact, in all EM Strategies, we assume that the EMS receives all the information it requires. Yet, we have to consider whether this is feasible or not. The communication architecture carrying the  $\mu$  grid information is made of small-capacity sensors and channels that are not very robust. Transmitting massive data on a real-time basis for the EM purpose is questionable.

## Conflicts of Interest

The authors declare that they have no conflicts of interest.

## References

- [1] M. A. M. Ramli, H. R. E. H. Bouchekara, and A. S. Alghamdi, "Optimal sizing of PV/wind/diesel hybrid microgrid system using multi-objective self-adaptive differential evolution algorithm," *Renewable Energy*, vol. 121, pp. 400–411, 2018.
- [2] Z. Wang, C. Gu, and F. Li, "Flexible operation of shared energy storage at households to facilitate PV penetration," *Renewable Energy*, vol. 116, pp. 438–446, 2018.
- [3] S. Proietti, P. Sdringola, F. Castellani, D. Astolfi, and E. Vuillermoz, "On the contribution of renewable energies for feeding a high altitude smart mini grid," *Applied Energy*, vol. 185, pp. 1694–1701, 2017.
- [4] P. Couty, M. J. Lalou, C. Peter, S. Cotture, and V. Saade, "Positive energy building with PV facade production and electrical storage designed by the swiss team for the U.S. Department of Energy Solar Decathlon 2017," *Energy Procedia*, vol. 122, pp. 919–924, 2017.
- [5] L. M. Halabi and S. Mekhilef, "Flexible hybrid renewable energy system design for a typical remote village located in tropical climate," *Journal of Cleaner Production*, vol. 177, pp. 908–924, 2018.
- [6] D. Morin, Y. Stevenin, C. Grolleau, and P. Brault, "Evaluation of performance improvement by model predictive control in a renewable energy system with hydrogen storage," *International Journal of Hydrogen Energy*, vol. 43, no. 45, pp. 21017–21029, 2018.
- [7] N. T. Mbungu, R. C. Bansal, R. Naidoo, V. Miranda, and M. Bipath, "An optimal energy management system for a commercial building with renewable energy generation under real-time electricity prices," *Sustainable Cities and Society*, vol. 41, pp. 392–404, 2018.
- [8] F. Sehar, M. Pipattanasomporn, and S. Rahman, "An energy management model to study energy and peak power savings from PV and storage in demand responsive buildings," *Applied Energy*, vol. 173, pp. 406–417, 2016.
- [9] G. Ahmad and M. Enayatzare, "Optimal energy management of a renewable-based isolated microgrid with pumped-storage unit and demand response," *Renewable Energy*, vol. 123, pp. 460–474, 2018.
- [10] V. Kamala Devi, K. Premkumar, and A. Bisharathu Beevi, "Energy management using battery intervention power supply integrated with single phase solar roof top installations," *Energy*, vol. 163, pp. 229–244, 2018.
- [11] A. Chauhan and R. P. Saini, "Techno-economic optimization based approach for energy management of a stand-alone integrated renewable energy system for remote areas of India," *Energy*, vol. 94, pp. 138–156, 2016.
- [12] R. Rahmani, I. Moser, and M. Seyedmahmoudian, "Multi-agent based operational cost and inconvenience optimization of PV-based microgrid," *Solar Energy*, vol. 150, pp. 177–191, 2017.
- [13] G. Prinsloo, A. Mammoli, and R. Dobson, "Discrete cogeneration optimization with storage capacity decision support for dynamic hybrid solar combined heat and power systems in isolated rural villages," *Energy*, vol. 116, pp. 1051–1064, 2016.
- [14] F. Najibi, T. Niknam, and A. Kavousi-Fard, "Optimal stochastic management of renewable mg (micro-grids) considering electro-thermal model of PV (photovoltaic)," *Energy*, vol. 97, pp. 444–459, 2016.
- [15] T. M. Kneiske, M. Braun, and D. I. Hidalgo-Rodriguez, "A new combined control algorithm for PV-CHP hybrid systems," *Applied Energy*, vol. 210, pp. 964–973, 2018.
- [16] L. N. An, T. T. Minh Dung, and T. Quoc-Tuan, "Optimal energy management for an on-grid microgrid by using branch and bound method," in *Proceedings of the 2018 IEEE International Conference on Environment and Electrical Engineering and 2018 IEEE Industrial and Commercial Power Systems Europe (EEEIC/I CPS Europe)*, pp. 1–5, Palermo, Italy, June 2018.
- [17] C. Keles, A. Kaygusuz, and B. B. Alagoz, "Multi-source energy mixing by time rate multiple PWM for microgrids," in *Proceedings of the 2016 4th International Istanbul Smart Grid Congress and Fair (ICSG)*, pp. 1–5, Istanbul, Turkey, April 2016.
- [18] C. Keles, B. B. Alagoz, and A. Kaygusuz, "Multi-source energy mixing for renewable energy microgrids by particle swarm optimization," in *Proceedings of the 2017 International Artificial Intelligence and Data Processing Symposium (IDAP)*, Malatya, Turkey, September 2017.
- [19] K. Rahbar, J. Xu, and R. Zhang, "Real-time energy storage management for renewable integration in microgrid: an off-line optimization approach," *IEEE Transactions on Smart Grid*, vol. 6, no. 1, pp. 124–134, 2015.
- [20] K. Rahbar, C. C. Chai, and R. Zhang, "Energy cooperation optimization in microgrids with renewable energy integration," *IEEE Transactions on Smart Grid*, vol. 9, no. 2, pp. 1482–1493, 2018.
- [21] A. T. Eseye, D. Zheng, and J. Zhang, "Optimal energy management strategy for an isolated industrial microgrid using a modified particle swarm optimization," in *Proceedings of the 2016 IEEE International Conference on Power and Renewable Energy (ICPRE)*, pp. 494–498, Vienna, Austria, October 2016.
- [22] W. Huang, Z. Fu, and L. Hua, "Research on optimal capacity configuration for distributed generation of island micro-grid with wind/solar/battery/diesel engine," in *Proceedings of the 2018 2nd IEEE Conference on Energy Internet and Energy System Integration (EI2)*, pp. 1–6, Beijing, China, October 2018.
- [23] U. B. Tayab, F. Yang, M. El-Hendawi, and J. Lu, "Energy management system for a grid-connected microgrid with photovoltaic and battery energy storage system," in *Proceedings of the 2018 Australian New Zealand Control Conference (ANZCC)*, pp. 141–144, Melbourne, Australia, December 2018.
- [24] M. H. F. Ahamed, U. D. S. D. Dissanayake, H. M. P. De Silva, H. R. C. G. P. Pradeep, and N. W. A. Lidula, "Modelling and simulation of a solar PV and battery based DC microgrid system," in *Proceedings of the 2016 International Conference on Electrical, Electronics, and Optimization Techniques (ICEEOT)*, pp. 1706–1711, Chennai, India, March 2016.
- [25] S. R. Alvarez, A. M. Ruiz, and J. E. Oviedo, "Optimal design of a diesel-PV-wind system with batteries and hydro pumped storage in a colombian community," in *Proceedings of the 2017 IEEE 6th International Conference on Renewable Energy Research and Applications (ICRERA)*, pp. 234–239, San Diego, CA, USA, November 2017.
- [26] H. Wang and J. Huang, "Joint investment and operation of microgrid," *IEEE Transactions on Smart Grid*, vol. 8, no. 2, pp. 833–845, 2017.
- [27] L. An and T. Quoc-Tuan, "Optimal energy management for grid connected microgrid by using dynamic programming method," in *Proceedings of the 2015 IEEE Power Energy Society General Meeting*, pp. 1–5, Denver, CO, USA, July 2015.

- [28] W. Shi, X. Xie, C.-C. Chu, and R. Gadh, "Distributed optimal energy management in microgrids," *IEEE Transactions on Smart Grid*, vol. 6, no. 3, pp. 1137–1146, 2015.
- [29] R. S. Karki and S. Chanana, "Simulation of energy management system for local energy market in microgrids," in *Proceedings of the 2016 IEEE Students' Conference on Electrical, Electronics and Computer Science (SCEECS)*, pp. 1–6, Bhopal, India, March 2016.
- [30] M. R. Sandgani and S. Sirouspour, "Coordinated optimal dispatch of energy storage in a network of grid-connected microgrids," *IEEE Transactions on Sustainable Energy*, vol. 8, no. 3, pp. 1166–1176, 2017.
- [31] L. Han, A. T. Eseye, J. Zhang, and D. Zheng, "Optimal energy management for industrial microgrids with high-penetration renewables," *Protection and Control of Modern Power Systems*, vol. 2, no. 1, p. 12, 2017.
- [32] I. Fatima, A. Khalid, S. Zahoor et al., "Home energy management system using ant colony optimization technique in microgrid," in *Advances on Broad-Band Wireless Computing, Communication and Applications*, B. Leonard, F. Xhafa, and Jordi Conesa, Eds., Springer International Publishing, Cham, Switzerland, 2018.
- [33] E. Cruz May, L. J. Ricalde, E. J. R. Atoche, A. Bassam, and E. N. Sanchez, "Forecast and energy management of a microgrid with renewable energy sources using artificial intelligence," in *Intelligent Computing Systems*, C. Brito-Loeza and A. Espinosa-Romero, Eds., Springer International Publishing, Cham, Switzerland, 2018.
- [34] P. G. Harhammer and A. Schadler, "Optimal energy management," in *System Modelling and Optimization*, A. Prékopa, J. Szelezsán, and B. Strazicky, Eds., Springer Berlin Heidelberg, Berlin, Heidelberg, Germany, 1986.
- [35] L. Raju, A. A. Morais, and R. S. Milton, "Advanced energy management of a micro-grid using Arduino and multi-agent system," in *Intelligent and Efficient Electrical Systems*, M.C. Bhuvaneshwari and J. Saxena, Eds., Springer, Singapore, 2018.
- [36] T. Bogaraj and J. Kanakaraj, "Intelligent energy management control for independent microgrid," *Sādhanā*, vol. 41, pp. 755–769, 2016.
- [37] S. Ghorbani, R. Rahmani, and R. Unland, "Multi-agent autonomous decision making in smart micro-grids' energy management: a decentralized approach," in *Multiagent System Technologies*, J. O. Berndt, P. Petta, and R. Unland, Eds., Springer International Publishing, Cham, Switzerland, 2017.
- [38] J. L. Ruiz Duarte and N. Fan, "Operations of a microgrid with renewable energy integration and line switching," *Energy Systems*, vol. 10, no. 3, 2018.
- [39] R. Jansen and R. Karki, *Sustainable Energy Optimization in a Smart Microgrid*, Springer, Singapore, 2017.
- [40] Z. Luo, W. Gu, Z. Wu, Z. Wang, and Y. Tang, "A robust optimization method for energy management of CCHP microgrid," *Journal of Modern Power Systems and Clean Energy*, vol. 6, no. 1, pp. 132–144, 2018.
- [41] G. Aghajani and N. Yousefi, "Multi-objective optimal operation in a micro-grid considering economic and environmental goals," *Evolving Systems*, vol. 10, no. 7, 2018.
- [42] H. Shayeghi and E. Shahryari, *Integration and Management Technique of Renewable Energy Resources in Microgrid*, Springer International Publishing, Cham, Switzerland, 2017.
- [43] T. Madiba, R. C. Bansal, J. J. Justo, and K. Kusakana, *Optimal Control System of under Frequency Load Shedding in Microgrid System with Renewable Energy Resources*, Springer International Publishing, Cham, Switzerland, 2017.
- [44] J. Klaimi, R. Rahim-Amoud, and L. Merghem-Boulahia, *Energy Management in the Smart Grids via Intelligent Storage Systems*, Springer International Publishing, Cham, Switzerland, 2017.
- [45] T. Brandt, *Designing an Energy Information System for Microgrid Operation*, Springer, Wiesbaden, Germany, 2016.
- [46] A. Awasthi, V. Karthikeyan, V. Das, S. Rajasekar, and A. K. Singh, *Energy Storage Systems in Solar-Wind Hybrid Renewable Systems*, Springer International Publishing, Cham, Switzerland, 2017.
- [47] *Energyplus Web-Based Documentation*, 2015, <https://bigladdersoftware.com/epx/docs/8-0/engineering-reference/page-076.html>.
- [48] G. Dutta and K. Mitra, "A literature review on dynamic pricing of electricity," *Journal of the Operational Research Society*, vol. 68, no. 10, pp. 1131–1145, 2017.
- [49] M. M. D. Ross, D. Turcotte, and S. Roussin, "Comparison of AC, DC, and AC/DC bus configurations for PV hybrid systems," Report Submitted to CETC-Varennes in Fulfillment of Contract, 2005.
- [50] J. S. del Moral and M. Á. Egido, *Simulation of AC, DC, and AC-DC Coupled Mini-Grids in Search of the Most Efficient System*, Universidad Politécnica de Madrid, Madrid, Spain, 2012.
- [51] M. Ourahou, W. Ayrir, B. El Hassouni, and A. Haddi, "Review on smart grid control and reliability in presence of renewable energies: challenges and prospects," *Mathematics and Computers in Simulation*, vol. 167, pp. 19–31, 2018.
- [52] P. G. Arul, V. K. Ramachandaramurthy, and R. K. Rajkumar, "Control strategies for a hybrid renewable energy system: a review," *Renewable and Sustainable Energy Reviews*, vol. 42, pp. 597–608, 2015.
- [53] M. Faccio, M. Gamberi, M. Bortolini, and M. Nedaei, "State-of-art review of the optimization methods to design the configuration of Hybrid Renewable Energy Systems (HRESS)," *Frontiers in Energy*, vol. 12, no. 4, pp. 591–622, 2018.
- [54] T. Weise, *Global Optimization Algorithms-Theory and Application*, Institute of Applied Optimization, Hefei University, Hefei, China, 2009.
- [55] S. S. Reddy, V. Sandeep, and C.-M. Jung, "Review of stochastic optimization methods for smart grid," *Frontiers in Energy*, vol. 11, no. 2, pp. 197–209, 2017.

## Review Article

# Solar Photovoltaic Power Forecasting

Abdelhakim El hendouzi <sup>1</sup> and Abdennaser Bourouhou<sup>2</sup>

<sup>1</sup>Lab Research in Electrical Engineering,  
Mohammed V University of Rabat National School of Computer Science and Systems  
Analysis and Higher Normal School of Technical Education,  
Avenue of Mohammed Ben Abdallah Regragui, Madinat Al Irfane, PB 713, Agdal Rabat, Morocco

<sup>2</sup>Lab Research in Electrical Engineering, Mohammed V University of Rabat Higher Normal School of Technical Education,  
Avenue of the Royal Army, Madinat Al Irfane, District Riad, Rabat 100100, Morocco

Correspondence should be addressed to Abdelhakim El hendouzi; [abdelhakim.elhendouzi@um5s.net.ma](mailto:abdelhakim.elhendouzi@um5s.net.ma)

Received 25 September 2020; Revised 8 December 2020; Accepted 11 December 2020; Published 31 December 2020

Academic Editor: Anna Diva Plasencia Lotufo

Copyright © 2020 Abdelhakim El hendouzi and Abdennaser Bourouhou. This is an open access article distributed under the Creative Commons Attribution License, which permits unrestricted use, distribution, and reproduction in any medium, provided the original work is properly cited.

The management of clean energy is usually the key for environmental, economic, and sustainable developments. In the meantime, the energy management system (EMS) ensures the clean energy which includes many sources grouped in a small power plant such as microgrid (MG). In this case, the forecasting methods are used for helping the EMS and allow the high efficiency to the clean energy. The aim of this review paper is providing the necessary data about the basic principles and standards of photovoltaic (PV) power forecasting by stating numerous research studies carried out on the PV power forecasting topic specifically in the short-term time horizon which is advantageous for the EMS and grid operator. At the same time, this contribution can offer a state of the art in different methods and approaches used for PV power forecasting along with a careful study of different time and spatial horizons. Furthermore, this current review paper can support the tenders in the PV power forecasting.

## 1. Introduction

The demand of energy by miscellaneous areas and the worldwide energy exploitation are really highest than any time before. In addition to the uppermost energy demand, oil and other planet's resources in fossil are becoming scarce. In this case, the environmentalists, the socialists, and the economists are supporting the climatic agreements and adopting the clean energy as a solution to retort the global energy demand, the cost effectiveness, and the ecological consequences such as the universal challenge caused by global warming and the greenhouse effect.

In this situation, the clean energy which includes the variable renewable energy, particularly the wind and solar PV, which provides free fuel source to the global energy market, consequently will improve the leveled cost of electricity (LCOE) in the medium and long terms. In this case, the solar PV is in the head of interest by the global investment, and also, Green Banks are leading the low-

carbon energy rebellion, helping to avoid the climate risk and serving the consumer and their concerns. According to the reports by the International Energy Agency (IEA), the solar PV pushed up for more growth, in spite of a decade of acceleration. In this detail, the cumulative solar PV capacity reached 398 GW, which represents around 2% of the global power energy [1]. Despite of the policies and regulation, the innovation, and the corporate commitments, the integration of solar PV in the power grids is suffering from both problems of unpredictability of weather parameters and poor infrastructure grids, which minimize the high penetration of solar PV. In this way, the forecasting techniques can help the rise of solar PV and promise the optimality of energy transition management between intermittent and conventional energies by providing the PV power forecasts in various time and spatial horizons. Subsequently, the PV power forecasting can support the grid operator by providing the future energy generated through the solar PV installations, which can help the planning and scheduling of



the effective unit commitments to meet the market demands. In addition, the PV power forecasting is advantageous for the benefit of new power generation such as the microgrids, in which they are smart, small microgenerations, based on numerous microsources including the solar PV. The microgrids, meanwhile, are a very ambitious technological asset for energy savings. However, their technology must meet certain stringent standards to integrate them into the power grids. The microgrids also need nearly smart regulations and controls. Therefore, the PV power forecasting methods can afford them motivated sustenance, and so, they can help the energy management system (EMS).

This review paper suggests the best strategy for building a PV power forecasting model, which, firstly, includes the analysis of the time horizons that means the time between the present and the future times. Several time horizons are considered by the literature. They include the very short term also called the “now-cast” or “intrahour,” which often begins from nearly seconds and ends in few minutes. 0–6 h which is also considered by the literature, as well as the short term, considers 24 hours or day-ahead forecasts; these time periods are generally expedient for utility scheduling and microgrids. In addition, other time horizons including the medium term, which is planned from several hours to several days, and the long term, which is organized from several days to several months, are used for the engine maintenance. Furthermore, the spatial horizon is revealed in the literature, which is strategic for PV power forecasting since it can display the total space foreseen by a forecasting method. This forecasting horizon, meanwhile, can include the single site and the multisite (regional forecasting) [2]. Secondly, the process of PV power forecasting consists of choosing the accurate methods and approaches of forecasting. In this case, the survey of the literature detailed that the PV power forecasting is possible by the direct and indirect methods. The direct methods consist of estimating directly the quantity of PV power foreseen in a future time horizon. In this situation, the experts suggest the artificial intelligence and machine learning techniques for short-term PV power forecasting [3, 4]. The indirect methods consist of transforming the result of solar irradiation forecasting to the PV power forecasts through the solar PV model [5]. For instance, the literature examination showed three main possible approaches destined for PV power forecasting [6]. They involve the physical performance or real PV model, the statistical approach including the methods of artificial intelligence and machine learning, and the hybrid approach, which consists of the combination of multiple techniques of different approaches or cooperation between techniques of the same approach. Indeed, other approaches exist which include the time series models, regressive models, and probabilistic models.

The objective of this review paper is abridging and expounding the principal components of PV power forecasting design by presenting the insightful analysis of several research publications. To that end, this deep analysis conducted through this review paper has shown a gap in the application of some standard accuracy metrics (SAMs) that are often used to validate the right forecasting method. Such as the research paper by Dong et al.[7] that indicated the

result of Error Maximization-Kalman Filter model implementation which is best in the term of MAPE and does not it really in the term of RMSE. Therefore, the one can find the best result by using a specific metric and does not find it by using another one. In this case, the present review paper opens a way to do the research in the normalization and generalization of standard metrics. The research papers by Vallance et al. and Zhang et al. [8, 9] in the standard accuracy metrics are very helpful for the future research, in which they contain an ensemble of new assessment criteria for enhancing the quality and accuracy of PV power forecasting models. The analysis conducted through these papers showed two new metrics: the first one is called the temporal distortion mix, and the second one is called the ramp metric.

Moreover, this review paper presents a complete study on time horizons by focusing the attention on the short-term PV power forecasting due to the expediency of this time horizon in several applications including the planning and scheduling, the unit commitments, the microgrids, and the electric vehicles (EVs). In addition, this review paper tackles the utility of PV power forecasting in numerous fields, which is the novelty and the value added.

The remainder of this paper is structured as follows: the first section covers the overview of spatial and time horizons, methodologies, and models recently applied for PV power forecasting. The second section recommends the artificial intelligence models and machine learning techniques as the benefit value to the PV power forecasting. The third section puts in a current literature analysis of several research papers conducted in different time and spatial horizons along with a profound study regarding the technical and economic benefits of PV power forecasting in the smart energy. Finally, the last section displays the feasibility study concerning the time utility scale for PV power forecasting.

## 2. PV Power Forecasting Spatial and Time Horizons

The modelling of PV power forecasting is pertinent when picking up the right time horizon and the resolution of forecasts. Therefore, the time horizons are defined as the time between the present and the future times of forecasting, and they can include the very short term that is considered from few seconds to few minutes, also including the “now-cast” and the “intrahour,” the time horizon of 0–6 h, the short term or day ahead that is considered up to 24 hours, the medium term that starts from several hours to several days, and the long term that begins from several days to several months.

In addition to the time horizons, the spatial horizons are also relevant in the forecasting system design and can be ranged from the single site to the regional area including several PV plants (multisite forecasts) [10].

*2.1. Very Short-Term, 0–6 h, and Short-Term Time Horizons.* The time horizons are the key for clustering forecasts. In addition, the forecasts made in various time horizons are

very stimulating in the diverse phases of grid operating, such as maintaining the grid permanency, the scheduling of rotating reserves, load monitoring, unit commitments, and other integrated generations such as microgrid planning.

*2.1.1. Very Short-Term Time Horizon.* The very short-term time horizon for PV power forecasting, also called the PV power immediate forecasting, covers time scales from few seconds to few minutes. This time horizon, meanwhile, is the key to ensure the grid operator by planning the energy reserves and meeting the consumption demand. This becomes a critical issue when considering stand-alone grid with deprived quality and strong solar penetration. Therefore, the very short-term time horizon is advantageous for controlling the power distribution, and it can help in dropping the number of transformer operations.

In addition, the very short-term time horizon is applicable for particular bids such as the manufacturing applications (e.g., solar airplanes and solar cars). However, this time horizon strongly obeys to the weather parameters such as the clouds' motion which comply with the physical rules; their stormy deportment is stochastic and not simple to model [11]. In this item, several research studies were proposed such as a system based on sky imaging which is used to decide the speed and the stability of clouds by [12]. A useful review paper including deep study of very short-term PV power forecasting with several useful techniques regarding this time horizon is available in [13]. For more literature study and analysis, Table 1 presents a summary of the literature in the very short-term time horizon, and Table 2 corresponds to a current literature review which carried out the methods, time, and spatial horizons and results. As a result, from the literature study, the techniques of artificial intelligence are the most important models for the very short-term time horizon. Nevertheless, this time prospect needs further accomplishment materials and additional advances in the digital technologies such as high-resolution cameras and unconventional satellites.

*2.1.2. 0–6 h Time Horizon.* The 0–6 h or intraday time horizon generally ranged from zero to six hours (0–6 h). This time horizon was used for both load control and monitoring and the power system operators, particularly for solar energy markets [16]. This time horizon was already revealed by several research papers. In this review paper, we discuss some research papers such as Zhang et al. employed the persistence model of cloud in order to improve the forecasting modelling of PV power, respectively, in one hour-ahead and one day-ahead. This forecasting approach employed the data of past PV power and NWP [9]. The hybrid techniques are also practical for 0–6 h PV power forecasting which consisted of combining multiple techniques to forecast the PV power, as well as the hybrid approach is more powerful in the front of other approaches [32].

Indeed, other references and techniques used in the 0–6 h time horizon are presented in Tables 2 and 3 which

show some precious references regarding the methods, the results, and the data sources.

*2.1.3. Short-Term Time Horizon.* The weather conditions greatly affect the capacity of solar PV power generation. At the same time, the daily energy produced by PV systems depends on the weather such as the relativeness of PV power to the irradiance in the plane of array, the air temperature, and the wind speed, which themselves depend on the day, the month, the year, and the season. However, this dependability makes the energy planned for grid integration variable, which consequently makes out undesirable scenarios to the electric grids regarding their stability, reliability, and operation scheduling, sideways of the economy losses. For that reason, the forecasting techniques can answer this stropy condition of weather variability and get back the information about the quantity of solar PV power generation in the future time horizons. Therefore, the forecasts from 6 am until the day before are also called short-term forecasts. They cover the times beginning from 6 hours to 48 hours ahead. They are typically practical for planning and unit commitments. In addition, they support the EMS to answer the grid operator demand. However, they are relative to the rent of the PV system, methods, and input data as shown in Tables 2 and 4, which summarize various research studies conducted in the short-term time horizon by focusing on the methods, the inputs, and the results.

In addition to the techniques shown in Tables 2 and 4, other worthwhile research studies were found in the literature such as Das et al. added a review paper in the topic of solar PV power forecasting which consisted of methods used for various time horizons including the short term along with the optimization techniques used for improving the results of forecasting. At the same time, they included genetic algorithm (GA), PSO, grid-search, FOA, firefly algorithm (FF), CO, chaotic ant swarm optimization (CASO), chaotic artificial bee colony algorithm (CABCA), and artificial intelligence [68]. Furthermore, the recent review papers by [3, 4] put on the literature review of recent methods that are used in PV power forecasting which includes the methods of artificial intelligence, machine learning, and deep learning algorithms. These models are considered by this review paper as the boosted techniques for PV power forecasting reliability.

*2.2. The Spatial Scale for PV Power Forecasting.* The techniques of forecasting used to predict the power produced by a single module or by a solar plant are useful for a single site (city, a rural area) or a regional area (utility-scale solar power system forecasting) [10]. The regional forecasts are practical for providing the grid operator by the information on the future energy and consequently maintaining the balances between supply and demand. In the order to make some differences between the solar forecasting applied to the single and the regional area, the experts suggest the study of variability of PV power in the short-term time horizon. This variability is due to the nature of solar resources and geographical specifications.

TABLE 1: Summary of the literature review in the very short-term time horizon.

References	Methods	Inputs	Best results
[12]	Cloud speed forecast (VOF and CCM forecasting techniques)	PNG images	FS = 0.19
[13]	NWP model, sky images, satellite images, cloud cover, and the time series models	—	—
[14]	SVR-2D	Past PV power and weather data	MRE = 9.65% MAID = 108.33 kW ICP = 73.07%
[15]	Cloud speed persistence	Solar power output data of 96 inverters and cloud motion data	RMSE = 4%
[16]	Machine learning techniques based on ANNs and support vector regression (SVR)	Past data of PV power and weather parameters	—
[17]	Regression tree (RT) method applied for 3 cases (cloudy day, clear day, and yearlong)	Past data of weather parameters and PV power	NRMSE = 13.8 %

Furthermore, the regional forecasts are characterized by the decrease in the error. This error, meanwhile, has an exponential curve of the distance between stations [31]. Subsequently, the process of regional forecasts can include the following: (a) the knowledge of the PV power generation from all PV systems. (b) The knowledge of PV power only at certain PV plants and not at the regional level. (c) The knowledge of the amount of energy produced by only regional sites. (d) If no photovoltaic energy data are available, in this case, it is always possible to use the solar irradiance forecasts and then their conversion to the power through a PV system model.

The literature survey, in the meantime, showed several approaches that tackled the regional forecasts. However, they depend on the data availability. The summation of individual forecasts is still used by da Silva Fonseca et al. [69], whereas Persson et al. presented a nonparametric machine learning approach applied for multisite PV power. In this case, the past data of power generation and relevant meteorological variables related to 42 rooftop installed PV power systems are used to form the forecasting model [10].

In addition, for calculating the installed capacity of PV panels in an area, the following equation can be used:

$$P_{\text{pred}}^{\text{reg}} = \frac{P_{\text{cap}}^{\text{reg}}}{I_{\text{ref}}} K \sum_{i=1}^n A_i I_{\text{POA},i} \quad (1)$$

where  $I_{\text{ref}}$  is the nominal irradiance,  $P_{\text{cap}}^{\text{reg}}$  is the PV power capacity,  $K$  is the ratio between the system coefficients,  $I_{\text{POA}}$  is the irradiance on the plane of array, and  $A$  is the accumulation of weights specified to the forecast of solar irradiation that ranges the PV panels correspondingly to a certain tilt angle and orientation; consequently, its form is given by the following equation:

$$\sum_{i=1}^n A_i = 1. \quad (2)$$

### 3. PV Power Forecasting Approaches and Methods

The selection of convenient forecasting time and/or spatial horizon and the appropriate forecasting approach are primal in

the forecasting process. In this case, the methods are classified into three important approaches: firstly, the physical approach which is based on the PV power model, secondly, the statistical approach which is based on the artificial intelligence and machine learning methods, and thirdly, the hybrid approach, which is based on the mix of the techniques of the same approach or the techniques belonging to the other approaches.

**3.1. Naïve Models.** The PV power is also foreseeable by the techniques of persistence, also called the naïve models, which are commonly practical as the benchmarking models.

**3.1.1. Naïve Persistence.** A naïve model assumes that the expected power over the future time horizon is similar to the power in the past time horizon as shown by equation (3). This model, meanwhile, is normally used for the stationary time series. Since the solar time series are not stationary,

$$P_n(T+h) = P(T). \quad (3)$$

In general, the naïve persistence is restricted to very short-term or intrahour applications. This technique involves breaking down of the PV power production into a stationary and a stochastic component. However, the stationary term is typically allied with the production in the clear sky condition, whereas the stochastic term is associated to the cloud that induced the changes in the PV power production [5].

**3.1.2. Smart Persistence.** A smart persistence model is usually used when the variable is no longer stationary. The mathematical form of a smart persistence model is given by equation (4) which corresponds to the best implementation of this technique:

$$P_i(T+h) = \begin{cases} P_{nc}(T+h), & \text{if } P_{nc}(T) = 0, \\ P_{nc}(T+h) \frac{P}{P_{nc}(T)}, & \text{otherwise,} \end{cases} \quad (4)$$

where  $P_{nc}(T)$  is the projected power when the sky is clear. In the periods of low variability and short-term time horizons, the power  $P_{nc}(T)$  is very accurate [70].

TABLE 2: Current literature review in the PV power forecasting including the references, methods, time and spatial horizons, and results.

References	Methods	TH	Inputs	Best results
[18]	Persistence, MPL, CNN, LSTM, and LSTM full.	VST	Past PV power data and sky images.	RMSE = 15.3%.
[19]	The component methods including SARIMA, ETS, MLP, STL, TBATS, theta, NWP, MOS, temporal reconciliation (TmpRec), and geographical reconciliation (GeoRec). The combined forecasts including simple averaging, Var, ordinary least squares (OLS), least absolute deviation (LAD), constrained least squares (CLS), subset, AIC, lasso, and Oracle.	ST	Past PV power.	NRMSE = 15.4%.
[20]	Probabilistic forecast based on the Gaussian process (GP) and the reference model based on ARIMA.	0–6 h	Household electricity consumption and past PV power.	NRMSE = 8.2% PINAW: 12.4% PICP: 87.57%.
[21]	GA + PSO + ANFIS compared to BPNN, and LRM.	ST	Past PV power data and NWP data.	NRMSE = 5.48%.
[22]	WT, FNN, ELM, and cascade forward BPNN (NewCF) learned with different learning methods.	ST	Past PV power, air temperature, wind speed, and humidity.	MAPE = 3.10%.
[23]	RF, fuzzy C-means (FCM), sparse Gaussian process (SPGP), and improved grey wolf optimizer (IMGWO).	ST	Past PV power data.	NRMSE = 6.5%.
[24]	Models for clear sky weather: SARIMA, W-SARIMA, RVFL, W-RVFL, and SVR. Models for cloudy/rainy weather: SARIMA-RVFL hybrid model.	VST	PV power data.	RMSE = 9.34%.
[25]	SVM, MLP, multivariate adaptive regression spline (MARS), and SVM-MLP-MARS.	ST	Past PV power, wind speed, wind direction, temperature, relative humidity, GHI, and DHI.	RMSE = 21.41%.
[26]	CNN	VST	PV power and sky images.	RMSE = 2.5 kW.
[27]	CNN, LSTM, and the hybrid model of CNN-LSTM.	ST	Wind speed, temperature, relative humidity, GHI, DHI, wind direction, current phase average, and active power.	RMSE = 0.9 kW.
[7]	Uncertain basis function method (UBF): UBU (uniform), UBG (Gaussian), and UBP (Laplace). Stochastic state-space method (STS): prediction minimization error and expectation maximization and Kalman filter (EM-KF).	VST	Past PV power and solar irradiance.	NRMSE = 8.11% MAPE = 5.81 %.
[28]	CNN with the rectified linear activation function (RLAF), the multiheaded CNN of 4 CNNs, the CNN-LSTM, and the ARMA.	ST	PV power, irradiation, module and ambient temperatures, and wind speed.	RMSE = 0.046 kW.
[29]	CNN, residual network (RN), dense convolutional network (DCNN), theta, ETS, SVR, RFR, physical, MPL, and the hybrid of RN-DCNN.	ST	Past PV power and NWP data.	MSE = 0.152 kW.
[30]	Hoff, Perez, Lave, variability reduction index (VRI)—gene expression programming (GEP) and WT-ANFIS models.	0–6 h	Irradiance data and weather conditions.	RMSE = 9.52 %.
[31]	Similarity algorithm (SA), KNN, NARX, and smart persistence models (SPMs).	ST	Past PV power, air and module temperatures, wind speed, wind direction, humidity, and solar irradiance.	RMSE = 2.3% RMSE = 0% RMSE = 5.9%.

TABLE 3: Summary of the literature review in data sources for the intraday time horizon.

References	Data sources
[16, 33–54]	NWP data
[9, 55, 56]	Endogenous data
[14, 55–58]	Meteorological records
[39, 59, 60]	Records from nearby PV plants
[61]	Past GHI data

A smart persistence model can be separated into stochastic and clear sky PV power production parts as shown by equations (5) and (6) [5]:

$$P(T) = P_{nc}(T) + P_{nl}(T + h), \quad (5)$$

$$P_i(T + h) = P_{nc}(T + h) + P_{nl}(T), \quad (6)$$

where  $P_{nl}(T)$  is the stochastic term.

TABLE 4: Summary of the literature review in the short-term time horizon.

References	Methods	Inputs	Best results
[62]	Quantile regression forest (QRF) method and 3 selecting methods, which are previous, KT, and Kolmogorov–Smirnov distance (KS). The result classification is based on the daily clearness index (KTd). At the same time, 3 classes are cloudy, partially cloudy, and clear days.	The past values of power, POA, temperature, wind, and NWP data.	NRMSE = 3.29%.
[63]	Prediction interval centred on the maximum likelihood estimation method, SVR for analysing the relationship between the input data and the NWP data (mesoscale model, GPV-MSM).	The past values of power and NWP of temperature, RH and cloud cover (CC), and extraterrestrial irradiance (EI).	The annual forecast error coverage with prediction intervals = 85–95% and the error aggregation of 1.5%.
[64]	Machine learning with functional analysis of variance (FANOVA), North American mesoscale model (NAM), (NOAA), rapid refresh (RAP), and high-resolution rapid refresh (HRRR).	GHI, DNI, temperature, and wind speed taken from NWP. However, the vertical atmospheric and cloud profiles and surface albedo are used to calculate the DNI.	RAP/HRRR/NAM: MAE is less than 2 MW.
[39]	The gradient boosting (GB) technique for the deterministic prediction technique and K-nearest neighbour (KNN) regression for probabilistic forecasts.	The NWP variables taken from ECMWF and past values of the PV system and from the adjacent PV power plants.	—
[16]	ANN and SVR techniques.	Inverter historical power data, NWP of temperature, wind direction (WD), and solar geometry (SG).	RMSE = 182.6 kWh.
[51]	Probabilistic forecasting based on the voted set of QRF and fixed random forest (RF) methods.	The NWP data and earlier values of power.	—
[65]	The prediction bands based on time series equations and algebraic viewpoint and the test of normality based on the algebraic setting of Jarque–Bera, Kolmogorov–Smirnov, and Lilliefors theories.	The data for one day collected from the rent of two PV systems based in France country.	The mean interval length (MIL), the prediction interval coverage probability (PICP), and the best cooperation between MIL and PICP obtained according to the clear sky index.
[66]	MLP, PHANN, and clear sky radiation model (CSR) for sunny and cloudy conditions.	Irradiance, temperature, day, and clear sky index.	MAPE = 10%.
[67]	Adaptive-network-based fuzzy inference system (ANFIS) and PSO-ANN models.	One year of input data including actual recorded PV power from the PV system rent in the northeast of Thailand country, solar irradiance, module temperature, and air temperature.	RMSE = 0.1184%.

3.1.3. *The Persistence of the Ramp.* In the short-term time horizon, the persistence of the ramp is normally practical. Therefore, it is beneficial for prolonging the deviation of the electricity production during the previous second to stay on the forecasting time horizon as shown by equations (7) and (8) [5, 15]:

$$P_r(T+h) = P(T) + k_{ASC}[P_{nc}(T+h) - P_{nc}(T)], \quad (7)$$

where  $k_{ASC}$  is the fraction of the current power and that in a clear sky condition

$$P_r(T+h) = P(T) + h[P(T) - P(T-1 \text{ second})]. \quad (8)$$

Furthermore, in the case of clear sky conditions and the clarity clue relations, the readers are invited to check

equations (1) and (2) in the review paper by Antonanzas et al. [5].

3.2. *Physical Approach.* The conversion of GHI into the PV power is not a technique of forecasting. In the meantime, other variables such as the temperature and wind forecasts are typically coming from NWP models. A physical approach employs the PV system parameters and does not require any further historical data; however, it is totally depended on the NWP models. Therefore, inaccurate NWP data can be a source of errors [71]. For that reason, the MOS are used to escape these errors, but they are strongly relative to the weather forecasts, and they involve the past meteorological data. To deepen the understanding of the PV power

modelling, bookworms are referred to check the research papers by Do et al. and Bessa et al. [71, 72].

In this case, this review paper wants to update the readers by the fresh references available in the physical approach part; however, the literature review does not cover enough research in this section. Furthermore, the analysis of the literature covered by this present review paper does not include the techniques used for the solar irradiance forecasting. To that end, the readers are invited to check out some beneficial references on the solar irradiance forecasting such as [73, 74].

**3.3. Statistical Approach.** A statistical approach corresponds to the data-driven model. The main process of this approach is often based on the extraction of the relationships for the earlier data in order to forecast the future performance of a PV power plant. The statistical models have the capacity to adjust the systematic errors; consequently, they have shown better performances than the PV performance models [75]. In the meantime, the inputs of models are optimized and organized by an application of optimization algorithms that selects the inputs that give the best results and make a compromise between stress and accuracy. The literature analysis revealed that the statistical approach is commonly used and often provides better results in comparison to the physical approach. Some techniques such as the stepwise regression by Fonseca et al. [76] and the principal component analysis (PCA) by Monteiro et al. [63] presented better results. Furthermore, Tables 2 and 5 offer some worthwhile references related to the application of statistical methods in the solar PV power forecasting.

**3.4. Hybrid Approach.** A hybrid approach consists of combining the forecasting techniques belonging to the same approach or the mix of techniques belonging to other approaches. Therefore, the combination of models is achievable by many conducts, such as the bagging, strengthening, voting, or stacking. A hybrid forecasting approach, meanwhile, can be realized through a combination of statistical, physical, and probabilistic methods, and it is often used in the literature. In this section, we present to the reader the most combinations found in the literature which are the autoregressive integrated moving average (ARIMA) technique combined with the ANN technique employed by Fonseca et al. [76] and the ANN and NARX models tested by Lorenz et al. [60]. In addition, grouping of the gradient-descent optimization technique and ANNs is used to establish the forecasting model. In this point, the metaheuristic optimization model, called shuffled frog leaping algorithm (SFLA), is developed to check the optimal parameters of ANNs by using the initial individuals found by the gradient-descent optimization method. In the meantime, the past solar power values of 5-, 10-, and 15-minute periods are used to feed the forecasting model. In this study, the forecasting model has given the best results in terms of MAPE [83]. In addition, grouping of ensemble forecasting methods was based on 142 models from six families that are the SARIMA family (36 models), ETS family (30 models), MLP (1 model), STL decomposition (2 models), TBATS family (72

models), and the theta model (1 model). The forecasts, meanwhile, were made by (1) simple averaging, (2) the variance-based grouping, (3) the least squares regression, (4) the least absolute deviation regression, (5) the constrained least squares regression, (6) the complete subset regressions, (7) the Akaike information criterion- (AIC-) weighted subset regressions, and (8) the lasso regression. This study, meanwhile, was established for the one day-ahead operational PV power forecasting and based on both the data diversity and the NWP data. Therefore, the forecasting model has given better results in terms of AIC, NMBE, FS, Kolmogorov-Smirnov test integral (KSI), and NRMSE [19]. At the same time, a research paper proposed a forecasting tool based on time-series models and their analysis which taken into account the nonstandard analysis which corresponds to the infinitely small and infinitely large numbers, this analysis take a time interval  $[0,1]$ . Furthermore, the Cartier-Perrin theorem is also used for time series analysis. This study, meanwhile, was established for a time horizon of short term and based on the full-year data collected from two sites located at Nancy in the east of France and Ajaccio in Corsica, a French island in the Mediterranean Sea. Consequently, the forecasting process has given a better-quality model in terms of MIL stems from the MRL and the prediction interval coverage probability (PICP) [65].

As a conclusion of this section, the hybrid approach is considered by the literature as the boosted technique for the reason that it takes the advantages from both physical and statistical approaches. For more research studies in this section, Table 2 affords the recent references available in the hybrid forecasting approaches and applied for different time horizons.

**3.5. Probabilistic Approach.** The probabilistic methods considered by the literature as the advanced approach of PV power forecasting added the concept of limits (upper and lower) in the aim to provide more accurate data by using the probability density function (PDF). The survey of the literature showed many research papers that used the probabilistic methods such as Lorenz Kühnert et al. who used the grouping between the statistical and probabilistic methods to generate the PV power forecasting in the time horizon of 0–6 h ahead. The proposed model, meanwhile, was based on the vector autoregression framework, whereas the parameters of forecasting used in this study were the solar PV power time series and distributed time-series information collected from the smart grid infrastructure. Therefore, the proposed forecasting tool presented better results in terms of RMSE and continuous ranking probability score (CRPS) in which they were susceptible for evolving the grid management functions [59]. Moreover, Sperati et al. developed a model based on the grouping between the statistical and probabilistic approaches which were based on the PDF method. The ANNs, meanwhile, were used to reduce the model bias and to generate the PDF of PV power. At the same time, the variance deficit (VD) and the ensemble model output statistics (EMOS) methods combined with the ensemble prediction system (EPS) were used to produce the skillful probabilistic forecast (SPF) in numerous weather

TABLE 5: The references of the statistical methods used in the forecasting approach.

References	Approaches
[14]	Grid-tie PV power-forecasting model for 0–6 h ahead, also called the 2D-interval forecasts based on SVR-2D, that computes directly the 2D-interval forecasts from the previous historical solar power and meteorological data by using the SVR method. The parameters of the forecasting model were the solar and the weather data that included the solar irradiance, temperature, humidity, and wind speed provided from the “Australian photovoltaic data” for two years sampled for every 1, 5, and 30 min along with the past data of PV power. At the same time, the mean absolute interval deviation (MAID), MRE, and interval coverage probability (ICP) were used to perform the forecasting model accuracy.
[77]	AR model that had comparable performances with the ARMA model to produce the short-term PV power forecasting, and the forecasting parameters include the climate state of previous time samples. Therefore, the forecasting model used for false data injection attacks (FDIAs) detection showed performance results in the security and the control of power grid. To that end, the phase-phase correlation (PPC) was used for evaluating the accuracy of forecasts.
[78]	Cloud and irradiance forecasting of 15 min to 5 hours ahead based on the satellite images and SVM. The 4 years of historical satellite images, meanwhile, were used to learn the model. Consequently, this application showed an improvement for the EMS in terms of RMSE, MRE, and the coefficient of determination $R^2$ .
[79]	The parametric approach that relied on the mathematical models with several parameters that describe the PV system, whereas the nonparametric approach was based on quantile regression forests with training and forecast stages. In the meantime, the forecasting parameters are the meteorological variables from the NWP models. In this case, this forecasting model showed better results in terms of mean-based error (MBE), RMSE, MAE, and skill scores (SS). Therefore, the forecasting engine has been used for calculating the hourly power delivered to the grid.
[80]	Multilinear adaptive regression splines and persistence method used for the short-term PV power forecasting model. The forecasting parameters, meanwhile, include the weather forecasts from the “US Global Forecasting Service (GFS)” and PV power output data (estimated to 1.3 MW) of a PV power plant located in the Borkum city of Germany country. Therefore, the application of this forecasting model showed better results in terms of $R^2$ , RMSE, MAE, and MBE, and in this situation, the forecasting process was advantageous for calculating the day-ahead production from a PV power plant.
[81]	A classical statistical method based on neural network modelling. The forecasting model parameters, meanwhile, are the number of sunny hours, length of the day, air pressure, maximum temperature, insolation of the day, and cloudiness. The forecasting model showed better results in terms of Pearson’s linear correlation coefficients, kurtosis, skewness, and RMS, and it was developed to perform the short-term PV power forecasting model.
[82]	A multistep method used for forecasting the PV power in different ranges of time, respectively, 10 s, 1 min, 5 min, 30 min, and 2 hours. The forecasting model, meanwhile, was based on the persistence method and the auto regressive exogenous (ARX) model, which presented better results in terms of RMSE and MAE once trained by the forecasting parameters, which included the data from the NREL radiometer grid, Hawaii (USA), and the Microgen database, East Midlands (UK).

conditions, as well as the persistence ensemble (PE) technique was used as the benchmarking model. In addition, the PV power forecasting model parameters were derived from three solar farms located at different sites in Italy. Therefore, the forecasting model was established for the time horizon of 0 to 72 hours ahead and had given better results in terms of Brier skill score (BSS), relative operating characteristic (ROC) skill score (ROCSS), CRPS, and the missing rate error [53]. In addition, Ayompe et al. added a research paper that consisted of a probabilistic approach used for short-term (24 hours ahead) PV power forecasting. The proposed algorithm, meanwhile, was integrated with the demand-side management (DSM) algorithm. In addition, the performance of forecasting models was confirmed by the cloudiness data that included the cloud classification (low-level clouds, midlevel clouds, and high-level clouds), the weighted relative root mean squared error (WRRMSE), and self-consumed energy, as well as the RMSE, MAE, MBE, and CRPS. Consequently, the probabilistic forecasting model was beneficial for increasing the skilfulness of the DSM algorithm under various load generations in a household [84].

To conclude this section, the probabilistic approach remains as the undeveloped method; however, it needs more growth. For more studies conducted in this section, Table 2 offers the recap of some recent studies in the probabilistic models.

**3.6. Regressive Methods.** The principal role of the regressive methods is estimating the correlations between dependent variables (PV power) and certain independent variables called forecasters (e.g., solar irradiance and ambient temperature). The time series, meanwhile, can have the linear or nonlinear forms, and they can be stationary or nonstationary, whereas the regression methods such as the support vector machine (SVM) including the supervised methods are used in the classification problems. However, in the regression problems, this technique is known as the vector support regression (SVR). Therefore, this technique is stronger in the capacity of generalization and has the capacity to deal with the nonlinear problems.

Furthermore, the study of the literature showed many related research papers such as the research study conducted by Das et al. which presented a complete and methodical study in the PV power forecasting. They also examined the status of relationships between the input and the output data and the preprocessing of input data [68]. In addition, González Ordiano et al. appended a contribution in the PV power forecasting topic that consisted of the time-series forecasting techniques, probabilistic forecasting techniques of point forecast, and an outline of time horizons [85]. Moreover, Sobri et al. added a clustering of PV power forecasting methods, in which three main categories were distinguished in this paper. They consisted of time-series

models, statistical approaches, physical techniques, and overall methods [6]. In addition, van der Meer et al. proposed a comprehensive study about the practice of Gaussian methods for probabilistic forecasting of the residential electricity consumption, PV power generation, and net demand of the single household [20]. For more references and methods in this section, Tables 2 and 6 offer a recap of recent regressive methods used for PV power forecasting.

**3.7. Ensemble Methods.** The literature review indicated that this approach sets two kinds of methods that are the competitive and the cooperative. The first method, meanwhile, consisted of making the forecasting by using the individual training of models. The training process is based on heterogeneous data and parameters. The result of forecasting is consequently equal to the average of all forecasting models. The second method consisted of the split of the forecasting process into several subprocesses. Therefore, the selection of the convenient forecasting model is adaptable with the characteristics of each subtask. The forecasting result, meanwhile, corresponds to the sum of all forecasting subprocesses [33, 89].

Furthermore, the survey of the literature showed some concomitant research papers that debated this topic such as the work by Raza et al. which proposed a contribution in the ensemble methods through the multivariate neural network ensemble forecast (MNNEF) methods, including the Bayesian model averaging (BMA) technique, namely FNN, Elman backpropagation network (ELM), and cascade forward backpropagation network (CFN). In this case, the WT is used to smooth the historical of PV power data used to train the MNNEFs ensemble methods. Therefore, this forecasting tool is based on Neural Networks ensembles which generates one day-ahead PV power forecasting, whereas the forecasting parameters considered by this study are the historical PV power, air temperature, wind speed, humidity, and solar irradiance. In addition, the MAPE and  $R^2$  are used to test the forecasting model performances [22]. For more research studies and contributions in the ensemble forecasting techniques, Table 2 provides some recent studies in this field.

**3.8. Data Mining Approach.** Data mining is defined in simple terms as the process of finding useful patterns in the data. In other terms, it consisted of the knowledge discovery, machine learning, and predictive analytics, in addition to the methods of data exploration, preprocessing, modelling, evaluation, and knowledge extraction [90].

**3.8.1. Data Exploration.** Data exploration firstly clusters the descriptive statistics that are the process of summarizing the key characteristics in the dataset. The communal metrics used in this process are the mean, standard deviation, and correlation. Secondly, the process of data visualization consisted of projecting the data in a multidimensional space. In the context of data mining, the data exploration,

meanwhile, used both the descriptive statistics and the visualization techniques [90].

**3.8.2. Classification.** The predictive analytic problems are of two categories: the classification and the numeric prediction problems. In classification or class prediction, the information from the predictors or independent variables is used to categorize the data samples into two or more distinct classes or buckets, but in the case of numeric prediction, the numeric value of a dependent variable is predictable by using the values assumed by the independent variables such as the traditional regression modelling [90].

**3.8.3. Fitting Data.** The basic idea at the back of fitting function is its practicality for forecasting the value (or class) of a dependent variable. In the meantime, the function of fitting involved several methods. The most common ones are of two categories: the linear regression for the numeric forecasting technique and the logistic regression for the classification technique [90].

**3.8.4. Association Analysis.** The objective of this class of data mining algorithms is finding usable patterns in the co-occurrences of the items by measuring the strength of the co-occurrence between one item and another [90].

**3.8.5. Clustering.** The principal role of clustering is simply to capture the possible natural groupings in the data by clustering all meaningful groups' data. The clustering, meanwhile, is usable for describing the dataset and used as a preprocessing step for other predictive algorithms [90].

**3.8.6. Time-Series Forecasting Models.** The time-series forecasting models are the oldest known predictive analytic techniques including the supervised models that consisted on collecting the data from several different attributes of a system that are used to fit a function in order to predict the desired quantity or target variable, for example, in our case of PV power forecasting, the target variable corresponds to the PV power. Some recommendations for time series models are that, firstly, they needed the choice of the appropriate forecasted variable. However, the presence of the noise component also called the nonsystematic component which is by definition random [90].

**3.8.7. Time-Series Analysis Methods.** The process of time series forecasting corresponds to the descriptive models or time series analysis and the predictive models. This process is based on the decomposition of the data into a trend component, a seasonal component, and a noise component. The trend and seasonality are also called the systematic components that are predictable. However, the noise component is called the nonsystematic component, and it is random [90].



TABLE 6: The most popular regressive models in the literature.

References	Methods
[86]	Artificial intelligence (AI) techniques including the MLP, NN Delay, recurrent Elman NN, NN radial basic function, ANFIS, adaptive resonance theory (ART), and $k$ -NN techniques.
[59]	Point and probabilistic forecasts based on multivariate models such as autoregressive (AR), vector AR (VAR), and vector ARX (VARX). Therefore, VARX is the most accurate model with NRMSE = 8.5%.
[14]	The techniques of SVM and SVR.
[87]	Nonlinear stationary models including nonlinear-AR exogenous (NARX).
[88]	Random forests (RFs) that are the set of decision RTs. The analysis of the literature in the PV power forecasting showed the best results from RFs in terms of average forecasting for individual trees. In addition, the bagging technique that involved the increasing analysis to understand the complete trees, respectively, with a sample initiated from the entire training set. Nevertheless, the RFs deal with this problematic with a feature encapsulation that involves the choice of an unplanned subgroup of entities at each node. The feature encapsulation, meanwhile, reduced the error of correlation.

**3.8.8. Feature Selection Methods.** The feature selection methods are simply filters that eliminate some attributes; they are of two categories: filter type and wrapper type. The filter approach is based on selecting the only attributes that meet certain stated criteria, whereas the wrapper approaches randomly selected the feedback of attributes that improve the performance of the algorithm. The filter approach, meanwhile, does not require any learning algorithm. However, the wrapper type is based on the optimization through a learning algorithm [90].

**3.8.9. The Quality of a Predictive Model.** The survey of the literature showed three best techniques which were used to test the quality of predictive models including the confusion matrices (or truth tables), lift charts, and receiver operator characteristic (ROC) curves. The evaluation of regression models, meanwhile used for numeric predictions, is based on conventional statistical tests [90].

**3.8.10. Anomaly Detection.** The process of finding the outliers in the dataset is called anomaly detection. The outliers, meanwhile, are the data objects that stand out amongst other data objects and do not conform to the expected performance. The outliers usually bias the forecasting process result [90].

**3.9. Machine Learning Approach.** The machine learning (ML) approach is actually the advanced algorithm that upholds the use of data at their raw form [91]. In the meantime, the survey of the literature showed several applications of ML in the process of PV power forecasting, as well as model implementation, such as the research paper by Amaro e Silva and Brito who carried out a study in the PV power forecasting for a time horizon of one day ahead. The approach, meanwhile, based on the extreme learning machine (ELM), that is a novel algorithm is used to train the feedforward neural networks. At the same time, this method was used for elaborating three models designed for three weather types (sunny, cloudy, and rainy), whereas the input data are the past PV power records from a PV plant. In order to compare their results, the method ELM was used in this study alongside the BP neural network

technique. The MAPE and NRMSE were used to test the accuracy of models [92]. In addition, Teneketzoglou et al. appended a basic ML approach that consisted of implementing ELM without exogenous inputs. At the same time, the ELM algorithm was used in this study for training a single hidden layer feedforward neural network. The ELM algorithm, meanwhile, used to forecast the PV power for a time horizon of very short term (5 min ahead) was based on 10 historical days of PV power. Subsequently, ELM was excellent in the front of the gradient-based learning method in terms of overtraining and local minima. Furthermore, the proposed model in this study has been compared to the time delay neural network (TDLNN) technique in terms of RMSE and NRMSE [93]. Moreover, Zhang et al. added a study based on the ML approach which consisted of using a mix of probabilistic intervals (PIs) for point forecast and the stochastic gradient boosting machine (SGBM) that are used for total loss function optimization. The association of SGBM, least square error (LSE), and least absolute error (LAE), meanwhile, was used to process the point forecast generation, unlike the PIs with multiple quantiles that were used for both probabilistic and point forecasting. At the same time, the input data of models were based on weather data such as the air temperature, humidity, solar irradiance, and wind speed, along with one year of PV power recorded (from 2012 to 2013); for precision, the time between samples was one minute. Therefore, the model assessment indicates that the SGBM method was very accurate than the ELM method in terms of MAE and RMSE [94]. At the same time, Luo et al. proposed a model of ML that consisted of mix of the fuzzy clustering method along with the grey correlation coefficient algorithm that was used in this study to select the similar days. In the meantime, the ELM method generated forecasts of PV power and was based on historical data of similar days. Furthermore, the GA was engaged in this process to overawe the problem of overfitting. The input data, meanwhile, correspond to the historical similar days of meteorological data including the highest, lowest, and mean value of solar radiation, humidity, and temperature and wind speed of the desired forecasted day. Additionally, the RMSE and MAPE were used in this study for testing the accurateness of forecasting models [95]. In addition, Theocharides et al. appended a recent study in the short-term PV power forecasting based

on ML algorithms that include the ANNs, SVR, and RTs along with the varied hyperparameters and feature methods. The input data of models are the forecasts of weather variables provided by NWP, satellite images, sky images, and other yearly historical data. In the meantime, the MAE, MAPE, RMS, SS, and NRMSE were used for testing the accurateness of models [96]. Moreover, for more techniques and studies in this field, Table 2 provides more information about ML that was used for PV power forecasting in various time horizons.

**3.10. Deep Learning Algorithms.** The basic idea of the deep learning neural network (DNN) comes from the use of multilayer perceptron that consisted of organizing the nonlinear modules of a given task into multiple layers. They are part of the artificial intelligence techniques, and they have many utilizations in the real life such as in the health care (tumour predictions), in the traffic (vehicle speed prediction), and in the renewable energy (detection of wind turbines fault, etc.). Furthermore, the DNN techniques are practical in the renewable energy forecasting for both PV and wind power. At the same time, they have many pros such as their usefulness in the noisy environment, in which they can filter and extract the data needs. In the meantime, they can display some visual analytic graphics after the training process. In addition, they offer the data discrimination possibility. In addition, they can classify the unstructured data as structured ones by applying some strategies such as deep belief method (DBM) or convolutional neural networks (CNN), as well as they can solve many problems by a near similar manner to the human brain. However, the deep learning algorithms are not far from challenges that are the need to supplement CPUs or GPUs. For the prerequisite of high volume data for the success of such networks, they have the problem with overfitting and suffer from the hyperparameter optimization problem [91].

The analysis of the literature showed some outstanding research studies in the PV power forecasting based on the DNN approach such as the research conducted by Zhang et al. who proposed a study on the deep PV now-casting forecasting model that consisted of PV power forecasting by using the DNN fed by multiple historical sky images. This model was compared to the CNN, long short-term memory (LSTM), and MLP methods [18]. In addition, Lee et al. appended a new study on one day-ahead PV power forecasting based on the DNN algorithm. This research paper, meanwhile, consisted of a question about the usefulness of the short-term memory recurrent neural network algorithm for data pattern recognition. In this case, the TensorFlow tool was used for the training process and based on data provided from multisite PV power. The input data are the total generation, output voltage and current, power factor, wind speed, wind direction, PV module temperature, ambient temperature, and weather information from the Korea Meteorological Administration. Consequently, the forecasting process was used to connect with the EMS [2]. Recently, the review papers by Ahmed et al. and Mellit et al.

[3, 4] offered the detailed studies on PV power forecasting models in which they confirmed that the capacity of deep learning methods is clear in the handling of big data and can afford a better solution for solar PV power forecasting; therefore, they can be considered as the revolutionary methods in this topic. Moreover, for more data about DNN techniques, [97, 98] give a deepen knowledge.

As a conclusion to this part of this review paper, the DNNs are characterized by an important number of neurons in which they suffer from two problems that consist of less fitting when the number of iterations is too few and overfitting when the number of iterations is too many. Therefore, the experts confirmed that the larger the number of hidden layers, the deeper the depth of the DNN. Moreover, the commonly used activation functions in a learning process include sigmoid, tanh, ReLU, and Leaky ReLU. In the meantime, ReLU is typically the most used activation function [99]. For more information about the literature review and the applications of the DNN, Table 2 shows the recap of some recent studies in the DNN and used for PV power forecasting.

#### **4. Study of the Current Literature in the PV Power Forecasting**

This section offers a careful study and analysis of the recent literature from the period of 2015 to 2020 of some selected research papers in the PV power forecasting as presented in Table 2. The aim of this table is to bring the reader useful information on the PV power forecasting methods and their corresponding time horizons (THs) alongside the inputs that have been used and the findings. The results found are presented by using the standard average metrics (SAMs). Therefore, this approach can help the reader to pick the PV power forecasting method easily without returning to the main paper.

#### **5. Study of the Current Literature in the PV Power Forecasting Operations**

The presence of renewable energy in the electrical systems needs the management, planning, and scheduling of power systems and the grid's power control. Subsequently, the forecasting methods can be used for resolving those problems. In the meantime, this review paper presents the literature review of some applications of PV power forecasting such as follows.

**5.1. The Employment of the Forecasting Methods in the Dynamic Economic Dispatch.** The forecasting techniques can be useful for the power system management as well as the dynamic economic dispatch (DED). In this case, Mahmoud et al. [100] tackled the DED with solar PV of various profiles' (clear and cloudy) proliferation. Therefore, the Salp swarm algorithm (SSA) method and the LSTM with adaptive moment estimation (ADAM) methods were used in this study. The short-term forecasting utility, meanwhile,

was based on the LSTM-ADAM method and presented the best results for DED. Moreover, Bedawy et al. [101] added a study on voltage regulations and their effect on distributed systems with the solar PV penetration. Consequently, the multiagent system (MAS) was used for voltage sensitivity control. Therefore, this study showed best results in terms of voltage deviation minimization tested for different sun profiles (sunny or cloudy), as well as the IEEE test systems were used for benchmarking utility. Furthermore, Mahmoud and Abdel-Nasser [17] appended 3 case studies relative to the weather states (cloudy day, clear day, and yearlong) in the distribution systems including high solar PV penetration. Therefore, the very short term including times of 1 sec, 30 sec, 1 min, 15 min, 30 min, and 1 hour was considered as the time observation of the distribution systems analysis. In this case, the RT method was used, and consequently, the best result was found for case 1. Therefore, the best numeric results in terms of NRMSE = 0.0138, 0.0141, 0.014, 0.0141, 0.0146, and 0.0153, respectively, for 1 sec, 30 sec, 1 min, 15 min, 30 min, and 1 hour in which they represent good results. In addition, Abdel-Nasser et al. [102] appended a study on the efficient state estimation methods (the estimation of voltages and active and reactive power losses) using the quadratic-based backward/forward sweep (QBBFS) which is a kind of ANNs. As a result, the best outcomes were obtained for NRMSE = 0.0110, 0.0312, and 0.0315, respectively, for the voltages, active, and reactive state estimations. In addition, Mahmoud and Abdel-Nasser [103] presented a research paper concerning the analysis of sequential power flow (SPF) for the active distribution systems including the solar PV. The RT method, meanwhile, was proposed for the voltage estimation. The final algorithm contained the SPF-RT and SPF-RTC with additional correction method. In the meantime, the PV and load data were used for algorithm feeding. Consequently, the best results in terms of NRMSE = 0.000263 and MRE = 0.120477 were found by the SPF-RTC method. Nevertheless, this study neglected the effect of uncertainties of PV and load which can affect the clearness of the final results. Furthermore, Marzband et al. [104] proposed a statistical approach based on the neural network combined with a Markov chain (ANN-MC) method. This technique, for now, presented an advantage for economic dispatch considering the generation, storage, and responsive load offers through the minimization of generation cost and the market-clearing price. Furthermore, the proposed approach of forecasting was used for one day-ahead and very short-term forecasts. This study taken into account the effect of uncertainties, as well as the wind-speed signal considered as the main model parameter. Moreover, Ying et al. [105] proposed a probabilistic approach based on the approximate probability distribution of the light intensity along with the dichotomy method. The proposed approach, meanwhile, was used to obtain the PV power forecasting with the interval [PV min, PV max]. In this case, the forecasting system was based on historical data of light intensity. Therefore, this forecasting model was effective to reinforce the optimality dispatching of the electrical grid.

*5.2. The Employment of the Forecasting Techniques in the Planning of Power Systems.* The PV power forecasting can be applicable in the planning of power systems. In this situation, Mahmoud et al. [106] proposed an approach for minimizing the power losses in the electrical distribution systems. In the meantime, the RPL formulation, the RPL including distributed generation (DG), and the RPL with multiple DGs were used with the IEEE test systems such as 33-bus and 69-bus for the DG allocation problem. Later, Mahmoud et al. [107] appended an efficient analytical method (EA) for optimal multiple DG installations with the power loss minimization. The method, meanwhile, included the optimal power flow (OPF) algorithm. In addition, the IEEE test systems such as 33-bus and 69-bus were used in this study for testing the RPL formulation, the RPL including distributed generation (DG), and the RPL with multiple DGs. Moreover, Mahmoud and Naoto [108] added a study about the optimal allocation of DGs including the solar PV. In the meantime, the optimal power flow (OPF) method was used for deciding the optimal sizing and the locations, as well as the promising of the best mix of various DGs, consequently reducing the power losses in the electric distribution networks. In addition, Ali et al. [109] proposed the active power curtailment (APC) for determining the optimal oversize of DG inverters as well as the voltage regulation. The approach, meanwhile, passed through the renewable energy sources and the load modelling based on the probability (beta and Weibull PDF) methods. Consequently, the results confirmed that the APC showed the best results and encouraging optimal voltage regulation with minimum total costs, as well as this method is helpful for the optimal inverter oversizing and voltage regulation, especially at different levels of DG penetration. Moreover, Luo et al. [110] added a study concerning the home energy management system (HEMS) with the penetration of renewable energy sources (RESs) such as the solar PV. Therefore, this study meant to minimize the energy cost and the peak-to-average ratio (PAR), and consequently, the proposed methods are PSO and BPSO which showed the best outcome for the energy cost of HEMS (19.7% reduced), and for both the energy cost and PAR, the reduction was 10%.

As a recommendation, the DGs can include the forecasting techniques for planning the nondispatchable energy resources such as the solar PV for power loss recovery. At the same time, the integration of the forecasting techniques can help the HEMS by getting the future data about the peak of power and, therefore, managing the load when there is less production by RESs.

*5.3. The Employment of the Forecasting Techniques in the Electric Vehicles.* The PV power forecasting can be practical for managing the changing of the electric vehicles (EVs). In this case, Ali et al. [111] added a research paper concerning the optimal day-ahead scheduling of EVs considering the uncertainty of renewable energy source generation and loads. In the meantime, the model of EV was based on the state of charge (SOC), and the PV model was based on the mathematical equations alongside the wind turbine model.

In addition, the IP method was used for interval optimization modelling, as well as the Karush–Kuhn–Tucker (KKT) condition was used for introducing uncertainties. The IEEE 33-bus, meanwhile, was used for testing the results. Consequently, this study proved that the reactive power of PV inverters and the active power of EV are preferable for minimizing the total losses as well as ensuring the voltage security. Furthermore, Ali et al. [112] appended a research paper about the plug-in hybrid electric vehicles (PHEVs). The subject of this study is optimizing the reactive power of PV inverters and the active power of PHEV smart charging, consequently controlling the voltage deviation. Therefore, the sensitivity-based (SB) and the optimization-based (OB) methods were used in this study alongside the SOS. As a result, this study demonstrated that the proposed methods are capable to mitigate the negative impacts of PV. At the same time, the reactive power from the PV inverters can reduce the required capacity of PHEVs reducing the voltage fluctuations and the voltage rise. Later, Ali et al. [113] added a research paper that tackled the problematic of optimizing the reactive power used for charging EV and, at the same time, maintaining the voltage deviations. In this case, the hull moving average (HMA) was proposed for alleviating the voltage fluctuations, as well as the gravitational search algorithm (GSA) was employed for solving the optimization model. Therefore, the IEEE 90-bus and IEEE 33-bus were used for testing the results which effectively improved the voltage deviations and optimized the charging/discharging rate of EVs. Other studies were found in the literature which carried out the EVs such as [114, 115].

Nevertheless, after the careful study and the analysis conducted through the proposed references, we did not see the use of the PV power forecasting; therefore, we recommend future studies for the application of short-term PV power forecasting.

*5.4. The Employment of the Forecasting Techniques in the Smart Grids and Microgrids.* The forecasting techniques can be helpful for the smart grids as well as the microgrids management. In this item, Wason [21] proposed the hybrid of PV power forecasting methods that was based on grouping the GA, PSO, and ANFIS. In the meantime, the binary GA with Gaussian process regression model based on the fitness function was applied to select the significant parameters of the forecasting model that significantly influence the amount of PV power generation. Therefore, the hybrid algorithm based on GA and PSO is used for optimizing the ANFIS model. This was used for one-day ahead PV power forecasting for a solar PV plant in the Goldwind Microgrid system located at China. Consequently, this PV power forecasting process was practical for the utility of electricity generation from the microgrid with high PV power penetration. In addition, Girbau-Llistuella et al. [116] developed a tool of an innovative EMS that was used to optimize the grid operation based on economic and technical criteria. The EMS, meanwhile, is used to process

the output from the forecasting model which was created by using the parameters such as the demand and renewable generation forecasts, electricity prices, and the status of distributed storages through the network. In addition, the time horizons considered in this study are, respectively, 3 days, 1 day, and 6 hours ahead. Furthermore, Abedinia et al. [117] added a study that consisted of a hybrid model for effective PV power forecasting created by using the VMD method, information theoretic, feature selection, and the forecasting engine (FE) with high learning capability. The feature selection method, meanwhile, was based on the IT criteria and an optimization algorithm. However, the FE was an MPL neural network equipped with a modified Levenberg–Marquardt learning algorithm. The forecasting model was based on the parameters such as the historical data of PV power and historical data of irradiance, weather temperature, and cell temperature. This strategy of forecasting, consequently, showed the best rate return in the Hungarian solar power plant. In addition, Galván et al. [118] added a study that consisted of using the neural networks to create the complex and nonlinear models with the output limits (upper and lower forecasting intervals). In the meantime, the proposed strategy was based on four traditional methods that are delta, Bayesian, bootstrap, and mean-variance. Furthermore, the ANNs, fuzzy logic, and PSO were used as the optimizer tools. Additionally, the effectiveness of this approach was tested by using the hypervolume that was typically used for multiobjective approaches which are employed to evaluate the excellence of the final Pareto fronts. The utility of this study, meanwhile, was the optimization of forecasting models. Moreover, Bao et al. [119] used a hybrid approach that was held in a random fuzzy theory method. The aim of this approach, meanwhile, is optimizing the scheduling model by optimizing the short-term line maintenance of the grid by taking into account the uncertainties of the PV power modelling which were based on the historical data driven out from NASA. In addition, Kroposki [120] tackled the question about the high-level penetration of variable renewable energy in the local grids and how to sustain the equilibrium between the load and the generation at all timescales. Recently, Gomes et al. [121] appended a research paper concerning the microgrid smart management with the peer-to-peer energy transaction model. In the meantime, the multiagent method was used in this study alongside the eight forecasting methods including three methods of baselines, two of weighted arithmetic average forecasts using the last periods, and three of the SVM method. As a result, the microgrid forecasting generation showed best results in terms of MAPE = 7.16% calculated for one week.

As a conclusion to this part, the research and development requirements are mostly in the PV power forecasting topic as shown in Figure 1 that pointed out the need of solar PV power forecasting that is necessary for the utilities of smart grid management, grid operations, and solar market scheduling. The most required time horizon, meanwhile, is the short-term PV power forecasting [5].

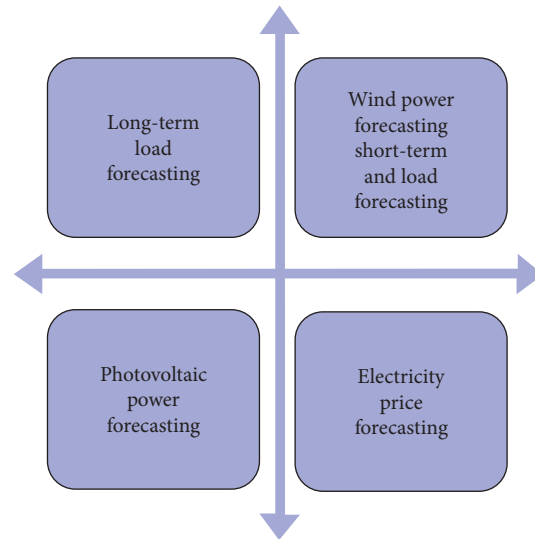


FIGURE 1: Development flowchart of different energy forecasts [5].

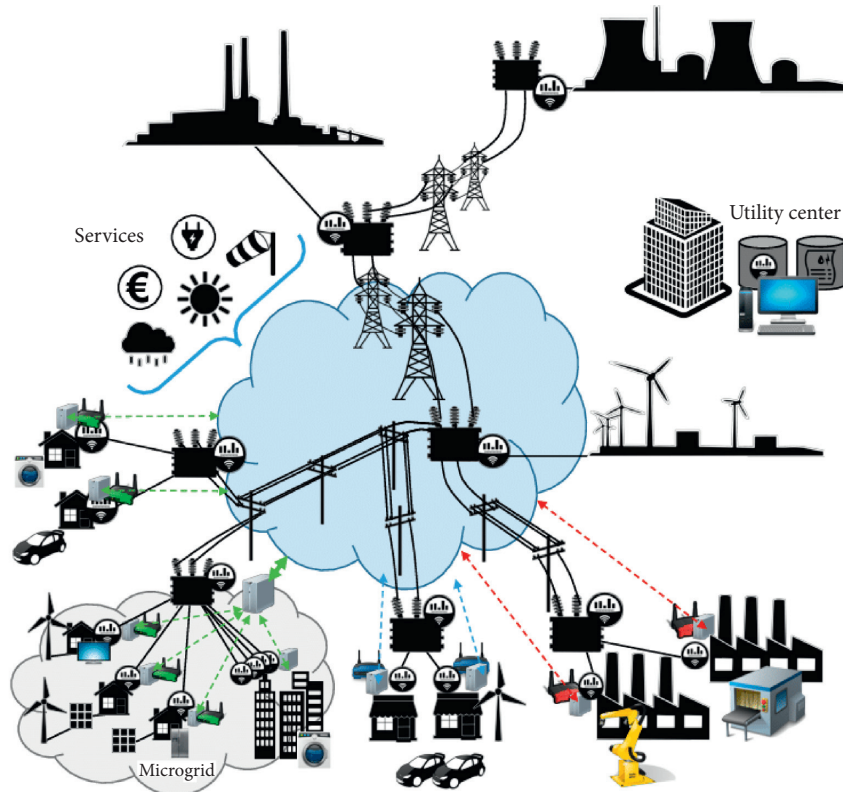


FIGURE 2: Energy penetration from numerous sources including microgrids with clean energy integration to the power grid.

## 6. Feasibility Study of PV Power Forecasting Time Horizons

The utility time scale of the short-term PV power forecasting extends to one day ahead. This time horizon, meanwhile, is applicable in the utilities of clean energy management (e.g., PV power trend curve in the near future), the solar energy market that includes planning and scheduling, and unit commitments that have used the PV power forecasting when

the PV plants cogenerate with other sources of power. In the meantime, the short-term PV power forecasting is helpful for the benefit of microgrids which hold the energy-side management system (ESMS) that rules the PV power forecasting algorithms which are used to provide the near upcoming data from the solar PV power plants. Furthermore, the data provided by the forecasting system to the ESMS are useful for the optimization of other generation sources based on fuel, natural gas, and coal by maximizing

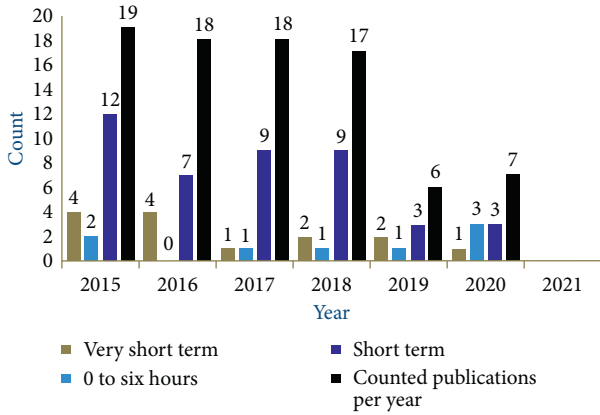


FIGURE 3: Research papers discussed by this review paper since 2015 to 2020.

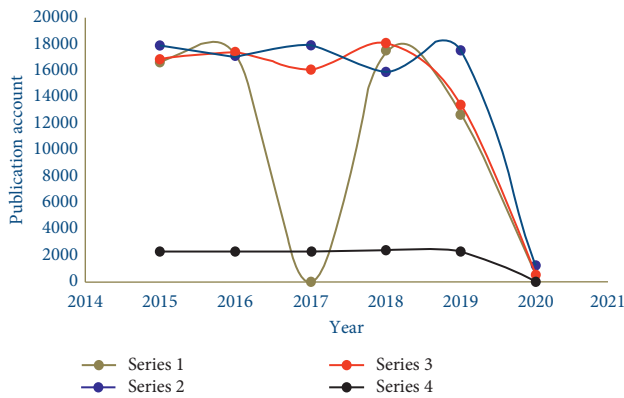


FIGURE 4: Number of publications since 2015 to 2020 for each time horizon returned by Google Scholar research.

the penetration of clean energy in the energy mix as shown in Figure 2.

Furthermore, this review paper is including the time scale from 0 to 6 h that is convenient for the same effectiveness as the short term. In addition, other time horizons such as the very short term were also called the now-cast or online forecasting. This time scale, meanwhile, is useful for the solar PV power monitoring and is usable for the systems that request minimum time forecasting such as the industrial applications. In addition, the very short-term time horizon has been introduced in the solar car industry that was recently developed by the manufacturers (e.g., Toyota manufacturer). Subsequently, the utility of now-cast forecasting in the solar car is its effectiveness to prevent sides including shadows and is also used to provide the weather forecasts [122]. Moreover, the time horizons including the medium term and long term were used in the planning of engine maintenance (e.g., power plants) and for the energy analysis and policy which aided the policy makers to choose the right decisions about the long-term investment return in the energy market.

Additionally, this present review paper provides the research about the time horizons used in the forecasting time utility scale as well as to brighter the time horizon value.

Therefore, two case studies were presented in this review paper: the first one concerns the publications discussed above as illustrated in Figure 3; the second study is based on Google Scholar research platform which provided all studies conducted in the PV power forecasting time horizons since 2015 to 2020. In the meantime, a simple comparison based on Google Scholar research has showed the best-used time horizon in 2019 that is the time horizon of 0–6 h, which returned 17,700 results as shown in Figure 4. To that end, the terminologies used in this website research are short-term photovoltaic power forecasting, very short-term photovoltaic power forecasting, zero to six hours photovoltaic power forecasting, and medium-term photovoltaic power forecasting.

### 7. Conclusion

This review paper revealed the checkup of several research papers available in the arena of PV power forecasting. After the attending analysis, the literature presented that the solar PV power forecasting depends upon the unpredictable parameters of weather as well as the intrinsic parameters of solar PV systems themselves such as the temperature of PV modules and the irradiance on the plane of PV array. In this case, the study of the forecasting parameters including both variables of weather and PV system can be considered before the modelling such as the use of similarity algorithm which can help the designer to select the best parameters and fast modelling [31]. At the same time, after a careful analysis of methods used to forecast the PV power, this study ascertains the need for developing more skillful methods and approaches in this area alongside the generalization methods that are capable to generalize the forecasting results. Indeed, this review paper suggests the practise of the hybrid models including the methods of artificial intelligence and machine learning such as the deep learning and CNN algorithms alongside the probabilistic models, in which they are efficient methods which are able to improve the accuracy of PV power forecasting models and resolve the complexity of solar PV power forecasting. In addition, there is a need for driving more research studies in the standard accuracy metrics (SAMs). Many research papers in the literature, meanwhile, showed several SAMs that were applied for testing the accuracy of forecasting results by comparing the forecasted data with the measured ones; however, these SAMs needed more generalization in their applications as shown previously in Table 2. Furthermore, the standardization of time horizons needs more research and development.

As a conclusion of this recent review paper, we recommend for the benefit of the industrials and practitioners the integration of PV power forecasting algorithms along with the EMS, the HEMS, and the optimal DG planning and dispatching. The PV power forecasting is also useful in the cases of microgrids and EVs. It provides the necessary information about the PV power available in the future time horizon and going to join the input of PV inverters. Further recommendation concerning the PV power forecasting modelling consisted on the PV power forecasting model for each time horizon which means, for example, a model for

short-term time horizon cannot be used for a time horizon of very short-term. This conclusion is proved through the analysis conducted on research papers [55, 60].

## Nomenclature

AR:	Autoregressive	LVQ:	Learning vector quantization
ART:	Adaptive resonance theory	LSTM:	Long short-term memory
AMVs:	Atmospheric motion vectors	LSE:	Least square error
ARMA:	Autoregressive moving average	LS-SVM:	Least square support vector machines
ARX:	AR exogenous	LS-SVR:	Least-square SVR
ARMAX:	ARMA with exogenous variables	MLR:	Multiple linear regression
ARIMA:	AR integrated with MA	MAE:	Mean absolute error
ANN-MC:	Artificial neural network combined with a Markov chain	MOS:	Model output statistics
ANEN:	Analog ensemble	MSE:	Mean square error
ANFIS:	Adaptive-network-based fuzzy inference system	MRE:	Mean relative error
AIC:	Akaike information criterion	MBE:	Mean-based error
BMA:	Bayesian model averaging	MAPE:	Mean absolute percentage error
BSS:	Brier skill score	MLP:	Multilayer perceptron
CC:	Cloud cover	MARS:	Multivariate adaptive regression spline
CASO:	Chaotic ant swarm optimization	MR:	Multivariate regression
CABCA:	Chaotic artificial bee colony algorithm	MIL:	Mean interval length
CI:	Clarity index	MNNEF:	Multivariate neural network ensemble forecasts
CFN:	Cascade forward backpropagation network	MAID:	Mean absolute interval deviation
CNNs:	Convolutional neural networks	MABC:	Multiperiod ABC
CRPS:	Continuous ranking probability score	MM5:	Fifth-generation Penn state
DPC:	Dual-population chaotic	MA:	Moving average
DNN:	Deep learning neural network	NOAA:	National Oceanic Atmospheric Administration
DBM:	Deep belief method	NRMSE:	Normalized root mean square error
DSM:	Demand-side management	NSDE:	Normalized standard deviation of the error
EMOS:	Ensemble MOS	NARX:	Nonlinear AR with exogenous input
EPS:	Ensemble prediction system	NWP:	Numerical weather prediction
ECMWF:	European Centre for Medium-Range Weather Forecasts	PICP:	Prediction interval coverage probability
ELM:	Elman backpropagation network	PDF:	Probability density function
EI:	Extraterrestrial irradiance	PE:	Persistence ensemble
ELMs:	Extreme learning machines	PINAW:	Prediction interval normalized average width
EMS:	Energy management system	PCA:	Principal component analysis
FF:	Firefly algorithm	POA:	Plane of array irradiance
F-FNN:	Feedforward neural network	PHANN:	Physical hybridized artificial neural network
FDIAs:	False data injection attacks	PPC:	Phase-phase correlation
GP:	Gaussian process	QR:	Quantile regression
GB:	Gradient boosting	QRFs:	Quantile regression forests
FCM:	Fuzzy C-means	RPS:	Ranked probability score
GA:	Genetic algorithm	RH:	Relative humidity
GSO:	Genetic swarm optimization	ROC:	Relative operating characteristic
GTNN:	GHI-temperature neural network	RMSE:	Root mean square error
GBRT:	Gradient boosted regression trees	RFs:	Random forests
GPU:	Graphic processing unit	RMS:	Root mean square
GRNN:	Generalized regression neural network	SPF:	Short-term probabilistic solar power forecasts
GEMS:	Global energy management system	SOM:	Self-organized map
HIRLAM:	High-resolution limited area model	RTs:	Regression trees
IMGWO:	Improved grey wolf optimizer	SSE:	Sum squared error
ICP:	Interval coverage probability	SG:	Solar geometry
IA:	Immune algorithm	SR:	Stepwise regression
KSI:	Kolmogorov-Smirnov test integral	SAM:	Solar advisor model
KNN:	K-nearest neighbours	SFLA:	Shuffled frog leaping algorithm
LAE:	Least absolute error	SDE:	Standard deviation of error
		SAMs:	Standard accuracy metrics
		SVM:	Support vector machine
		SMA:	Simple moving average
		SGBM:	Stochastic gradient boosting machine
		SGBQR:	Stochastic gradient boosting quantile regression
		SS:	Skill scores
		SSO:	Shark smell optimization



SARIMA:	Seasonal ARIMA
SPF:	Skillful probabilistic forecast
SPGP:	Sparse Gaussian process
SVR:	Support vector regression
TDLNN:	Time delay neural network
VD:	Variance deficit
TCWB:	Taiwan Central Weather Bureau
VARX:	Vector ARX
VMD:	Variational mode decomposition
VAR:	Vector AR
WT:	Wavelet transform
WRFM:	Weather research and forecasting model
WRRMSE:	Weighted relative root mean squared error
VST:	Very short term
ST:	Short term
0–6 h:	Zero to six hours
PINAW:	Prediction interval normalized average width
MABC:	Multiperiod ABC.

## Data Availability

The data used to support the findings of the study are available from the corresponding author upon request.

## Conflicts of Interest

The authors declare that they have no conflicts of interest.

## References

- [1] OECD, *Renewables 2017: Global Status Report*, OECD, Paris, France, 2017.
- [2] J.-I. Lee, I.-W. Lee, and S.-H. Kim, "Multi-site photovoltaic power generation forecasts based on deep-learning algorithm," in *Proceedings of the 2017 International Conference on Information and Communication Technology Convergence (ICTC)*, pp. 1118–1120, Jeju, Republic of Korea, October 2017.
- [3] R. Ahmed, V. Sreeram, Y. Mishra, and M. D. Arif, "A review and evaluation of the state-of-the-art in PV solar power forecasting: techniques and optimization," *Renewable and Sustainable Energy Reviews*, vol. 124, Article ID 109792, 2020.
- [4] A. Mellit, A. Massi Pavan, E. Ogliari, S. Leva, and V. Lughi, "Advanced methods for photovoltaic output power forecasting: a review," *Applied Sciences*, vol. 10, no. 2, p. 487, 2020.
- [5] J. Antonanzas, N. Osorio, R. Escobar, R. Urraca, F. J. Martinez-de-Pison, and F. Antonanzas-Torres, "Review of photovoltaic power forecasting," *Solar Energy*, vol. 136, pp. 78–111, 2016.
- [6] S. Sobri, S. Koohi-Kamali, and N. A. Rahim, "Solar photovoltaic generation forecasting methods: a review," *Energy Conversion and Management*, vol. 156, pp. 459–497, 2018.
- [7] J. Dong, M. M. Olama, T. Kuruganti et al., "Novel stochastic methods to predict short-term solar radiation and photovoltaic power," *Renewable Energy*, vol. 145, pp. 333–346, 2020.
- [8] L. Vallance, B. Charbonnier, N. Paul, S. Dubost, and P. Blanc, "Towards a standardized procedure to assess solar forecast accuracy: a new ramp and time alignment metric," *Solar Energy*, vol. 150, pp. 408–422, 2017.
- [9] J. Zhang, A. Florita, B.-M. Hodge et al., "A suite of metrics for assessing the performance of solar power forecasting," *Solar Energy*, vol. 111, pp. 157–175, 2015.
- [10] C. Persson, P. Bacher, T. Shiga, and H. Madsen, "Multi-site solar power forecasting using gradient boosted regression trees," *Solar Energy*, vol. 150, pp. 423–436, 2017.
- [11] D. P. Larson, L. Nonnenmacher, and C. F. M. Coimbra, "Day-ahead forecasting of solar power output from photovoltaic plants in the American Southwest," *Renewable Energy*, vol. 91, pp. 11–20, 2016.
- [12] C. W. Chow, S. Belongie, and J. Kleissl, "Cloud motion and stability estimation for intra-hour solar forecasting," *Solar Energy*, vol. 115, pp. 645–655, 2015.
- [13] F. Barbieri, S. Rajakaruna, and A. Ghosh, "Very short-term photovoltaic power forecasting with cloud modeling: a review," *Renewable and Sustainable Energy Reviews*, vol. 75, pp. 242–263, 2017.
- [14] M. Rana, I. Koprinska, and V. G. Agelidis, "2D-interval forecasts for solar power production," *Solar Energy*, vol. 122, pp. 191–203, 2015.
- [15] M. Lipperheide, J. L. Bosch, and J. Kleissl, "Embedded nowcasting method using cloud speed persistence for a photovoltaic power plant," *Solar Energy*, vol. 112, pp. 232–238, 2015.
- [16] Z. Li, S. Rahman, R. Vega, and B. Dong, "A hierarchical approach using machine learning methods in solar photovoltaic energy production forecasting," *Energies*, vol. 9, no. 1, p. 55, 2016.
- [17] K. Mahmoud and M. Abdel-Nasser, "Fast yet accurate energy-loss-assessment approach for analyzing/sizing PV in distribution systems using machine learning," *IEEE Transactions on Sustainable Energy*, vol. 10, no. 3, pp. 1025–1033, 2019.
- [18] J. Zhang, R. Verschae, S. Nobuhara, and J.-F. Lalonde, "Deep photovoltaic nowcasting," *Solar Energy*, vol. 176, pp. 267–276, 2018.
- [19] D. Yang and Z. Dong, "Operational photovoltaics power forecasting using seasonal time series ensemble," *Solar Energy*, vol. 166, pp. 529–541, 2018.
- [20] D. W. van der Meer, M. Shepero, A. Svensson, J. Widén, and J. Munkhammar, "Probabilistic forecasting of electricity consumption, photovoltaic power generation and net demand of an individual building using Gaussian processes," *Applied Energy*, vol. 213, pp. 195–207, 2018.
- [21] Y. K. Semero, J. Zhang, J. Zhang, and D. Zheng, "PV power forecasting using an integrated GA-PSO-ANFIS approach and Gaussian process regression based feature selection strategy," *CSEE Journal of Power and Energy Systems*, vol. 4, no. 2, pp. 210–218, 2018.
- [22] M. Q. Raza, N. Mithulananthan, and A. Summerfield, "Solar output power forecast using an ensemble framework with neural predictors and Bayesian adaptive combination," *Solar Energy*, vol. 166, pp. 226–241, 2018.
- [23] Z. Cheng, Q. Liu, and Y. Xing, "A hybrid probabilistic estimation method for photovoltaic power generation forecasting," *Energy Procedia*, vol. 158, pp. 173–178, 2019.
- [24] V. Kushwaha and N. M. Pindoriya, "A SARIMA-RVFL hybrid model assisted by wavelet decomposition for very short-term solar PV power generation forecast," *Renewable Energy*, vol. 140, pp. 124–139, 2019.
- [25] L. Liu, M. Zhan, and Y. Bai, "A recursive ensemble model for forecasting the power output of photovoltaic systems," *Solar Energy*, vol. 189, pp. 291–298, 2019.



- [26] Y. Sun, V. Venugopal, and A. R. Brandt, "Short-term solar power forecast with deep learning: exploring optimal input and output configuration," *Solar Energy*, vol. 188, pp. 730–741, 2019.
- [27] K. Wang, X. Qi, and H. Liu, "A comparison of day-ahead photovoltaic power forecasting models based on deep learning neural network," *Applied Energy*, vol. 251, Article ID 113315, 2019.
- [28] V. Suresh, P. Janik, J. Rezmer, and Z. Leonowicz, "Forecasting solar PV output using convolutional neural networks with a sliding window algorithm," *Energies*, vol. 13, no. 3, p. 723, 2020.
- [29] H. Zang, L. Cheng, T. Ding, K. W. Cheung, Z. Wei, and G. Sun, "Day-ahead photovoltaic power forecasting approach based on deep convolutional neural networks and meta learning," *International Journal of Electrical Power & Energy Systems*, vol. 118, Article ID 105790, 2020.
- [30] H. A. H. Al-Hilfi, A. Abu-Siada, and F. Shahnia, "Combined ANFIS-wavelet technique to improve the estimation accuracy of the power output of neighboring PV systems during cloud events," *Energies*, vol. 13, no. 7, p. 1613, 2020.
- [31] A. El hendouzi, A. Bourouhou, and O. Ansari, "The importance of distance between photovoltaic power stations for clear accuracy of short-term photovoltaic power forecasting," *Journal of Electrical and Computer Engineering*, vol. 2020, Article ID 9586707, 14 pages, 2020.
- [32] D. Yang, J. Kleissl, C. A. Gueymard, H. T. C. Pedro, and C. F. M. Coimbra, "History and trends in solar irradiance and PV power forecasting: a preliminary assessment and review using text mining," *Solar Energy*, vol. 168, pp. 60–101, 2018.
- [33] M. Ahmed and Aung, "Ensemble learning approach for probabilistic forecasting of solar power generation," *Energies*, vol. 9, no. 12, p. 1017, 2016.
- [34] S. Alessandrini, L. Delle Monache, S. Sperati, and G. Cervone, "An analog ensemble for short-term probabilistic solar power forecast," *Applied Energy*, vol. 157, pp. 95–110, 2015.
- [35] D. AlHakeem, P. Mandal, A. U. Haque, A. Yona, T. Senjyu, and T.-L. Tseng, "A new strategy to quantify uncertainties of wavelet-GRNN-PSO based solar PV power forecasts using bootstrap confidence intervals," in *Proceedings of the 2015 IEEE Power & Energy Society General Meeting*, pp. 1–5, Denver, CO, USA, July 2015.
- [36] P. Bacher, H. Madsen, and H. A. Nielsen, "Online short-term solar power forecasting," *Solar Energy*, vol. 83, no. 10, pp. 1772–1783, 2009.
- [37] L. A. Fernandez-Jimenez, A. Muñoz-Jimenez, A. Falces et al., "Short-term power forecasting system for photovoltaic plants," *Renewable Energy*, vol. 44, pp. 311–317, 2012.
- [38] T. Hong, P. Pinson, and S. Fan, "Global energy forecasting competition 2012," *International Journal of Forecasting*, vol. 30, no. 2, pp. 357–363, 2014.
- [39] J. Huang and M. Perry, "A semi-empirical approach using gradient boosting and k-nearest neighbors regression for GEFCom2014 probabilistic solar power forecasting," *International Journal of Forecasting*, vol. 32, no. 3, pp. 1081–1086, 2016.
- [40] S. Jafarzadeh, M. S. Fadali, and C. Y. Evrenosoglu, "Solar power prediction using interval type-2 TSK modeling," *IEEE Transactions on Sustainable Energy*, vol. 4, no. 2, pp. 333–339, 2013.
- [41] J. G. d. S. F. Junior, T. Oozeki, H. Ohtake, K.-I. Shimose, T. Takashima, and K. Ogimoto, "Forecasting regional photovoltaic power generation - a comparison of strategies to obtain one-day-ahead data," *Energy Procedia*, vol. 57, pp. 1337–1345, 2014.
- [42] J. G. d. S. F. Junior, T. Oozeki, H. Ohtake, K.-I. Shimose, T. Takashima, and K. Ogimoto, "Characterizing the regional photovoltaic power forecast error in Japan: a study of 5 regions," *IEEE Transactions on Power and Energy*, vol. 134, no. 6, pp. 537–544, 2014.
- [43] Y. Li, Y. Su, and L. Shu, "An ARMAX model for forecasting the power output of a grid connected photovoltaic system," *Renewable Energy*, vol. 66, pp. 78–89, 2014.
- [44] V. P. A. Lonij, A. E. Brooks, A. D. Cronin, M. Leuthold, and K. Koch, "Intra-hour forecasts of solar power production using measurements from a network of irradiance sensors," *Solar Energy*, vol. 97, pp. 58–66, 2013.
- [45] J. Lorenz Kühnert, B. Wolff, A. Hammer, O. Kramer, and D. Heinemann, "PV power predictions on different spatial and temporal scales integrating PV measurements, satellite data and numerical weather predictions," in *Proceedings of the 29th EUPVSEC*, Amsterdam, Netherlands, September 2014.
- [46] E. Lorenz, D. Heinemann, and C. Kurz, "Local and regional photovoltaic power prediction for large scale grid integration: assessment of a new algorithm for snow detection," *Progress in Photovoltaics: Research and Applications*, vol. 20, no. 6, pp. 760–769, 2012.
- [47] E. Lorenz, T. Scheidsteger, J. Hurka, D. Heinemann, and C. Kurz, "Regional PV power prediction for improved grid integration," *Progress in Photovoltaics: Research and Applications*, vol. 19, no. 7, pp. 757–771, 2010.
- [48] E. Lorenz, J. Hurka, D. Heinemann, and H. G. Beyer, "Irradiance forecasting for the power prediction of grid-connected photovoltaic systems," *IEEE Journal of Selected Topics in Applied Earth Observations and Remote Sensing*, vol. 2, no. 1, pp. 2–10, 2009.
- [49] A. Mellit, A. Massi Pavan, and V. Lughi, "Short-term forecasting of power production in a large-scale photovoltaic plant," *Solar Energy*, vol. 105, pp. 401–413, 2014.
- [50] C. Monteiro, T. Santos, L. Fernandez-Jimenez, I. Ramirez-Rosado, and M. Terreros-Olarte, "Short-term power forecasting model for photovoltaic plants based on historical similarity," *Energies*, vol. 6, no. 5, pp. 2624–2643, 2013.
- [51] G. I. Nagy, G. Barta, S. Kazi, G. Borbély, and G. Simon, "GEFCom2016: Probabilistic solar and wind power forecasting using a generalized additive tree ensemble approach," *International Journal of Forecasting*, vol. 32, no. 3, pp. 1087–1093, 2016.
- [52] S. Pelland, G. Galanis, and G. Kallos, "Solar and photovoltaic forecasting through post-processing of the Global Environmental Multiscale numerical weather prediction model," *Progress in Photovoltaics: Research and Applications*, vol. 21, no. 3, pp. 284–296, 2011.
- [53] S. Sperati, S. Alessandrini, and L. Delle Monache, "An application of the ECMWF ensemble prediction system for short-term solar power forecasting," *Solar Energy*, vol. 133, pp. 437–450, 2016.
- [54] A. Yona, T. Senjyu, T. Funabashi, and C.-H. Kim, "Determination method of insolation prediction with fuzzy and applying neural network for long-term ahead PV power output correction," *IEEE Transactions on Sustainable Energy*, vol. 4, no. 2, pp. 527–533, 2013.
- [55] M. G. De Giorgi, P. M. Congedo, M. Malvoni, and D. Laforgia, "Error analysis of hybrid photovoltaic power forecasting models: a case study of mediterranean climate,"

- Energy Conversion and Management*, vol. 100, pp. 117–130, 2015.
- [56] T. Soubdhan, J. Ndong, H. Ould-Baba, and M.-T. Do, “A robust forecasting framework based on the Kalman filtering approach with a twofold parameter tuning procedure: application to solar and photovoltaic prediction,” *Solar Energy*, vol. 131, pp. 246–259, 2016.
- [57] M. G. De Giorgi, M. Malvoni, and P. M. Congedo, “Comparison of strategies for multi-step ahead photovoltaic power forecasting models based on hybrid group method of data handling networks and least square support vector machine,” *Energy*, vol. 107, pp. 360–373, 2016.
- [58] M.-T. Do, T. Soubdhan, and B. Benoît Robyns, “A study on the minimum duration of training data to provide a high accuracy forecast for PV generation between two different climatic zones,” *Renewable Energy*, vol. 85, pp. 959–964, 2016.
- [59] R. J. Bessa, A. Trindade, C. S. P. Silva, and V. Miranda, “Probabilistic solar power forecasting in smart grids using distributed information,” *International Journal of Electrical Power & Energy Systems*, vol. 72, pp. 16–23, 2015.
- [60] A. G. R. Vaz, B. Elsinga, W. G. J. H. M. van Sark, and M. C. Brito, “An artificial neural network to assess the impact of neighbouring photovoltaic systems in power forecasting in Utrecht, The Netherlands,” *Renewable Energy*, vol. 85, pp. 631–641, 2016.
- [61] S.-I. Inage, “Development of an advection model for solar forecasting based on ground data. Part II: verification of the forecasting model over a wide geographical area,” *Solar Energy*, vol. 180, pp. 257–276, 2019.
- [62] M. P. Almeida, O. Perpiñán, and L. Narvarte, “PV power forecast using a nonparametric PV model,” *Solar Energy*, vol. 115, pp. 354–368, 2015.
- [63] da S. Fonseca, T. Oozeki, H. Ohtake, T. Takashima, and O. Kazuhiko, “On the use of maximum likelihood and input data similarity to obtain prediction intervals for forecasts of photovoltaic power generation,” *Journal of Electrical Engineering & Technology*, vol. 10, no. 3, pp. 1342–1348, 2015.
- [64] S. Lu, I. Khabibrakhmanov, F. J. Marianno, J. Zhang, B.-M. Hodge, and H. F. Hamann, “Machine learning based multi-physical-model blending for enhancing renewable energy forecast - improvement via situation dependent error correction,” in *Proceedings of the 2015 European Control Conference (ECC)*, pp. 283–290, Linz, Austria, July 2015.
- [65] M. Fliess, C. Join, and C. Voyant, “Prediction bands for solar energy: new short-term time series forecasting techniques,” *Solar Energy*, vol. 166, pp. 519–528, 2018.
- [66] A. Nespoli, E. Ogliari, S. Leva et al., “Day-ahead photovoltaic forecasting: a comparison of the most effective techniques,” *Energies*, vol. 12, no. 9, p. 1621, 2019.
- [67] P. Dawan, K. Sriprapha, S. Kittisontirak et al., “Comparison of power output forecasting on the photovoltaic system using adaptive neuro-fuzzy inference systems and particle Swarm optimization-artificial neural network model,” *Energies*, vol. 13, no. 2, p. 351, 2020.
- [68] U. K. Das, K. S. Tey, M. Seyedmahmoudian et al., “Forecasting of photovoltaic power generation and model optimization: a review,” *Renewable and Sustainable Energy Reviews*, vol. 81, pp. 912–928, 2018.
- [69] J. G. da Silva Fonseca, T. Oozeki, H. Ohtake, T. Takashima, and K. Ogimoto, “Regional forecasts of photovoltaic power generation according to different data availability scenarios: a study of four methods: regional forecasts of photovoltaic power generation,” *Progress in Photovoltaics: Research and Applications*, vol. 23, no. 10, pp. 1203–1218, 2015.
- [70] H. T. C. Pedro and C. F. M. Coimbra, “Assessment of forecasting techniques for solar power production with no exogenous inputs,” *Solar Energy*, vol. 86, no. 7, pp. 2017–2028, 2012.
- [71] A. Dolara, S. Leva, and G. Manzolini, “Comparison of different physical models for PV power output prediction,” *Solar Energy*, vol. 119, pp. 83–99, 2015.
- [72] L. M. Ayompe, A. Duffy, S. J. McCormack, and M. Conlon, “Validated real-time energy models for small-scale grid-connected PV-systems,” *Energy*, vol. 35, no. 10, pp. 4086–4091, 2010.
- [73] C. A. Gueymard and J. A. Ruiz-Arias, “Extensive worldwide validation and climate sensitivity analysis of direct irradiance predictions from 1-min global irradiance,” *Solar Energy*, vol. 128, pp. 1–30, 2016.
- [74] R. Urraca, J. Antonanzas, M. Alia-Martinez, F. J. Martinez-de-Pison, and F. Antonanzas-Torres, “Smart baseline models for solar irradiation forecasting,” *Energy Conversion and Management*, vol. 108, pp. 539–548, 2016.
- [75] G. Graditi, S. Ferlito, and G. Adinolfi, “Comparison of Photovoltaic plant power production prediction methods using a large measured dataset,” *Renewable Energy*, vol. 90, pp. 513–519, 2016.
- [76] P. Ramsami and V. Oree, “A hybrid method for forecasting the energy output of photovoltaic systems,” *Energy Conversion and Management*, vol. 95, pp. 406–413, 2015.
- [77] J. Zhao, G. Zhang, M. La Scala, Z. Y. Dong, C. Chen, and J. Wang, “Short-term state forecasting-aided method for detection of smart grid general false data injection Attacks,” *IEEE Transactions on Smart Grid*, vol. 8, no. 4, pp. 1580–1590, 2017.
- [78] H. S. Jang, K. Y. Bae, H.-S. Park, and D. K. Sung, “Solar power prediction based on satellite Images and support vector machine,” *IEEE Transactions on Sustainable Energy*, vol. 7, no. 3, pp. 1255–1263, 2016.
- [79] M. P. Almeida, M. Muñoz, I. de la Parra, and O. Perpiñán, “Comparative study of PV power forecast using parametric and nonparametric PV models,” *Solar Energy*, vol. 155, pp. 854–866, 2017.
- [80] L. Massidda and M. Marrocu, “Use of Multilinear Adaptive Regression Splines and numerical weather prediction to forecast the power output of a PV plant in Borkum, Germany,” *Solar Energy*, vol. 146, pp. 141–149, 2017.
- [81] A. Bugała, “Short-term forecast of generation of electric energy in photovoltaic systems,” *Renewable and Sustainable Energy Reviews*, vol. 81, pp. 306–312, 2018.
- [82] R. Amaro e Silva and M. C. Brito, “Impact of network layout and time resolution on spatio-temporal solar forecasting,” *Solar Energy*, vol. 163, pp. 329–337, 2018.
- [83] A. Asrari, T. X. Wu, and B. Ramos, “A hybrid algorithm for short-term solar power prediction-sunshine state case study,” *IEEE Transactions on Sustainable Energy*, vol. 8, no. 2, pp. 582–591, 2017.
- [84] W. El-Baz, M. Seufzger, S. Lutzenberger, P. Tzscheutschler, and U. Wagner, “Impact of probabilistic small-scale photovoltaic generation forecast on energy management systems,” *Solar Energy*, vol. 165, pp. 136–146, 2018.
- [85] J. Á. González Ordiano, S. Waczowicz, V. Hagenmeyer, and R. Mikut, “Energy forecasting tools and services,” *WIREs Data Mining and Knowledge Discovery*, vol. 8, no. 2, p. e1235, 2018.

- [86] A. El hendouzi and A. Bourouhou, "Contribution to the management of Microgrids by the application of short term photovoltaic power forecasting," in *Proceedings of the 2017 International Renewable and Sustainable Energy Conference (IRSEC)*, pp. 1–6, Tangier, Morocco, December 2017.
- [87] A. El hendouzi and A. Bourouhou, "Forecasting of PV power application to PV power penetration in a microgrid," in *Proceedings of the 2016 International Conference on Electrical and Information Technologies (ICEIT)*, pp. 468–473, Tangiers, Morocco, May 2016.
- [88] M. Taillardat, *Non-parametric Methods of Post-processing for Ensemble Forecasting*, University of Paris-Saclay, Paris, France, 2017.
- [89] Y. Ren, P. N. Suganthan, and N. Srikanth, "Ensemble methods for wind and solar power forecasting-A state-of-the-art review," *Renewable and Sustainable Energy Reviews*, vol. 50, pp. 82–91, 2015.
- [90] V. Kotu and B. Deshpande, *Predictive Analytics and Data Mining: Concepts and Practice with RapidMiner*, Elsevier, Amsterdam, Netherlands, 2015.
- [91] R. Wason, "Deep learning: evolution and expansion," *Cognitive Systems Research*, vol. 52, pp. 701–708, 2018.
- [92] Z. Li, C. Zang, P. Zeng, H. Yu, and H. Li, "Day-ahead hourly photovoltaic generation forecasting using extreme learning machine," in *Proceedings of the 2015 IEEE International Conference on Cyber Technology in Automation, Control, and Intelligent Systems (CYBER)*, pp. 779–783, Shenyang, China, June 2015.
- [93] A. Teneketzoglou, N. G. Paterakis, and J. P. S. Catala, "Nowcasting photovoltaic power with wavelet analysis and extreme learning machines," in *Proceedings of the 2015 18th International Conference on Intelligent System Application to Power Systems (ISAP)*, pp. 1–6, Porto, Portugal, September 2015.
- [94] W. Zhang, H. Quan, O. Gandhi, C. D. Rodriguez-Gallegos, A. Sharma, and D. Srinivasan, "An ensemble machine learning based approach for constructing probabilistic PV generation forecasting," in *Proceedings of the 2017 IEEE PES Asia-Pacific Power and Energy Engineering Conference (APPEEC)*, pp. 1–6, Bangalore, India, November 2017.
- [95] P. Luo, S. Zhu, L. Han, and Q. Chen, "Short-term photovoltaic generation forecasting based on similar day selection and extreme learning machine," in *Proceedings of the 2017 IEEE Power & Energy Society General Meeting*, pp. 1–5, Chicago, IL, USA, July 2017.
- [96] S. Theocharides, G. Makrides, G. E. Georghiou, and A. Kyprianou, "Machine learning algorithms for photovoltaic system power output prediction," in *Proceedings of the 2018 IEEE International Energy Conference (ENERGYCON)*, pp. 1–6, Limassol, Cyprus, June 2018.
- [97] A. Gensler, J. Henze, B. Sick, and N. Raabe, "Deep learning for solar power forecasting—an approach using AutoEncoder and LSTM neural networks," in *Proceedings of the 2016 IEEE International Conference on Systems, Man, and Cybernetics (SMC)*, pp. 2858–2865, Budapest, Hungary, October 2016.
- [98] M. Abdel-Nasser and K. Mahmoud, "Accurate photovoltaic power forecasting models using deep LSTM-RNN," *Neural Computing and Applications*, vol. 31, no. 7, p. 2727, 2019.
- [99] M. Yan, M. Li, H. He, and J. Peng, "Deep learning for vehicle speed prediction," *Energy Procedia*, vol. 152, pp. 618–623, 2018.
- [100] K. Mahmoud, M. Abdel-Nasser, E. Mustafa, and Z. M. Ali, "Improved salp-swarm optimizer and accurate forecasting model for dynamic economic dispatch in sustainable power systems," *Sustainability*, vol. 12, no. 2, p. 576, 2020.
- [101] A. Bedawy, N. Yorino, K. Mahmoud, Y. Zoka, and Y. Sasaki, "Optimal voltage control strategy for voltage regulators in active unbalanced distribution systems using multi-agents," *IEEE Transactions on Power Systems*, vol. 35, no. 2, pp. 1023–1035, 2020.
- [102] M. Abdel-Nasser, K. Mahmoud, and H. Kashef, "A novel smart grid state estimation method based on neural networks," *International Journal of Interactive Multimedia and Artificial Intelligence*, vol. 5, no. 1, p. 92, 2018.
- [103] K. Mahmoud and M. Abdel-Nasser, "Efficient SPF approach based on regression and correction models for active distribution systems," *IET Renewable Power Generation*, vol. 11, no. 14, pp. 1778–1784, 2017.
- [104] M. Marzband, F. Azarnejadian, M. Savaghebi, and J. M. Guerrero, "An optimal energy management system for islanded Microgrids based on multiperiod artificial bee Colony combined with Markov chain," *IEEE Systems Journal*, vol. 11, no. 3, pp. 1712–1722, 2017.
- [105] Y. Ying, Y. Wu, Y. Su, R. Fu, X. Liang, and H. Xu, "Dispatching approach for active distribution network considering PV generation reliability and load predicting interval," *The Journal of Engineering*, vol. 2017, no. 13, pp. 2433–2437, 2017.
- [106] K. Mahmoud, N. Yorino, and A. Ahmed, "Power loss minimization in distribution systems using multiple distributed generations," *IEEE Transactions on Electrical and Electronic Engineering*, vol. 10, no. 5, pp. 521–526, 2015.
- [107] K. Mahmoud, N. Yorino, and A. Ahmed, "Optimal distributed generation allocation in distribution systems for loss minimization," *IEEE Transactions on Power Systems*, vol. 31, no. 2, pp. 960–969, 2016.
- [108] K. Mahmoud and Y. Naoto, "Optimal siting and sizing of distributed generations," in *Electric Distribution Network Planning*, F. Shahnia, A. Arefi, and G. Ledwich, Eds., pp. 167–184, Springer, Singapore, 2018.
- [109] A. Ali, D. Raisz, and K. Mahmoud, "Optimal oversizing of utility-owned renewable DG inverter for voltage rise prevention in MV distribution systems," *International Journal of Electrical Power & Energy Systems*, vol. 105, pp. 500–513, 2019.
- [110] F. Luo, G. Ranzi, C. Wan, Z. Xu, and Z. Y. Dong, "A multistage home energy management system with residential photovoltaic penetration," *IEEE Transactions on Industrial Informatics*, vol. 15, no. 1, pp. 116–126, 2019.
- [111] A. Ali, D. Raisz, and K. Mahmoud, "Optimal scheduling of electric vehicles considering uncertain RES generation using interval optimization," *Electrical Engineering*, vol. 100, no. 3, pp. 1675–1687, 2017.
- [112] A. Ali, D. Raisz, and K. Mahmoud, "Sensitivity-based and optimization-based methods for mitigating voltage fluctuation and rise in the presence of PV and PHEVs," *International Transactions on Electrical Energy Systems*, vol. 27, no. 12, 2017.
- [113] A. Ali, D. Raisz, and K. Mahmoud, "Voltage fluctuation smoothing in distribution systems with RES considering degradation and charging plan of EV batteries," *Electric Power Systems Research*, vol. 176, Article ID 105933, 2019.
- [114] R. Fachrizal, M. Shepero, D. van der Meer, J. Munkhammar, and J. Widén, "Smart charging of electric vehicles considering photovoltaic power production and electricity consumption: a review," *Transportation*, vol. 4, Article ID 100056, 2020.

- [115] M. C. Mercan, M. Ö. Kayalica, G. Kayakutlu, and S. Ercan, "Economic model for an electric vehicle charging station with vehicle-to-grid functionality," *International Journal of Energy Research*, vol. 44, no. 8, p. 6697, 2020.
- [116] F. Girbau-Llistuella, F. Díaz-González, and A. Sumper, "Optimization of the operation of smart rural grids through a novel energy management system," *Energies*, vol. 11, no. 1, p. 9, 2017.
- [117] O. Abedinia, D. Raisz, and N. Amjady, "Effective prediction model for Hungarian small-scale solar power output," *IET Renewable Power Generation*, vol. 11, no. 13, pp. 1648–1658, 2017.
- [118] I. M. Galván, J. M. Valls, A. Cervantes, and R. Aler, "Multi-objective evolutionary optimization of prediction intervals for solar energy forecasting with neural networks," *Information Sciences*, vol. 418–419, pp. 363–382, 2017.
- [119] Z. Bao, C. Gui, and X. Guo, "Short-term line maintenance scheduling of distribution network with PV penetration considering uncertainties," *IEEE Access*, vol. 6, pp. 33621–33630, 2018.
- [120] B. Kroposki, "Integrating high levels of variable renewable energy into electric power systems," *Journal of Modern Power Systems and Clean Energy*, vol. 5, no. 6, pp. 831–837, 2017.
- [121] L. Gomes, Z. Vale, and J. M. Corchado, "Multi-agent microgrid management system for single-board computers: a case study on peer-to-peer energy trading," *IEEE Access*, vol. 8, pp. 64169–64183, 2020.
- [122] K. Araki, L. Ji, G. Kelly, and M. Yamaguchi, "To do list for research and development and international standardization to achieve the goal of running a majority of electric vehicles on solar energy," *Coatings*, vol. 8, no. 7, p. 251, 2018.

## Research Article

# Bus Voltage Stabilization Control of Photovoltaic DC Microgrid Based on Fuzzy-PI Dual-Mode Controller

Yu Zhang <sup>1,2,3</sup>, Shuhao Wei,<sup>1</sup> Jin Wang,<sup>1</sup> and Lieping Zhang <sup>1</sup>

<sup>1</sup>The College of Mechanical and Control Engineering, Guilin University of Technology, Guilin 541004, China

<sup>2</sup>Guangxi Key Laboratory of Building New Energy and Energy Saving, Guilin 541004, China

<sup>3</sup>The College of Electrical Engineering, Guangxi University, Nanning 530004, China

Correspondence should be addressed to Lieping Zhang; [zlp\\_gx\\_gl@163.com](mailto:zlp_gx_gl@163.com)

Received 29 February 2020; Revised 26 June 2020; Accepted 13 July 2020; Published 5 August 2020

Guest Editor: Mauro de Souza Tonelli-Neto

Copyright © 2020 Yu Zhang et al. This is an open access article distributed under the Creative Commons Attribution License, which permits unrestricted use, distribution, and reproduction in any medium, provided the original work is properly cited.

The photovoltaic DC microgrid has strong nonlinearity and time variation. Therefore, traditional dual closed-loop control strategy of voltage and current based on PI controller cannot effectively restrain the fluctuation and impact of DC bus voltage when the dynamic response of the system is improved. Under this situation, in this paper, the fuzzy-PI dual-mode controller is designed to upgrade the traditional dual closed-loop control, taking voltage outer ring into consideration, which is adopted to achieve good transient performance while the bus voltage deviation is large. While the bus voltage deviation is small, the PI controller is utilized for good steady-state performance. Hence, simulation and experimental results show that the fuzzy-PI dual-mode controller has the same advantages with both fuzzy control and PI control; in other words, it has the features of speedy response, low overshoot, good robustness, and strong anti-interference under different working conditions.

## 1. Introduction

In terms of the photovoltaic DC microgrid system, the bus voltage is the only standard to measure the systematic security and stability [1, 2]. However, as affected by the randomness and fluctuation of the power of photovoltaic power generation as well as the dynamic change of load, there is an unpredictable power disturbance of the PV DC microgrid in the practical function, bringing large fluctuation into the bus voltage. Therefore, how to maintain the stable operation of the DC bus voltage and how to ensure the quality of power are crucial problems to be solved urgently [3]. Currently, compensation is made through energy storage device (ESD) that is incorporated into the DC bus through the bidirectional DC/DC converter (BDC) [4]. The micropower source is able to supply energy and the load can store energy, relying on the amount of the bus voltage, so as to strengthen the systematic robustness [5–10].

At present, the converter of energy storage unit generally adopts the strategy of dual closed-loop control of voltage and current or its upgraded strategy. Furthermore, traditional

dual closed-loop control of voltage and current, with taking the bus voltage as the control outer ring and energy-storing inductive and current as the control inner ring, makes compensation by the PI controller under the classical control theory [11, 12]. This traditional control fails to effectively restrain the large fluctuation and impact of the DC bus voltage while improving the systematic dynamic response.

According to this problem, a great number of scholars introduce the method of feedforward control into the traditional dual closed-loop control [13, 14]. And these methods can be divided into current feedforward and power feedforward according to different variables of the feedforward. For example, Takei et al. put forward three methods for testing feedforward control of load current aiming at unstable zero point of Boost converter, which, compared with the feedback control, successfully restrained the voltage's change and enhanced systematic stability when reducing the output filter capacitance [15]. In addition, Hou et al. fed forward the load current to the control link based on direct power control. And experimental results and simulations showed that the load current feedforward

scheme significantly intensified the dynamic response of DC converters and kept the constant of output voltage under load's abrupt change [16]. Besides, Lu et al., based on the DC/DC buck converter, brought in ripple compensation link established by load current feedforward in the current inner ring control, so as to speed up the dynamic response speed of the inner ring and perfect the quality of the systematic output power [17]. The above current feedforward control strategy enhances the dynamic response performance of the system to some extent. But due to the delay of the voltage ring and current ring, the output current response will lag behind the load disturbance.

The power feedforward is similar to the current feedforward control, and it feeds forward the disturbance power to the control link to suppress the fluctuation of the bus voltage [18]. For example, Zhi-Lin et al., taking the fluctuation problem of the DC bus caused by the mismatch between output power and load consumption of renewable energy for the DC microgrid into consideration, raised the control method of power feedforward compensation based on the classical dual closed-loop control to lead power disturbance into controller through the feedforward channel, so as to restrain the fluctuation of the bus voltage and reinforce systematic stability [19]. Moreover, Song and Zhu, in order to elevate the antiload disturbance ability of the bidirectional DC/DC converter, came up with the strategy of virtual direct power control on the basis of direct power feedforward control which did not need to consider the parameters of converter's energy storage inductance and transformer's changing ratio and boosted systematic compatibility [20]. More importantly, the power feedforward accelerates the response speed of the system to power disturbance, which, to a certain degree, improves the system's ability to restrain the fluctuation of the bus voltage. However, similar to the current feedforward, the power feedforward needs going through the current inner ring as well, from which the output current still has certain delay compared with the load disturbance. Meanwhile, it should be noted that the feedforward control requires to simultaneously collect the real-time information of systematic parameters and increases the cost of the system while reducing its reliability at the same time, which is not conducive to the expansion of the microgrid and the popularization of plug-and-play functions. In view of the problems in the feedforward control, Ibrahim et al. introduce the methods of state observer, nonlinear perturbation observer into the control loop. When the state observer estimates the amount of disturbance, it is not necessary to establish an accurate mathematical model including the disturbance signal [21, 22]. As the models' construction is relatively simple, a great deal of mathematical calculation is avoided to meet the requirements of system's real-time property, whereas noises are inevitably introduced and affect the power quality of the microgrid at the time when the observer is used to observe the state variables of the system.

In terms of the strong nonlinearity and time variability of the photovoltaic DC microgrid [23–27], fuzzy-PI dual-mode controller upgrades the traditional dual closed-loop control in this paper. And for the voltage outer ring, the fuzzy

controller is adopted to obtain good transient performance when the deviation of the bus voltage is large. On the contrary, the PI controller is adopted to get good steady-state performance when the deviation of the bus voltage is small. The simulation and experimental results show that the fuzzy-PI dual-mode controller, boosting the advantages of the fuzzy control and the PI control, enjoys fast response speed, low overshoot, good robustness, and strong anti-jamming ability under different working conditions.

## 2. Topology Structure and Circuit Structure Diagram of the Photovoltaic DC Microgrid

### 2.1. Topology Structure of the Photovoltaic DC Microgrid.

The topology structure of the photovoltaic DC microgrid is shown in Figure 1, and it is mainly composed of photovoltaic arrays, batteries, loads, and various types of energy conversion devices, among which the photovoltaic arrays and batteries are connected to the DC bus by the Boost and BDC, respectively, and the loads include resistive load and constant power load. For the two loads, the first one is directly parallel connection to the DC bus, and the other one is connected to the DC bus through the Buck converter, which is equivalent to the constant power load together with the Buck converter. As the photovoltaic DC microgrid can work in grid-connected and off-grid working mode, this paper mainly takes the bus voltage stabilization of the photovoltaic DC microgrid when off-grid functions.

### 2.2. Circuit Diagram of the Photovoltaic DC Microgrid.

The main circuit construction of the photovoltaic DC microgrid during the off-grid operation is shown in Figure 2. In this figure,  $L_{pv}$ ,  $L_{bat}$ , and  $L_1$  represents the energy storage inductance ( $H$ ) of the Boost converter, the bidirectional DC/DC converter, and the Buck converter respectively;  $i_{pv\_dc}$  serves as the output current for the Boost converter, and  $i_{b\_dc}$  shows the output current that bidirectional DC/DC converter is connected behind the battery, which has bidirection;  $i_{load}$  represents the current of the Buck converter;  $i_R$  is the current of the resistive load;  $C_{dc}$  refers to the capacitance of the DC bus; and  $u_{dc}$  indicates the voltage of the DC bus.

If the battery modules are not considered, according to the current equation by Kirchhoff, the dynamic equation for the DC bus is

$$C_{dc} \frac{du_{dc}}{dt} = i_{pv\_dc} - i_{load} - i_R. \quad (1)$$

From formula (1), the DC bus voltage is influenced by output current as well as load current of the photovoltaic modules. And when photovoltaic output is equal to load consumption, the voltage of the DC bus is stable, but it is affected by the randomness and volatility of the photovoltaic output and the dynamic change of the load. Hence, it is difficult to ensure that the output current is exactly the same as the input current of the load of the Boost converters within all periods. After adding battery modules, the dynamic equation for the DC bus is

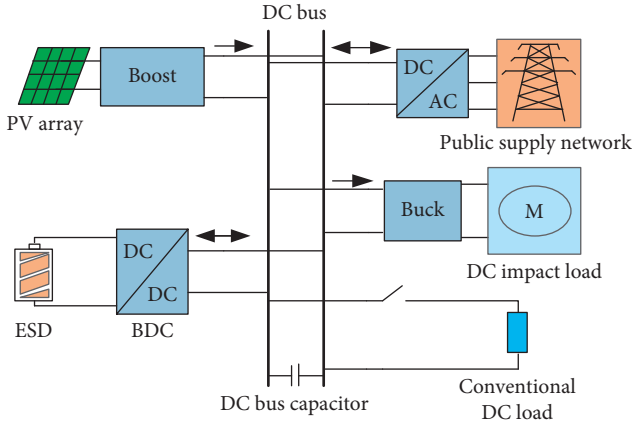


FIGURE 1: Topology structure of the photovoltaic microgrid.

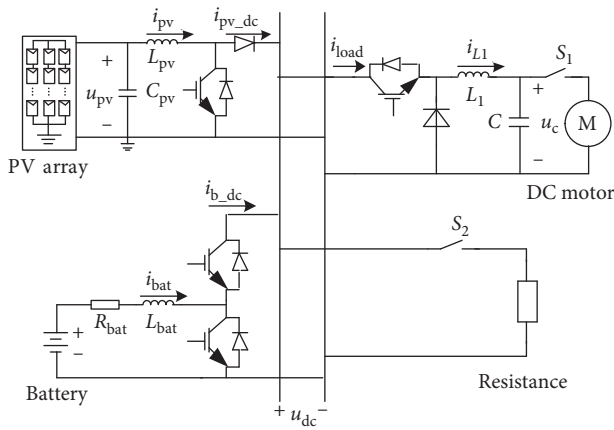


FIGURE 2: Circuit structure of the photovoltaic DC microgrid.

$$C_{dc} \frac{du_{dc}}{dt} = i_{pv\_dc} \pm i_{b\_dc} - i_{load} - i_R. \quad (2)$$

When  $i_{b\_dc}$  is expressed as “+,” it shows that the battery discharges, providing energy for the system. When  $i_{b\_dc}$  is expressed as “-,” it shows that the battery charges, absorbing system’s surplus energy. The system is guaranteed to function safely and stably through controlling the charge and discharge of the battery to restrain the fluctuation of DC bus voltage.

### 3. Fuzzy-PI Dual-Mode Controller

The classical PI controller not only has simple and strongly stable algorithm, but also has simple and effective control effects for precise linear system of mathematical models. However, the distributed power source is of diverse categories, the running states, the output characteristics, and the control methods, belonging to the typical nonlinear system in the microgrid. When systematic workload is large, especially in the case of largely sudden change of load or access to impact load, the robustness of microgrid system based on the PI control is less weak, which is difficult to suppress the impacts of system’s high-power disturbance on the DC bus voltage in a short time. The fuzzy control serves as a kind of

intelligent control algorithm based on fuzzy set theory, fuzzy language variables, and fuzzy logic reasoning. Importantly, it transforms natural language into control strategy not relying on the system’s precise mathematical models. Furthermore, its great robustness is suitable to solve the problems of nonlinearity, strong coupling time variation, and lag in the control process, and it is an important method for human beings to tackle complicated nonlinear systems, while the fuzzy control lacks the integral link, which is difficult to eliminate and leads to the reduction of the controlled accuracy and the dynamic quality of the system.

In order to effectively cope with the contradiction of the dual closed-loop control based on the PI in improving the steady accuracy and dynamic performance of the system, this paper proposes a PI controller that the fuzzy-PI dual-mode controller replaces the voltage outer ring with combining the advantages of the fuzzy controller and PI controller. If the system’s deviation is large, the fuzzy control scheme is selected to enhance the mediation range. If the error is small, the PI control scheme is chosen to elevate the steady-state accuracy. The control frame is shown in Figure 3.

In Figure 3,  $U_{dc}^*$  and  $i_{bat}^*$  are the given values of the voltage outer ring and the current inner ring, respectively;  $U_{dc}$  and  $i_{bat}$  are the sampling values of the voltage of the DC bus and the current of energy-storing inductance, respectively. In addition, the current inner ring adopts the PI controller, and the voltage outer ring applies the fuzzy-PI dual-mode controller, which chooses different controlling strategies according to the deviation of the bus voltage. Since application of the PI controller is so mature, the fuzzy controller and mode selector are primarily described as follows.

**3.1. Fuzzy Controller.** The fuzzy controller is also called fuzzy logic controller. Because the adopted fuzzy control rules are described by fuzzy conditional statements of fuzzy theory, the fuzzy controller is a language controller, also known as fuzzy language controller. This paper employs a two-dimensional fuzzy controller, and the system’s frame is shown in Figure 4.

In Figure 4,  $e$  and  $ec$  are the input of the fuzzy control, where  $e$  represents the systematic deviation;  $ec$  acts as the deviation’s changing rate  $ec = de/dt$ ;  $u$  is the amount of output control;  $k_e$  and  $k_{ec}$  as well as  $k_u$  are the quantitative factors of  $e$ ,  $ec$ , and  $u$  respectively;  $E$ ,  $EC$ , and  $U$  are the language variables of  $e$ ,  $ec$ , and  $u$  defined on its respective theory domains; and  $D/F$  acts as fuzzy modules, whose functions are to convert the real determinate input into fuzzy vector. And  $A^* \circ R$  module is the reasoning module. According to the input fuzzy vector and the fuzzy control rules, the fuzzy output  $U$  is worked out according to the fuzzy reasoning synthesis rules.  $F/D$  module is defined as clear modules, which is to convert the fuzzy quantity  $U$  into clear amount, then to obtain the actual control amount and to act on the executing agency through quantitative factor.

In the design of the fuzzy control, the universe of language variables is usually defined as the discrete universe of



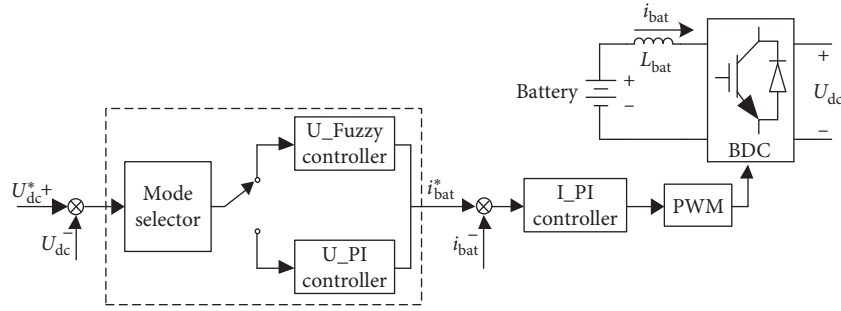


FIGURE 3: BDC controlling frame.

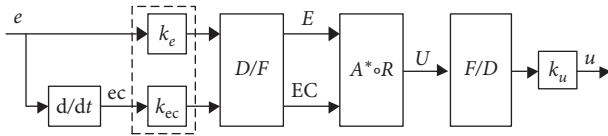


FIGURE 4: Fuzzy controller frame.

finite integers, and the input and output variables are transformed on dimension, so that they can fall within the scope of their respective universe. This paper regards the fuzzy universe of  $E$ ,  $EC$ , and  $U$  as  $N = [-5, 5]$  and, according to the various sensitivity of the controlled objects to the input variables, sets the fuzzy subset of  $E$  and  $U$  as negative big (NB), negative medium (NM), negative small (NS), negative zero (NO), positive zero (PO), positive small (PS), positive medium (PM), and positive big (PB) and sets the fuzzy subset as negative big (NB), negative small (NS), zero (ZO), positive small (PS), and positive big (PB). Reducing the number of ECfuzzy subset can reduce the number of subordinate functions in the reasoning module and can speed up the operation speed of fuzzy controller. Among them, the universe transformation schematic is shown in Figure 5, and subordinate functions of the input amount  $E$ ,  $EC$  and the output amount  $U$  are shown in Figures 6(a)–6(c).

The fuzzy reasoning rules of  $U$  are presented in Table 1 in accordance with the control theory and experience. Taking  $E = \text{NB}$  and  $EC = \text{NB}$  then  $U = \text{NB}$  as an example, it indicates that the current DC bus voltage is much larger than expected value, and the error is increasing continuously when the voltage deviation  $e$  of the DC bus is NB and the deviation's change rate is negative big. Therefore, it is necessary to rapidly reduce the output  $U$  of converters so that it operates in the Buck mode, absorbs redundant energy from the system, and maintains the stability of the bus voltage.

On the basis of the above fuzzy-control rules, the 3D effect diagram of input and output relationship of the fuzzy controller is shown in Figure 7.

**3.2. Mode Selector.** The mode selector is used to automatically switch the operating mode of the dual-mode controller, and it will calculate an error threshold based on the control blind field of the fuzzy controller. Hence, when the systematic deviation is greater than that of the threshold, the fuzzy controller is employed to render the controlled objects

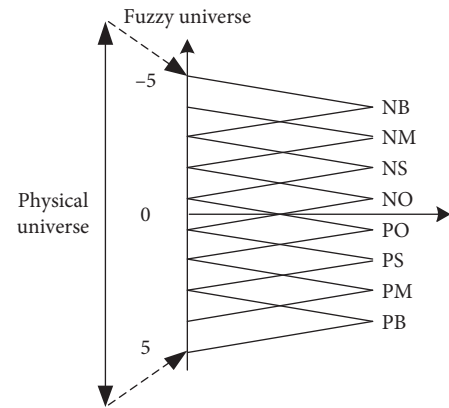


FIGURE 5: Universe transformation schematic diagram.

faster approaching the expected value to accelerate the dynamic response speed of the system. It is believed that the systematic adjustment accesses the adjust blind area of the fuzzy controller when systematic input error is less than that of the threshold. So, it automatically switches to the PI control mode, aiming at lowering the system's steady-state error and improving the system's controlling accuracy.

The fuzzy controller on the discrete universe has control blind area near the equilibrium points. Through setting the physical universe of systematic deviation as  $[-a, a]$  ( $a > 0$ ), the fuzzy universe as  $N_j = [-n_j, -n_j + 1, \dots, -1, 0, 1, \dots, n_j - 1, n_j]$  ( $n_j$  is usually a positive integer from 3 to 7), and the quantitative factor as  $k_e = n_j/a$  of  $e$ , it can be concluded that the corresponding fuzzy value of the systematic deviation is  $n = k_e \times e$ . If  $n$  is an integer, it is the value in the fuzzy universe  $N_j$ . And the calculated  $n$  is not an integer; the value of  $n$  is worked out from the following formula:

$$n = \begin{cases} n_j, & k_e \times e \geq n_j, \\ \text{sgn}(k_e \times e) \text{int}(|k_e \times e| + 0.5), & -n_j < k_e \times e < n_j, \\ -n_j, & k_e \times e \leq -n_j. \end{cases} \quad (3)$$

In the formula, the symbol operator "sgn" means plus-minus sign of the value in the parenthesis. The integer operator "int" represents the integer part in the parenthesis behind the sign. For example, if there is  $k_e \times e = -6.2$ ,  $n = n_j = -6$ . According to (3), if  $n = 0$  near the equilibrium points, the value of the system's deviation at this



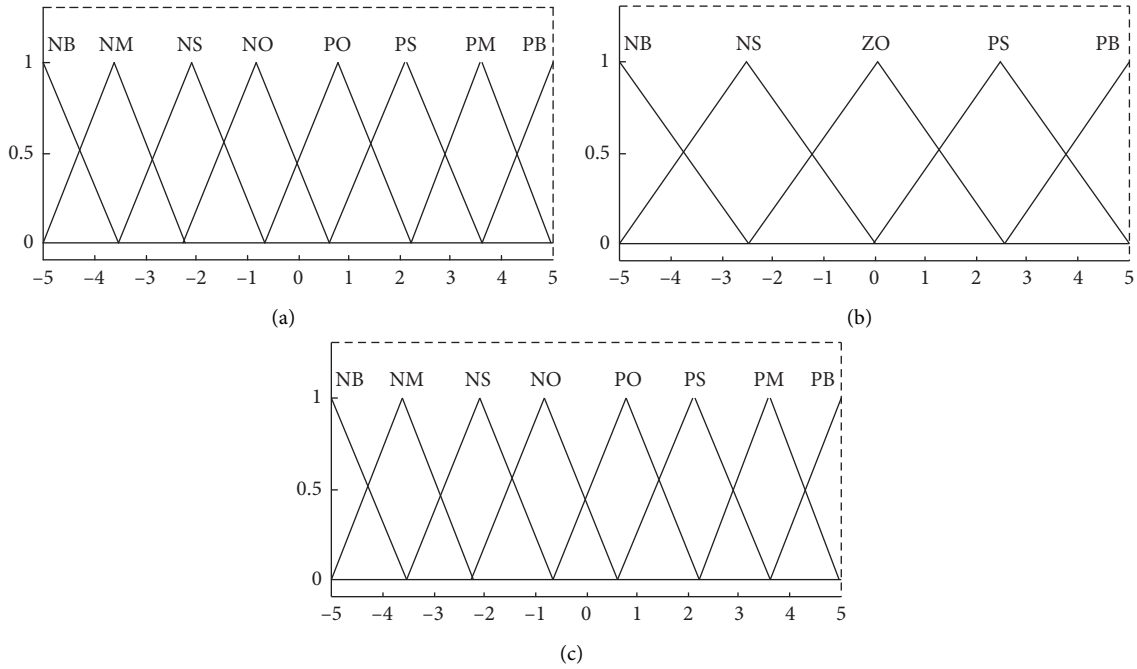


FIGURE 6: Relationship diagram of subordinate function. (a) Subordinate function of the input amount  $E$ , (b) subordinate function of the input amount  $EC$ , and (c) subordinate function of the output amount  $U$ .

TABLE 1: The table of fuzzy reasoning rules of  $U$ .

	$U$				
$EC/E$	NB	NS	ZO	PS	PB
NB	NB	NB	NB	NM	NM
NM	NB	NM	NM	NM	NS
NS	NM	NS	NS	NS	NO
NO	NS	NO	NO	NO	PO
PO	NO	PO	PO	PO	PS
PS	PO	PS	PS	PS	PM
PM	PS	PM	PM	PM	PB
PB	PM	PB	PB	PB	PB

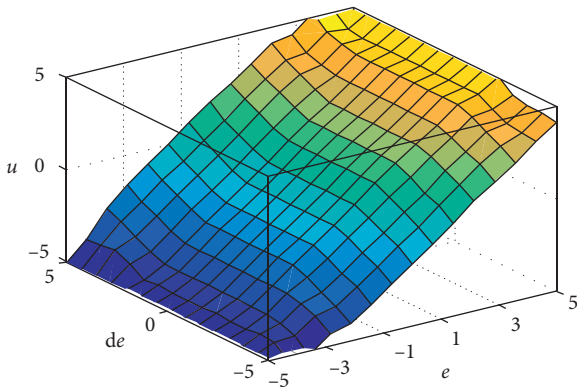


FIGURE 7: The input and output relationship figure of the fuzzy controller.

time may not equal zero. There is a controlled blind area, and its critical value is

$$|X| = \frac{0.5}{k_e} = \frac{0.5a}{n_j} \quad (4)$$

When the deviation  $e$  of the system satisfies  $|e| < 0.5a/n_j$ , the system enters into the blind area of the fuzzy controller, which is considered to have reached a steady state. Therefore, this deviation cannot be eliminated, seriously affecting the stable-state performance of the controlled system. As can be seen from formula (4), the larger  $a$  is, the greater the critical value of the blind regions will be and the more the system's error of the steady state will be. And the larger  $n_j$  is, the less the critical value of the blind area will be and the less the system's error of the steady state will be, while the system's calculation will increase at the same time. According to the size of the critical value of the fuzzy control blind area, the threshold is set, and generally the latter is greater than the former.

## 4. Simulations and Experimental Results

**4.1. Simulations and Results.** In the light of the circuit structure diagram of the photovoltaic DC microgrid shown in Figure 2, the simulation model is constructed in MATLAB/Simulink, as shown in Figure 8, and the systematic simulation parameters are shown in Table 2.

The expected value of the bus voltage is 650 V, and the PV module Boost converters make use of tracking control mode (MPPT) at the maximum power point. And the Buck

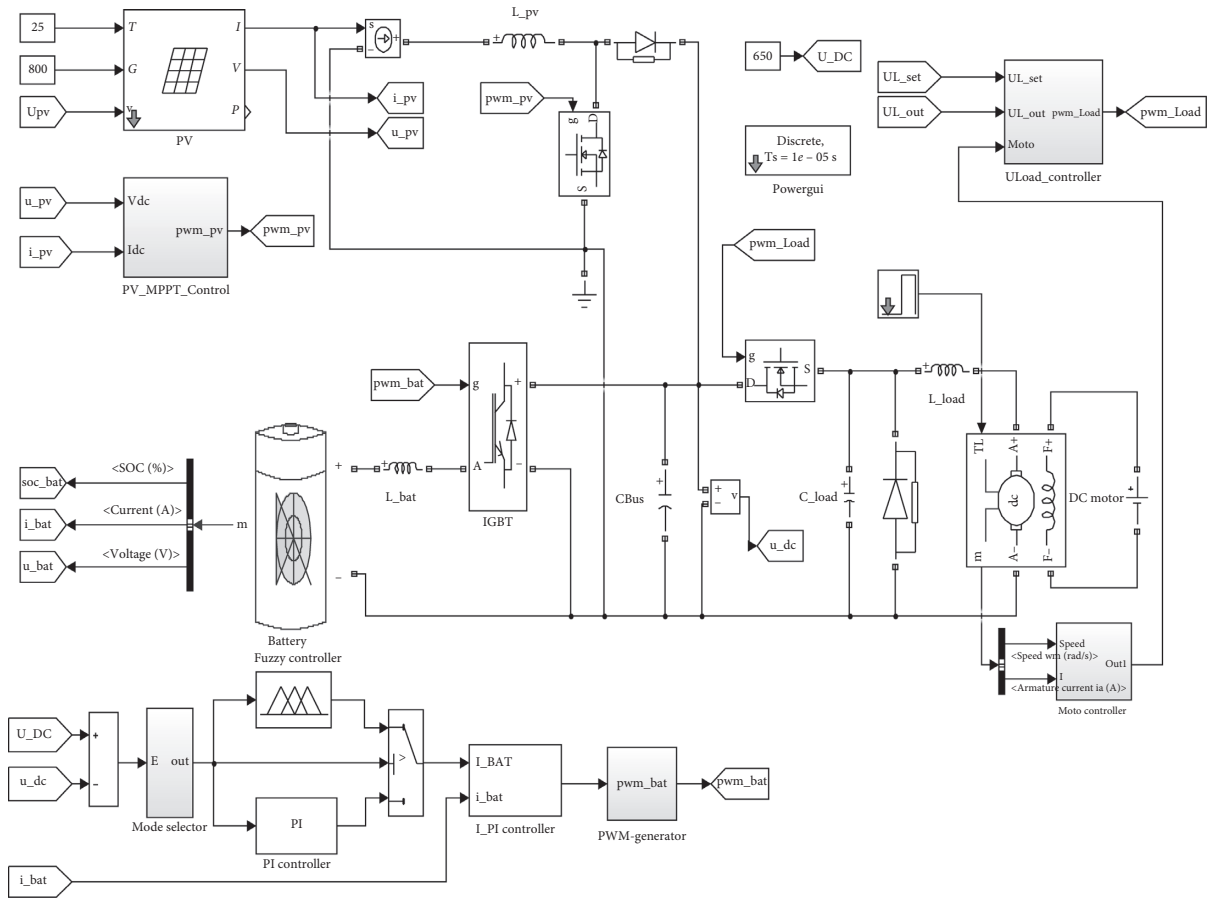


FIGURE 8: Simulation structure of the microgrid.

TABLE 2: Experimental parameters.

Parameter	Numerical value
Output voltage of photovoltaic battery (V)	12
Capacitance of the DC bus (uF)	1000
Rated voltage of battery (V)	12
Rated capacitance of battery (Ah)	38
Rated power of DC motor (W)	30
Rated voltage of DC motor (V)	24
Rated current of DC motor (A)	2.1

utilizes single closed-loop control of voltage to lower the bus voltage to the rating voltage of the load motor, in order to ensure the motor's properly working. The following studies are used to research three transient processes of the system's initial power-up, the surge, and reduction of the load. In addition, the outer ring of the energy storage converter voltage works on the system's ability to restrain the fluctuations ability and dynamic response performance under the PI control, fuzzy control, and fuzzy-PI dual-mode control.

The oscillogram of the DC bus voltage under different control strategies is shown in Figure 9. In order to more intuitively compare the control effects of the three control strategies in different transient processes, the three parts, initial power-up, load's surge, and load's plummet, are enlarged as shown in Figures 10–12, respectively.

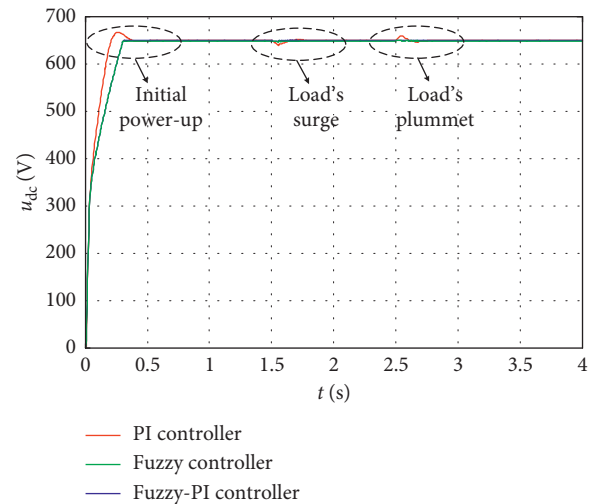


FIGURE 9: The comparison chart of the bus voltage.

The partial amplification chart of the DC bus voltage at the initial power-up is shown in Figure 10. As seen from Figure 10, when the voltage outer ring is controlled by the PI, the overshoot of the DC bus is 15.5 V, stable at 650 V at about 0.5 s, while the voltage outer ring is controlled by the fuzzy control, the DC bus voltage reaches stable at 0.3 s, and there is no overshoot. But due to the existence of control

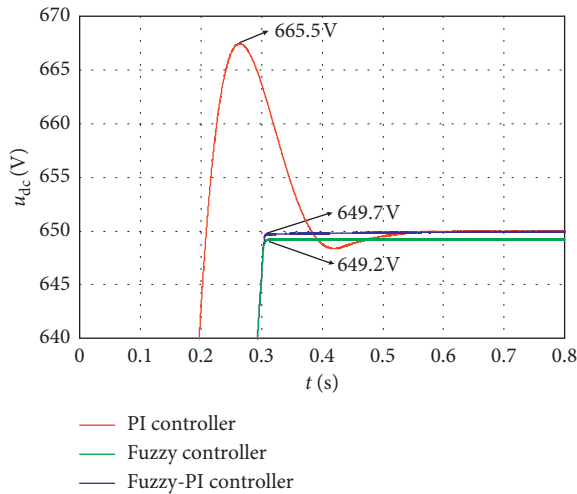


FIGURE 10: Initial power-up.

blind spots, the bus voltage is stable at 649.2 V and fails to achieve the expected value, and the system does not have the trend of farther adjustment, while the fuzzy-PI dual-mode controller using the fuzzy control is introduced; if the deviation of the bus voltage is large, the fuzzy control is used; if the deviation of the bus voltage is small, the PI control is adopted. On the basis of the figures above, due to the large voltage deviation of the bus, far greater than the threshold set by the mode selector, the control curves of the fuzzy control and fuzzy-PI dual-mode almost coincide, indicating that the fuzzy-PI dual-mode controller is operated in fuzzy control mode at this time. The bus voltage is 649.7 V at 0.3 s, reaching a steady state. From the above analysis, it can be seen that in the process of electrical transient state on the system, the fuzzy-PI dual-mode control improves the dynamic response performance of the system compared with the PI control. And compared with the fuzzy control, the fuzzy-PI dual-mode control reduces the steady-state error of the system.

Figure 11 is the partial magnification of the DC bus voltage during the load's surge. As can be seen from the figure, at the 1.5 s, the DC bus voltage under the PI control sharply drops, but it is stable at 650 V attachments at some 85 s with load power suddenly increasing, while in the recovery process there is an overshoot phenomenon. When adopting the fuzzy control, the load instantaneously elevates, the bus voltage reduces by 2.5 V and stabilizes at 650 V with 1.5 V steady-state error, and the system cannot be further adjusted. When using the fuzzy-PI dual-mode controller, the drop of the bus voltage is about 1 V, reaching stability at 1.6 s, gradually restoring to 650 V, and having no overshoot and steady-state error.

Figure 12 is a partial enlarged one of the DC bus voltage when the load is suddenly reduced. The load suddenly reduces at 2.5 s, the bus voltage uplifts 10 V under PI control, the overshoot phenomenon is presented in the recovery process, and the voltage is gradually stabilized to 650 V at about 2.9 s. On employing the fuzzy controller, the bus voltage reaches the steady-state value of 649.2 V after oscillating adjustment. When employing the fuzzy-PI dual-

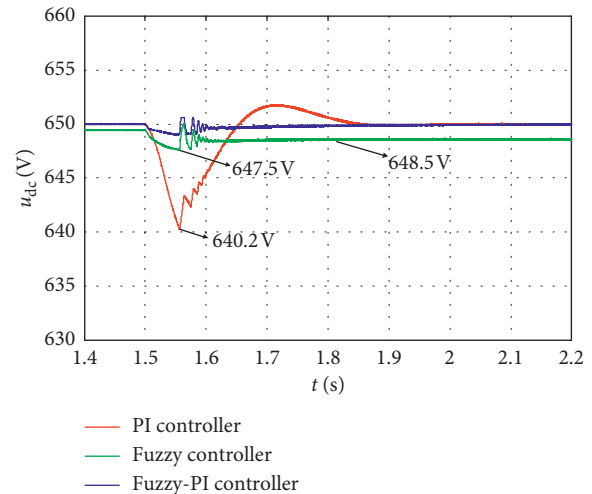


FIGURE 11: Load's surge.

mode controller, the voltage of the bus increases 1 V in the load's instantaneous reduction and recovers to about 650 V at 2.7 s.

The above analysis shows that in the three different transient processes, systematic initial power-up, load's surge, and load's reduction, relative to PI control and fuzzy control, the fuzzy-PI dual-mode controller combines the advantages between the fuzzy control and the PI control, which is able to effectively restrain the large fluctuations and impact on improving the dynamic response at the same time and enhance the robustness of the system.

**4.2. Experiments and Results.** Taking the safety factors into account, the voltage level will be lowered for experiments, and the DSPACE 1104 control platform is used to further test the effectiveness of the proposed fuzzy-PI dual-mode controller in this paper. With designing the bus voltage level of 24 V of experimental platform, the photovoltaic simulator and battery connected to the input of the experimental board as the distributed power source and energy storage equipment of the system, and output of the experimental board is connected to the DC motor load, and the specific experimental parameters are shown in Table 2.

Figure 13 is the oscillogram for the DC bus voltage, similar to the simulation part. In studying the three different transient processes of the initial power-up, load's surge, and load's reduction of photovoltaic DC microgrid, the voltage outer ring utilizes the PI control, fuzzy control, and fuzzy-PI dual-mode controller to research the fluctuation situations of the bus voltage. Figures 14–16 are the oscillograms of the bus voltage for these processes.

As can be seen from Figures 14–16, in the three different transient processes of the initial power-up, load's surge, and sudden reduction, when using the fuzzy control, the voltage outer ring has steady-state errors and has no further adjusting trend. There is less steady-state errors, while the overshoot and weak dynamic performance exists under the PI control. Using the fuzzy-PI dual-mode controller can effectively lower the steady-state errors under the fuzzy

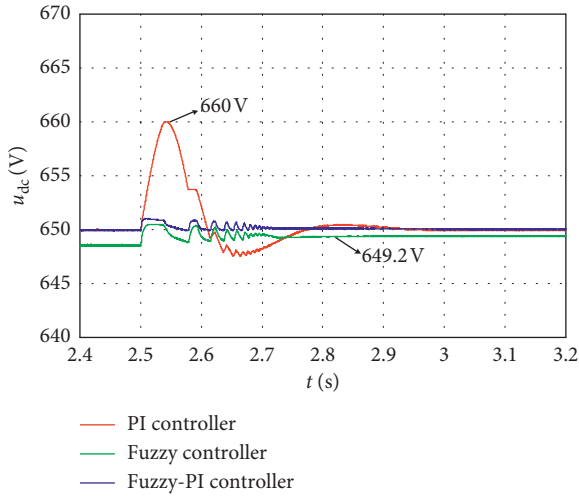


FIGURE 12: Load's plummet.

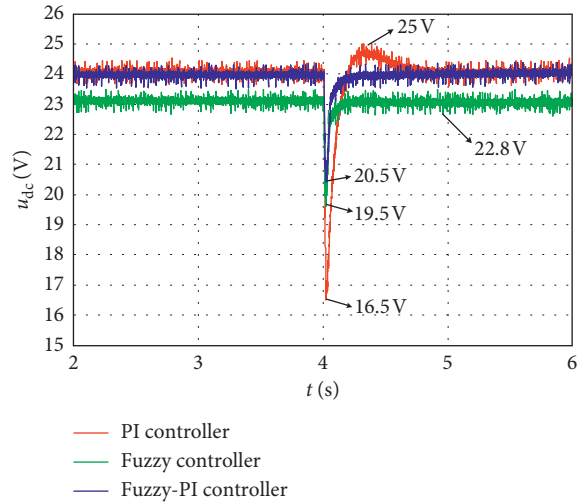


FIGURE 15: Load's surge.

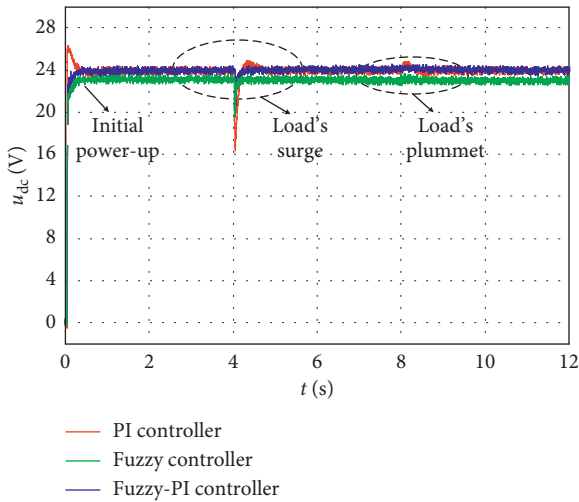


FIGURE 13: The oscillogram of the DC bus voltage.

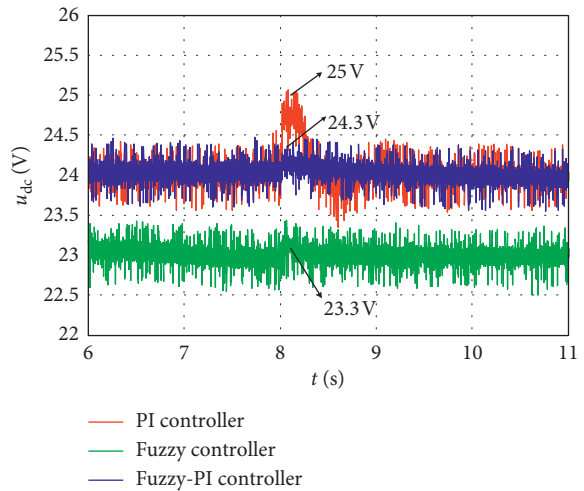


FIGURE 16: Load's plummet.

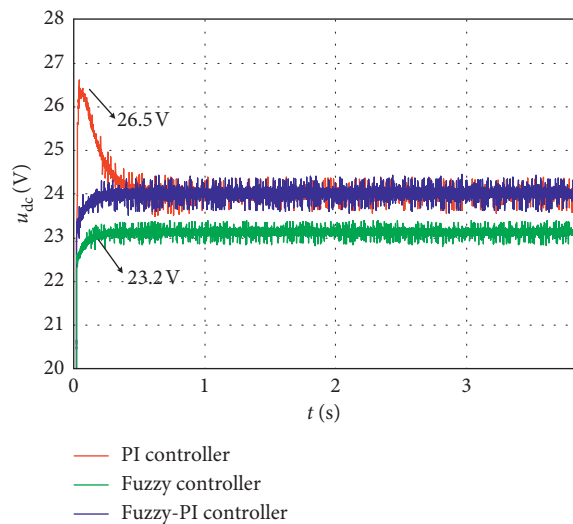


FIGURE 14: Initial power-up.

TABLE 3: Comparison of performance indexes under different controlling strategies.

		PI controller	Fuzzy controller	Fuzzy-PI controller
Initial power-up	Adjustment time (s)	0.4	0.2	0.2
	Voltage overshoot (V)	2.5	0	0
	Steady-state error (V)	0	0.8	0
Load's surge	Adjustment time (s)	0.8	0.2	0.2
	Voltage variation (V)	7.5	4.5	3.5
	Steady-state error (V)	0	1.2	0
Load's sharp reduction	Adjustment time (s)	0.8	0.2	0.2
	Voltage variation (V)	1	0.5	0.3
	Steady-state error (V)	0	0.8	0

control and improve the dynamic response performance under the PI control.

The results of the experiments mentioned above show that when the system is disturbed, the fuzzy-PI dual-mode controller can successfully enhance the adjusted speed and controlled accuracy of the system, meeting the requirements of rapid recovery of the DC bus voltage, better realizing the voltage stability of the DC bus. The specific performance indexes are shown in Table 3:

## 5. Conclusion

In terms of the problems of bus voltage stabilization in the photovoltaic DC microgrid, this paper adopts the fuzzy-PI dual-mode controller to upgrade the traditional dual closed-loop control. For the voltage outer ring, according to the bus voltage deviation, functioning mode automatically switches. When the bus voltage deviation is large, the fuzzy controller is used to obtain good transient performance. When the bus voltage deviation is small, the PI controller is used to obtain good steady-state performance. The specific conclusions are as follows:

- (1) Compared with the PI control and the fuzzy control, fuzzy-PI dual-mode controller combines the advantages of these two controllers, which can validly enhance the dynamic respond and restrain the fluctuation and impact of the DC bus voltage, so as to improve the robustness of the system
- (2) The fuzzy controller in the discrete universe has controlling blind areas near the equilibrium points. The larger the theoretical material universe interval is, the greater the critical value of the blind areas is and the more the system's errors of the steady state are. The more elements in the fuzzy universe, the smaller the critical value of the blind areas is, and the less the steady-state error of the system is, which will lead to an increase in the system's calculation amount
- (3) Simulation and experiments show that in the three different transient processes, including initial power-up, load's surge, and load's sudden reduction, the fuzzy-PI dual-mode controller control has flexible control, strong adaptability, and strong antijamming ability.

## Data Availability

The data used to support the findings of this study have been deposited in the Figshare repository ([https://figshare.com/articles/simulation\\_and\\_experimental\\_data\\_xlsx/9563897](https://figshare.com/articles/simulation_and_experimental_data_xlsx/9563897)).

## Conflicts of Interest

The authors declare that there are no conflicts of interest regarding the publication of this paper.

## Acknowledgments

This work was supported by the Natural Science Foundation of China (no. 51567002) and the Guangxi Natural Science Foundation (no. 2017GXNSFAA198161).

## References

- [1] Q. Yang, D. An, W. Yu, Z. Tan, and X. Yang, "Towards stochastic optimization-based electric vehicle penetration in a novel archipelago microgrid," *Sensors*, vol. 16, no. 6, p. 907, 2016.
- [2] B. Li, S. Huang, and X. Chen, "Performance improvement for two-stage single-phase grid-connected converters using a fast DC bus control scheme and a novel synchronous frame current controller," *Energies*, vol. 10, no. 3, 2017.
- [3] M. Yazdani and A. Mehrizi-Sani, "Distributed control techniques in microgrids," *IEEE Transactions on Smart Grid*, vol. 5, no. 6, pp. 2901–2909, 2014.
- [4] D. Xu, J. Liu, and X.-G. Yan, "A novel adaptive neural network constrained control for a multi-area interconnected power system with hybrid energy storage," *IEEE Transactions on Industrial Electronics*, vol. 65, no. 8, pp. 6625–6634, 2018.
- [5] Z. Lei, F. Wang, Y. Gao, and Y. Ruan, "Research status and application analysis of bidirectional DC-DC converters in DC micro-grids," *Transactions of China Electrotechnical Society*, vol. 31, no. 22, pp. 137–147, 2016.
- [6] C. Shuaixun, H. Beng Gooi, and M. Wang, "Sizing of energy storage for microgrids," *IEEE Transactions on Smart Grid*, vol. 3, no. 1, pp. 142–151, 2012.
- [7] C. Wang, Y. Liu, X. Li, L. Guo, L. Qiao, and H. Lu, "Energy management system for stand-alone diesel-wind-biomass microgrid with energy storage system," *Energy*, vol. 97, pp. 90–104, 2016.
- [8] C. Chen and S. Duan, "Optimal allocation of distributed generation and energy storage system in microgrids," *IET Renewable Power Generation*, vol. 8, no. 6, pp. 581–589, 2014.
- [9] B. Zhao, Q. Yu, and W. Sun, "Extended-Phase-shift control of isolated bidirectional DC-DC converter for power distribution in microgrid," *IEEE Transactions on Power Electronics*, vol. 27, no. 11, pp. 4667–4680, 2012.
- [10] M. Rana and L. Li, "An overview of distributed microgrid state estimation and control for smart grids," *Sensors*, vol. 15, no. 2, pp. 4302–4325, 2015.
- [11] N. Korada and M. K. Mishra, "Grid adaptive power management strategy for an integrated microgrid with hybrid energy storage," *IEEE Transactions on Industrial Electronics*, vol. 64, no. 4, pp. 2884–2892, 2017.
- [12] F. A. Inthamoussou, J. Pegueroles-Queralt, and F. D. Bianchi, "Control of a supercapacitor energy storage system for microgrid applications," *IEEE Transactions on Energy Conversion*, vol. 28, no. 3, pp. 690–697, 2013.
- [13] C. He, G. Hu, F. L. Lewis, and A. Davoudi, "A distributed feedforward approach to cooperative control of AC microgrids," *IEEE Transactions on Power Systems*, vol. 31, no. 5, pp. 4057–4067, 2016.
- [14] X. Li, L. Guo, S. Zhang, C. Wang, and Y. W. Li, "Observer-based DC voltage droop and current feed-forward control of a DC microgrid," *IEEE Transactions on Smart Grid*, vol. 99, p. 1, 2017.
- [15] D. Takei, H. Fujimoto, and Y. Hori, "Load current feedforward control of boost converter for downsizing the output filter capacitor," in *Proceedings of the 40th Annual Conference of the IEEE Industrial Electronics Society*, IEEE, Dallas, TX, USA, October 2014.
- [16] N. Hou, W. Song, and W. U. Mingyi, "A load current feedforward control scheme of dual active bridge DC/DC converters," in *Proceedings of the Chinese Society for Electrical Engineering*, pp. 2478–2485, Shanghai, China, November 2016.

- [17] W. Lu, N. Zhao, S. Lang, S. Liu, and L. Zhou, "Nonlinear control of a DC/DC buck converter and its ripple compensation strategy," in *Proceedings of the Chinese Society for Electrical Engineering*, pp. 35–46, Shanghai, China, August 2013.
- [18] Y. Li, Q. Sun, D. Wang, and S. Lin, "A virtual inertia-based power feedforward control strategy for an energy router in a direct current microgrid application," *Energies*, vol. 12, no. 3, 2019.
- [19] L. Zhi-Lin, W. Q. Tang, and X. J. Zeng, "Voltage stability control of isolated DC micro-grid based on power feed forward," *Power Electronics*, vol. 49, no. 8, pp. 32–36, 2015.
- [20] P. Song and W. Zhu, "Virtual direct power control strategy of dual active bridge DC-DC converter," *Electrical Measurement & Instrumentation*, vol. 55, no. 5, pp. 125–131, 2018.
- [21] O. Ibrahim, N. Z. Yahaya, N. Saad, and K. Y. Ahmed, "Development of observer state output feedback for phase-shifted full bridge DC-DC converter control," *IEEE Access*, vol. 99, p. 1, 2017.
- [22] W. Chengshan, L. Xianlin, G. Li, and Y. W. Li, "A nonlinear-disturbance-observer-based DC-bus voltage control for a hybrid AC/DC microgrid," *IEEE Transactions on Power Electronics*, vol. 29, no. 11, pp. 6162–6177, 2014.
- [23] L. Benadero, R. Cristiano, D. J. Pagano, and E. Ponce, "Nonlinear analysis of interconnected power converters: a case study," *IEEE Journal on Emerging and Selected Topics in Circuits and Systems*, vol. 5, no. 3, pp. 326–335, 2015.
- [24] G. Sun and Z. Ma, "Practical tracking control of linear motor with adaptive fractional order terminal sliding mode control," *IEEE/ASME Transactions on Mechatronics*, vol. 22, no. 6, pp. 2643–2653, 2017.
- [25] Y. Yin, J. Liu, J. A. Sanchez et al., "Observer-based adaptive sliding mode control of NPC converters: an rbf neural network approach," *IEEE Transactions on Power Electronics*, vol. 34, no. 4, pp. 3831–3841, 2019.
- [26] Y. Gao, F. Xiao, J. Liu, and R. Wang, "Distributed soft fault detection for interval type-2 fuzzy-model-based stochastic systems with wireless sensor networks," *IEEE Transactions on Industrial Informatics*, vol. 15, no. 1, pp. 334–347, 2019.
- [27] Z. Zhu, Z. Zhao, H. Cui, and F. Shi, "Improved T-S fuzzy control for uncertain time-delay coronary artery system," *Complexity*, vol. 473, pp. 227–238, 2019.